ELECTROCHEMICAL OXIDATION OF PHENOL FOR WASTE WATER TREATMENT

by

VIVIAN SMITH de SUCRE
B.Sc. Universidad Simon Bolivar, 1975

A THESIS SUBMITTED IN PARTIAL FULFILLMENT OF
THE REQUIREMENTS FOR THE DEGREE OF
MASTER OF APPLIED SCIENCE
in
THE FACULTY OF GRADUATE STUDIES
Department of Chemical Engineering

We accept this thesis as conforming
to the required standard

THE UNIVERSITY OF BRITISH COLUMBIA

August, 1979

In presenting this thesis in partial fulfilment of the requirements for an advanced degree at the University of British Columbia, I agree that the Library shall make it freely available for reference and study. I further agree that permission for extensive copying of this thesis for scholarly purposes may be granted by the Head of my Department or by his representatives. It is understood that copying or publication of this thesis for financial gain shall not be allowed without my written permission.

Department of CHEMICAL ENGINEERING

The University of British Columbia
2075 Wesbrook Place
Vancouver, Canada
V6T 1W5

Date 20-08-1979

ABSTRACT

The electrochemical oxidation of phenol for waste treatment applications was investigated on lead dioxide packed-bed anodes. The electrolytic cell was operated in both batch and continuous modes with feed streams up to 1100 mg/l phenol dissolved in aqueous solutions of Na_2SO_4 and H_2SO_4 or NaOH.

Electrodeposited lead dioxide was found to be a better anode for phenol oxidation, than the lead dioxide obtained by anodizing lead shot. Results showed that all the phenol in solution could be readily oxidized but complete total organic carbon (T.O.C.) removal was more difficult. Rates of phenol oxidation were similar in divided and undivided cells. The oxidation of phenol was favoured by an acidic pH, but an alkaline pH improved the further oxidation of intermediate products. In divided cells, an anionic membrane, which allowed migration of hydroxyl ions, proved to be superior than a cationic membrane for T.O.C. removal. The percent of phenol oxidized increased with increasing current density, and decreased as initial phenol concentration, electrolyte flow rate, and anode particle size were increased.

Comparisons of the experimental results with a mass transfer model are presented for the batch experiments, and a simplified model is proposed to interpret the results from continuous experiments in terms of relative mass transfer and electrochemical reaction resistances.

TABLE OF CONTENTS

LIST OF TABLES

LIST OF FIGURES

ACKNOWLEDGEMENTS

I would like to thank my supervisor Prof. Paul Watkinson for his advice and encouragement throughout the whole of this work. I am also grateful to Prof. Colin Oloman for his sincere interest in the project and for the many useful discussions we had together.

Thanks are also due to my husband, Gustavo Sucre for his suggestions, patience, and understanding.

I wish to express my appreciation to the Chemical Engineering staff for their cooperation and assistance and to the personnel of the Environmental Engineering Laboratory in the Civil Engineering Department for their generous help in the operation of analytical apparatus.

Also acknowledged are Mrs. Rima Kaplan for her translations from Russian papers, Mrs. Monica Gutierrez for the drafting of figures, and Mrs. Nina Thurston for typing the manuscript.

Financial support from the Venezuelan Government through FONINVES (Fondo para la Investigacion en Materia de Hidrocarburos) is gratefully appreciated.

CHAPTER 1

INTRODUCTION

1.1 Phenols as pollutants

"Phenols" in waste water treatment terminology includes not only phenol (C_6H_5OH), but all those derivatives of the aromatic ring that contain one or more hydroxyl groups.

Phenols are constituents of many industrial waste water streams. The major sources of phenolic wastes are oil refineries and coke plants. Phenols are finding increasing use in coatings, stripping agents, solvents, paint vehicles, plastics, explosives, rubber substitutes, fertilizers, wood preservatives, and drugs. Given the usefulness of phenolic compounds, they will undoubtedly continue to be a major product of the chemical industry. Unfortunately, some of the chemical characteristics that make phenols so useful, are also responsible for their high pollution potential.

Chlorine used in drinking water combines with phenols to form chlorophenols which are persistent pollutants, since they are not easily degradable in the environment. Concentrations as low as 5 µg/l of phenols will impart objectionable tastes and odours to drinking waters when phenols are combined with chlorine (1). For this reason the U.S. Public Health Service has set the allowable concentration of phenols in drinking waters at 1 µg/l (2). Phenols are toxic to fish at levels above 2 mg/l, but can cause taste in fish flesh at concentrations far

below the toxic level (3).

The chemical oxygen demand, C.O.D. of phenols is relatively high (theoretically 2.4 mg O_2/mg phenol) and in sufficient concentration can deplete the oxygen of a receiving body of water causing the death of vegetable and animal species.

Permissible levels of phenols have been established by the U.S. Environmental Protection Agency (E.P.A.) for different industrial wastes. These guidelines generally limited phenolic concentrations to 0.1 mg/l in 1977 and project a standard of 0.02 mg/l for 1983 (3).

1.2 Methods of treatment of phenolic wastes

The concentration of phenol in industrial effluents varies widely as do the effluent flow rates (4,5). Generally recovery is only applicable for wastes of at least 2000 mg/l of phenol and flows in excess of about 50 G.P.M. (2).

Phenols may be recovered by liquid-liquid extraction processes using organic solvents such as benzene, butyl acetate, or butyl alcohol. These methods show efficiencies of recovery up to 99.7%, but the concentrations remaining in the aqueous phase after recovery are still significant from the pollution control point of view. Therefore the waste stream requires further treatment before being discharged.

The choice between recovery or destruction of the phenolic content of a given stream is made on the basis of economics. Solvent extraction, for example, has been found to be an extremely expensive alternative in many cases (1).

There are several conventional methods for treating phenolic wastes that cannot be economically recovered. These include adsorption,

incineration, biological treatment, and chemical oxidation. Carbon adsorption is applicable for relatively low (100-200 mg/l) phenolic concentrations. Thus it may be necessary to pretreat or dilute the waste stream before it is applied to the carbon beds (3).

The main disadvantage of the activated carbon process is that the carbon has a finite capacity for removing phenols (0.09-0.4 g phenol/g activated carbon) and eventually the bed becomes fully loaded. To make the cost of the operation reasonable the carbon must be re-activated and re-used. Chemical and thermal regenerations are possible. The first produces a more concentrated phenol stream and the second destroys the adsorbed phenol completely. Very high temperatures are required for this purpose (900°C) and carbon losses of 5-10% can result from the operation. Operating costs of the activated carbon process have been compared with those of other proven treatment methods in a recent study (1) and it was found that activated carbon was the most expensive.

Incineration techniques are only applicable to concentrated wastes. In the case of dilute phenol solutions, the cost of energy to evaporate large amounts of water would be prohibitive. Typical operating temperatures for combustion of phenol to carbon dioxide and water are as high as 800°C.

Biological treatments for the degradation of phenolic wastes are applicable for concentrations up to several thousands mg/l. Many biological plants report treated effluents in the range of 0.1 mg/l for influent loads of about 1000 mg/l (6).

Different biological treatment flow schemes, such as alternating activated sludge, trickling filter, or lagoon can be used, but the

activated sludge system is the most common. A very critical aspect in the success of biological treatment is the control of shock loads to the system, because the microorganisms are only adaptable to a certain range of phenol concentration and stable conditions of pH and temperature. Therefore, in many cases it has been necessary to provide an equalization basin before the biological treatment. Operating costs of biological treatment are relatively low, but generally large land areas are required which may result in substantial capital costs.

Chemical oxidation of phenols includes treatment by hydrogen peroxide, potassium permanganate, ozone, and chlorine dioxide. Depending on the dose of oxidizing agent the phenol can be completely oxidized to carbon dioxide and water or only partly converted to certain intermediate, less harmful organic compounds. In the latter case, additional treatment may be required to reduce the total organic carbon (T.O.C.) or the chemical oxygen demand (C.O.D.) of the waste to acceptable levels.

Oxidation by hydrogen peroxide can provide 99% phenol removal and about 40% C.O.D. removal when using a ratio of 2 g H_2O_2/g phenol (3), but when substituted phenols are present the amount of peroxide necessary can increase to about 4 g H_2O_2/g substituted-phenol. The presence of a metal catalyst is required in the oxidation reaction which increases significantly the operating costs, and for this reason potassium permanganate is a more desirable oxidizing agent.

Potassium permanganate requires a higher oxidant to phenol weight ratio for the oxidation reaction--theoretically 15.7 g $KMnO_4$/g phenol. The main disadvantage is that the reaction produces a precipitate of manganese dioxide that has to be removed, complicating the operation and increasing its cost (1).

Ozonization can be very effective in the destruction of phenols. For example, starting at 2500 mg/1, 99% removal can be achieved in 60 min, when using a ratio of 1.7 g ozone/g phenol. Ozone can oxidize the phenol completely to CO_2 and water but the usual practice is to partially oxidize the phenol to organic compounds more easily biodegradable and then use a biological treatment. This is done since at low phenol concentrations the necessary ozone to phenol ratio is too high to be economical. Initial costs are relatively high because the ozone generating system has to be installed.

The products of the oxidation of phenol by chlorine dioxide are very dependent on pH. At near neutral pHs, in the range 7-8, phenol is oxidized to benzoquinone with a theoretical requirement of 1.5 g ClO_2/g phenol and above pH 10 the products are maleic and oxalic acid requiring a weight ratio of 3.3. Chlorophenols are not produced by this process because the benzene ring is completely destroyed. An economic study made on the oxidation of phenolic coking wastes by ClO_2 indicated that the process was excessively expensive unless the oxidizing agent was already being produced on site (3).

New methods for treating phenolic wastes are being sought, because of the importance of the pollution problem and the highly restrictive future pollution control standard.

Increasing interest is being shown in methods such as Gamma Irradiation (7), wet air, and catalytic oxidation (8), ultraviolet oxidation (9), and electrochemical oxidation, which is the subject of the present study. In the following chapter the fundamental bases of the electrochemical process are presented along with a literature review on previous attempts at electrochemical oxidation of phenol.

CHAPTER 2

BASES OF THE ELECTROCHEMICAL PROCESS

2.1 General concepts

For any electrochemical reaction j of the form

$$B + ze^- \rightleftarrows A$$

the reversible equilibrium potential is written as

$$V_j = V_j^\circ - \frac{RT}{zF} \ln\left(\frac{C_A}{C_B}\right) \qquad [1]$$

where the activity coefficient of each species (i.e., $f_A = a_A/C_A$) is equal to unity (10).

The electrode potential is defined as the difference between the potential of the metal of the electrode and the potential of the solution adjacent to the electrode (Fig. 1). Thus,

$$\text{Anode potential} = V_a^* = \phi_{ma} - \phi_{sa} \qquad [2]$$

$$\text{Cathode potential} = V_c^* = \phi_{mc} - \phi_{sc} \qquad [3]$$

The rate of an electrochemical reaction is a function of the overpotential, or difference between the electrode potential and the equilibrium potential for reaction j. The anodic and cathodic overpotentials for reaction j, are respectively,

$$\eta_{aj} = V_a^* - V_j \qquad [4]$$

$$\eta_{cj} = V_c^* - V_j \qquad [5]$$

The current density (i) is defined as the amount of current passing per unit area of the electrode, and may be related to the overpotential, either linearly at low overpotentials ($\eta \propto i$) or through the Tafel equation at high overpotentials,

$$\eta_j = a_j + b_j \log i \qquad [6]$$

In a given electrolyte, the Tafel constants a and b have specific values for each electrochemical reaction j occurring on a given electrode at determined conditions of pH and temperature. These have been reported for common electrode reactions on different electrodes (10,11). A side reaction will occur if the potential of the electrode is equal to the total potential required to drive the side reaction (equilibrium potential plus overpotential). Major side reactions associated with electrolytic processes in aqueous solutions are the reactions of water electrolysis, that is, the anodic formation of oxygen and the cathodic formation of hydrogen.

Depending on the pH of the electrolyte and potential of the electrode, different water electrolysis reactions may occur,

	(Standard reduction potentials)	
Oxygen evolution reactions:		
$2\ OH^- \rightleftarrows \frac{1}{2}\ O_2 + H_2O + 2e^-$	$V° = 0.4010$	[R1]
$H_2O \rightleftarrows \frac{1}{2}\ O_2 + 2H^+ + 2e^-$	$V° = 1.2290$	[R2]
Hydrogen evolution reactions:		
$H_2O + e^- \rightleftarrows \frac{1}{2}\ H_2 + OH^-$	$V° = -0.8277$	[R3]
$H^+ + e^- \rightleftarrows \frac{1}{2}\ H_2$	$V° = 0.0000$	[R4]

Side reactions will compete with the desired electrochemical reaction for current so that the applied current density will be the sum of the partial current densities supporting each reaction. Considering

the electrochemical reaction ($A \rightarrow B + ze^-$), the current efficiency for the oxidation of A is defined as the ratio between the theoretical amount of electricity needed to oxidize one equivalent of A, and the actual amount of electricity passed per equivalent of A oxidized.

Thus, an expression for the percent of current efficiency is:

$$\% \text{ C.E.} = \frac{F\ z\ m}{I\ t} \times 100 \qquad [7]$$

where, m = number of moles of A oxidized.

If the oxidation of A is the desired electrochemical reaction, sometimes it is necessary to suppress the reverse reduction reaction (depending on the relative reaction rates). In order to avoid contact between the oxidized species and the cathode, or to prevent mixing of anolyte and catholyte with possible reaction an ion exchange membrane or a diaphragm can be used to separate the anode and cathode chambers in a divided cell.

A diaphragm allows the transport of ions and molecules. An ion exchange membrane can be either anion selective or cation selective, in which case only anions or cations respectively will be transported through the membrane. Due to the selective properties of ion exchange membranes, they can also be used to control the pH of the anolyte and catholyte, since the transport of $[OH^-]$ or $[H^+]$ ions will be determined by the type of membrane used.

For the general case of plane electrodes and two separate chambers, the different potential drops through the cell are illustrated in Fig. 1.

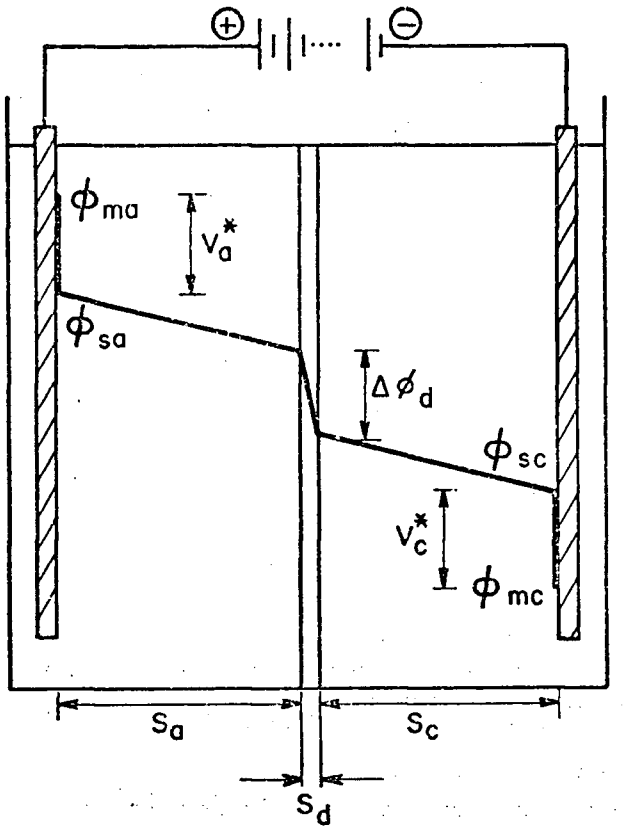

Fig. 1. Voltage components in a divided electrolytic cell.

If K_{e_a}, K_{e_d}, and K_{e_c} are the electrical conductivities of the anolyte, diaphragm, and catholyte, and are uniform, the Ohm's law can be written as follows:

$$i = \frac{K_{e_a}\,|\Delta\phi_{sa}|}{S_a} = \frac{K_{e_d}\,|\Delta\phi_d|}{S_d} = \frac{K_{e_c}\,|\Delta\phi_{sc}|}{S_c}$$

Therefore, the total ohmic drop is given by:

$$\Delta V_{ohmic} = \Delta\phi_{sa} + \Delta\phi_d + \Delta\phi_{sc} = i\left(\frac{S_a}{K_{e_a}} + \frac{S_d}{K_{e_d}} + \frac{S_c}{K_{e_c}}\right).$$

When the anolyte and catholyte have appreciably different compositions, an extra potential drop may exist, called "liquid junction potential"

(10) but usually it is relatively small.

The total electrolysing voltage for a current density i would be,

$$\Delta V = V_a^* + |V_c^*| + i\left(\frac{S_a}{K_{e_a}} + \frac{S_d}{K_{e_d}} + \frac{S_c}{K_{e_c}}\right) \qquad [8]$$

The total electrolysing voltage is of importance since the operating cost of the electrolytic process will depend on its power requirements which is directly related to the total voltage drop through the cell at a given current density.

Practically, the total electrolysing voltage is easier to measure than the particular electrode potentials because to measure V_a^* or V_c^* a reference electrode has to be connected at the surface of the anode or cathode to detect the difference in potential between the metal and the solution. The rate at which an electrochemical reaction occurs depends strongly on the electrode potential as will be shown below.

Consider a single reversible reaction that occurs on an electrode (anode or cathode),

$$A \underset{2}{\overset{1}{\rightleftarrows}} B + ze^- \qquad \begin{array}{l} 1: \text{ oxidation reaction} \\ 2: \text{ reduction reaction} \end{array}$$

The net rate of electrochemical reaction over the electrode is the modulus of the difference between the rates of oxidation and reduction of the reversible reaction

$$\frac{i}{zF} = |Kr_2 \, C_{B_s}^{m_2} - Kr_1 \, C_{A_s}^{m_1}| \qquad [9]$$

where C_{A_s} and C_{B_s} are the concentrations of A and B at the surface of the electrode, m_1 and m_2 are the orders of the oxidation and reduction reactions respectively, and Kr_1 and Kr_2 are the electrochemical reaction

rate constants, which can be expressed in terms of the electrode potential by using an Arrhenius type of rate constant-activation energy relationship,

$$Kr_1 = Kr_1^\circ \exp\left(\frac{\alpha\ zF\ |V^*|}{RT}\right) \qquad [10]$$

$$Kr_2 = Kr_2^\circ \exp\left(\frac{(1-\alpha)\ zF\ |V^*|}{RT}\right) \qquad [11]$$

Here Kr_1° and Kr_2° are rate constants referred to a particular electrode potential at standard conditions, and α is a constant known as the charge transfer coefficient. These equations imply that a fraction of the electrode potential $\alpha|V^*|$ drives the forward reaction and the remainder $(1-\alpha)\ |V^*|$ drives the reverse reaction.

The fact that the electrochemical rate constant depends exponentially on the electrode potential and not just on the temperature as in the case of a pure chemical reaction, illustrates that the reaction rate can be varied by orders of magnitude by simply adjusting the potential.

At a given reaction rate, the concentration of reactant at the surface of the electrode will be related to the rate of mass transfer from the bulk of the solution to the electrode surface,

$$\text{Mass transfer flux} = K_m(C_{A_b} - C_{A_s}) \qquad [12]$$

where K_m is the mass transfer coefficient, characteristic of the particular electrode configuration and fluid dynamics. Empirical and theoretical expressions for transfer coefficients, suitable for design purposes are available in standard texts (12).

2.2 Literature review on the electrochemical oxidation of phenol

A substantial literature exists related to the electrochemical oxidation of phenol. However, owing to the complexity of the oxidation reactions and the variety of operating conditions used in each study, reported findings are sometimes contradictory. Many different reaction mechanisms have been proposed, some of which appear highly speculative.

In order to consider possible rate determining factors, a review of the literature is presented here and some of the contradictions are discussed.

2.2.1 Reaction products

The anodic oxidation of phenol was extensively studied by Fichter and co-workers (13-15) during the early part of this century. They reported that when phenol is oxidized at a lead dioxide electrode in sulphuric acid media the products shown in Fig. 2 are involved.

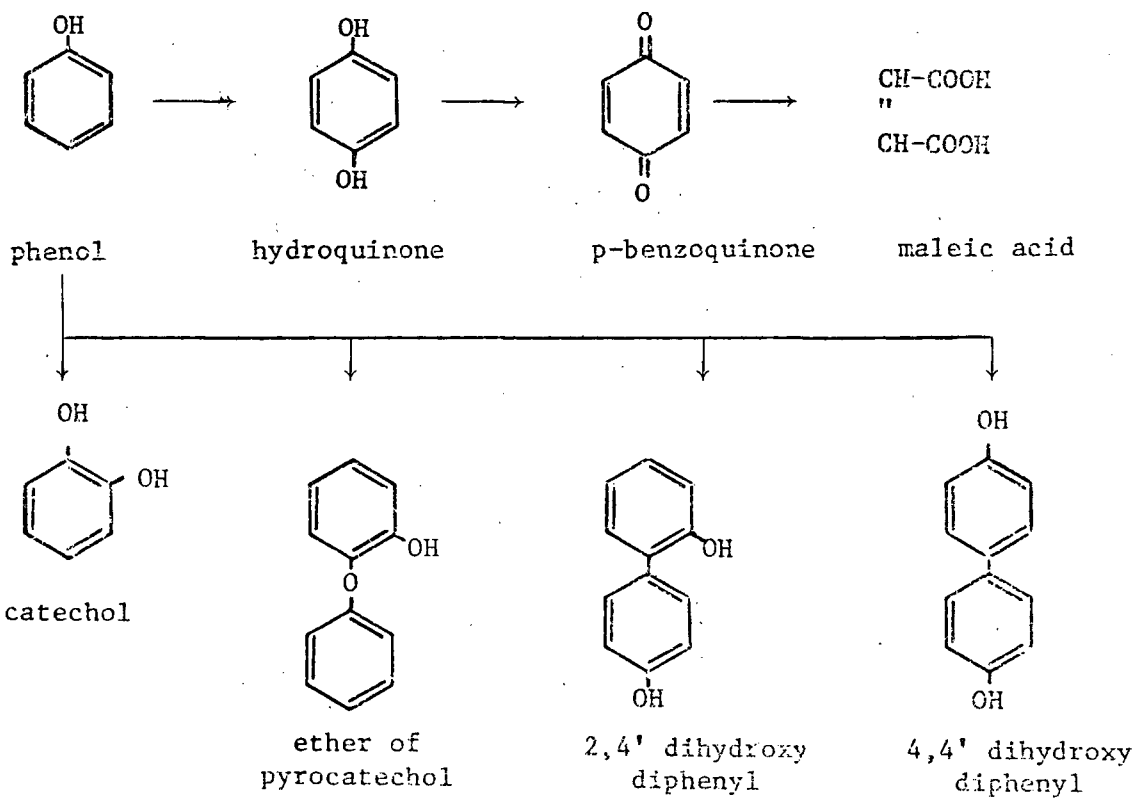

Fig. 2. Reaction products.

It was also found that if benzene (13) is electrochemically oxidized at a platinum electrode in sulphuric acid solution some of the same products were encountered, e.g., hydroquinone, p-benzoquinone, catechol, maleic, and oxalic acids. It was suggested (11,13) that probably phenol was first produced as an intermediate in the oxidation of benzene, even though phenol had not been isolated from the reaction mixture. Thus, information concerning benzene electrooxidation can be useful for the present study.

2.2.2 Proposed reaction mechanisms

a) Hydroxylation

The formation of hydroquinone and catechol was attributed to the introduction of hydroxyl groups into the aromatic ring, by the action of anodically generated oxygen. By the same mechanism phenol would be produced if benzene was the starting substrate (13). However, this assumption is contradicted in a more recent paper (16) where the oxidation of benzene to p-benzoquinone is reported at 100% current efficiency at potentials below those at which oxygen evolution occurs. But a clear explanation of the mechanism is not given in the paper.

b) Nuclear linkage

Fichter explained the formation of diphenyl derivatives by supposing that a linkage of two aromatic nuclei was brought about by a bond of oxygen,

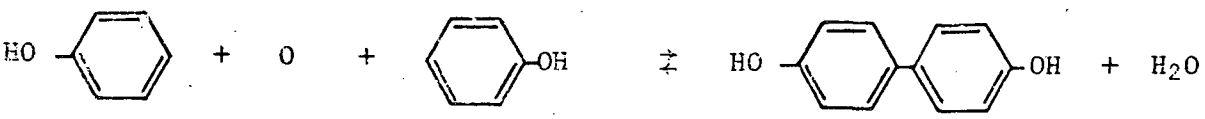

[R5]

A similar mechanism would produce all the diphenyl compounds indicated in Fig. 2. Those compounds were found when lead peroxide anodes were

employed at a relatively low current density ($25A/m^2$). Fichter also reported that the nuclear linkage is even more pronounced with phenol homologues like o-Cresol due to the presence of an electron donating group. The diphenols were found susceptible to further oxidation upon continuing the electrolysis or upon increasing the current density. In more recent publications (17-22) the presence of diphenyl derivatives has not been reported among the products of oxidation of pure phenol solutions. Generally the reported products are hydroquinone, benzoquinone, maleic acid, and carbon dioxide. It is possible that under the reported conditions the diphenyl derivatives either are not formed, or are further oxidized to the above mentioned end-products. However, in the case of substituted phenols, the presence of coupled products is always reported in recent studies (23,24) which is in agreement with Fichter's findings.

c) Primary electron transfer mechanism

In the oxidation of phenol, two different first-step mechanisms of electron transfer have been proposed (23,25), due to the ability of phenols to exist in the ionized or unionized form depending on the pH of the solution,

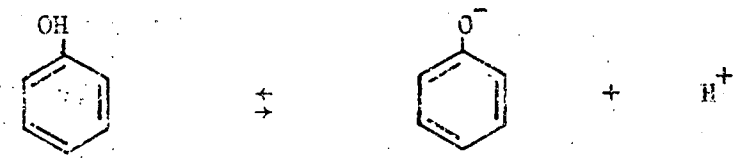

unionized form phenoxide ion [R6]

At low pH in aqueous solutions phenols will tend to be in the unionized form, and at high pH values will tend to be as a phenoxide ion.

The following mechanisms have been proposed, for the first step of the oxidation:

In acidic solutions the initial step involves two electrons where the

electrophilic attack of the aromatic nucleus produces the "phenoxonium ion",

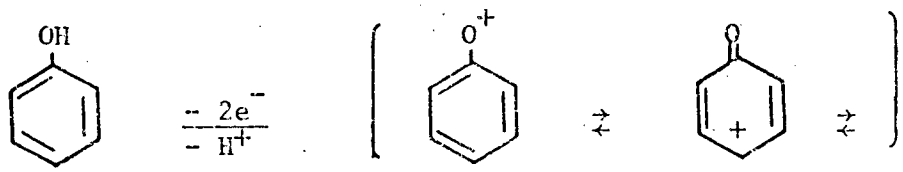

phenoxonium ion (mesomeric) [R7]

In alkaline solutions the primary anodic reaction of phenoxide ions is a one-electron transfer with the formation of a phenoxy free radical that is very reactive.

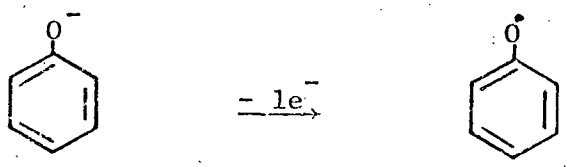

phenoxi radical [R8]

In appendix 5, the percentage phenol ionized as a function of pH is calculated from the dissociation constant for phenol at 20°C ($K_d \simeq 1.28 \times 10^{-10}$).

d) The divided or undivided cell and the reaction mechanism

A great deal of information regarding the electrochemical oxidation of phenol exists because of commercial interest in the production of hydroquinone or p-benzoquinone (19-22). Covitz studied the electrochemical oxidation of phenol for hydroquinone production at lead dioxide anodes in an undivided cell in acid media. He showed that the reaction can be controlled to produce hydroquinone at over 90% yield.

The simplified mechanism for the electrolytic process proposed is (26, p. 157):

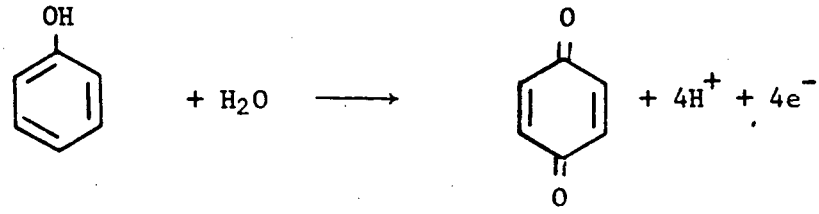

Anodic reaction [R9]

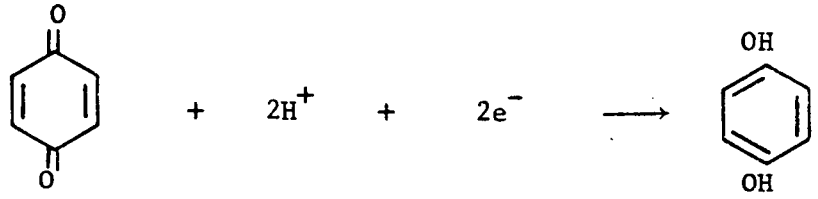

Cathodic reactions [R10]

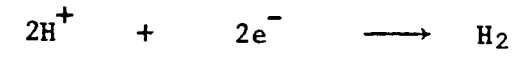

Overall reaction [R11]

It is of interest to note that in the anodic reaction, water is utilized to introduce an oxygen atom into the starting phenol molecule. In the undivided cell p-benzoquinone is reduced at the cathode to produce hydroquinone. From this reaction scheme it is obvious that if the process is carried out in a divided cell, by using a membrane or a diaphragm, p-benzoquinone would not contact the cathode and therefore would not be reduced back to hydroquinone. Covitz reported (19) that when using a semipermeable membrane, the only measurable product in the anolyte was p-benzoquinone.

Another possible reaction in an undivided cell is the oxidation of hydroquinone back to p-benzoquinone which would compete with the phenol for oxidation at the anode, thus lowering the current efficiency for phenol oxidation.

e) Electrolytic action of lead dioxide

Some authors (16,23,26) support the hypothesis of electrocatalytic oxidation of phenol on lead dioxide. In other words, phenol is oxidized chemically by lead dioxide and the reduced lead species so formed are rapidly oxidized back to PbO_2 by a charge transfer or electrolytic step.

1) $PbO_2 + ORGANIC \rightarrow PRODUCT + Pb^{+2}$ [R12]

2) $Pb^{+2} \xrightarrow[OXIDATION]{ELECTROLYTIC} PbO_2$ [R13]

This mechanism is suggested as an alternative explanation to electron transfer from the organic molecule.

Experiments have been carried out to determine the oxidative ability of PbO_2 in the absence of current. Clarke and co-workers (16) made studies with granular PbO_2 in stirred benzene emulsions. The analysis of the products showed that benzoquinone and maleic acid were rapidly formed. However, numerical results were not provided.

As discussed previously, the same paper contradicts the hypothesis of hydroxylation as a mechanism of introduction of oxygen into the organic molecule. Thus if PbO_2 is supposed to be the oxygen carrier it would be necessary to replace the oxygen lost in reaction [R12] by reaction [R13]. The ultimate source of oxygen, is of course, the water, whatever is the prevailing mechanism.

f) Further oxidation of intermediates

The available information concerning the last stages of the electrolytic oxidation of phenol to open chain organic compounds or eventually to carbon dioxide is very limited, probably because only a few investigations have been concerned with the total destruction of the organic substrate for waste treatment applications (i.e., 17,18,25).

A mechanism for the last-stage reactions has not ever been proposed. However, in the early investigations (14) it was shown that intermediates were susceptible to further disintegration. Catechol, for example, was well known as an easily oxidizable substrate, and p-benzoquinone, which offered a high resistance to chemical oxidation, was shown to be readily broken down by electrochemical means (27).

Fichter established that the decomposition process occurs faster at high current densities, when the aromatic nucleus is saturated with electrolytic oxygen. He reported less characteristic final products such as oxalic acid, formic acid, and carbon monoxide, which is in agreement with some of the products reported by Gladisheva (17).

A particularly interesting controlled potential study is presented for the electrolytic oxidation of benzene (16) where it is shown that as the potential is increased above that of oxygen evolution, fragmentation of the aromatic ring occurs and the current efficiency for maleic acid and carbon dioxide production increases.

Anodically generated oxygen is known as one of the most powerful oxidizing agents, and seems to be responsible for the further oxidation of the intermediates, even though the exact reaction mechanism has not been determined.

2.2.3 Electrode materials tested

Lead dioxide has been the most commonly used electrode in the electrochemical oxidation of phenol and in several cases is recommended as the electrode material of choice. However, it is of interest to review and compare the performances of different electrode materials.

In the paper by Gladisheva and Lavrenchuk (17) several anode materials were tested: nickel, smooth platinum, graphite, and lead dioxide

electrodeposited on a nickel base. The experiments showed that under the same operating conditions, the highest oxidation rate occurred on the lead dioxide electrode. The results are shown in Table 1 where the rate of oxidation is given at two phenol concentrations and two current densities. The chemical stability of the different electrodes tested was

TABLE 1

RATES OF PHENOL OXIDATION ON DIFFERENT ELECTRODE MATERIALS (17)

Electrode material	Initial phenol conc. (mg/l)	Rate of Oxidation (mg/min) $i = 50 A/m^2$	Rate of Oxidation (mg/min) $i = 1000 A/m^2$
Electro deposited lead dioxide	200	1.0	3.7
	1000	9.2	21.6
Graphite	200	0.7	2.4
	1000	6.3	17.0
Smooth platinum	200	0.4	2.4
Nickel	200	0.2	2.9

also discussed. The graphite anode was found relatively stable at current densities between 50-250 A/m^2 but at higher current densities the graphite started to break down, forming small particles that were difficult to remove by filtration. Nickel electrodes were unsuitable since at pH = 10 nickel dissolution occurred parallel to phenol oxidation, consuming a significant amount of current, and destroying the electrode.

The smooth platinum electrode was, of course, electrochemically stable but the rates of oxidation of phenol were much lower than expected, considering that platinum has a high oxygen overpotential. This fact was explained by the formation of a tar film on the surface

of the anode which did not dissolve in alkaline or acid solution. However, the presence of such a film was not mentioned in the case of the lead dioxide electrode.

In the study of electrochemical oxidation of phenol to quinone by Fioshin et al (22) the same result was obtained when comparing the platinum and lead dioxide electrodes. The chemical yield to quinone was 33% on the lead dioxide anode, whereas it was only 5% on platinum, although it is known that the overpotential of these electrodes in acidic solutions are practically the same. The reason suggested was the different adsorptive powers of the two electrodes towards the same organic substrate. However, the lower quinone yield on platinum could also have been caused by further disintegration of the quinone. This possibility was not suggested and other products analyses were not performed.

2.2.4 Effect of current density

Studies have been carried out over a wide range of current densities. For example, in reference (17) the current effect on phenol oxidation was studied in the range of 50-2000 A/m^2. It was concluded that among the variables studied, the current density was the strongest determining factor in the rate of electrochemical oxidation of phenol. The results are given in Tables 1 and 2. In Table 1 it can be observed that on the PbO_2 electrode, at the initial concentration of 1000 mg/l of phenol, the rate of phenol oxidation approximately doubled when the current density was increased 20 times.

Table 2 shows that in the sodium sulphate electrolyte, when starting at 466 mg/l of chemical oxygen demand (C.O.D.) at a current density of 50 A/m^2, the final C.O.D. was 420 mg/l after 5 h, whereas at 2000 A/m^2 the C.O.D. dropped to 30 mg/l in only 1 h.

TABLE 2

EFFECT OF CURRENT DENSITY AND TYPE OF ELECTROLYTE ON C.O.D. REMOVAL (17)

Current density A/m^2	Electrolyte type	Time of Electrolysis (h)	Final C.O.D. (mg/l of O_2)
50	I	5	307
	II	5	420
500	I	3	90
	II	5	120
1000	I	1	30
	II	2	75
2000	I	0.5	0
	II	1.0	30

Notes. Initial phenol concentration = 200 mg/l
Initial C.O.D. concentration = 466 mg/l of O_2
Electrolyte I - 1 g/l NaCl, 1.5 g/l Na_2SO_4
Electrolyte II - 3 g/l Na_2SO_4

2.2.5 Effect of nature of the electrolyte

In several studies on the electroxidation of phenol for waste treatment, chloride salts were used as electrolytes (17,18,25,28-30). In such media the oxidation of phenol follows totally different reaction paths.

When using NaCl or $CaCl_2$ as electrolytes, the following reactions have been proposed (17)

1. Evolution of chloride at the anode,

$$2\ Cl^- - 2e^- \rightarrow Cl_2 \qquad [R14]$$

2. a) Formation of hypochlorite followed by chemical reaction with phenol,

$$Cl_2 + H_2O \rightarrow HCl + HClO \qquad [R15]$$

$$8\ HClO + C_6H_5OH \rightarrow \begin{matrix} CH - CO\text{-}OH \\ \| \\ CH - CO\text{-}OH \end{matrix} + 2\ CO_2 + 8\ HCl + H_2O \qquad [R16]$$

b) Chlorination of phenol by molecular Cl_2 producing 2,4 dichlorophenol and 2,4,6 trichlorophenol

As can be seen, this process does not represent pure electrochemical oxidation of phenol, but instead it is equivalent to the electrolytic production of chlorine and hypochlorite followed by a chemical oxidation of phenol.

It also gives rise to undesirable chlorination products. Although these are claimed to be capable of further oxidation, to give products of the quinone type, the removal is never 100%. This was shown in reference (25) where experiments were carried out starting with p-chlorophenol, 2,4 dichlorophenol and 2,4,6 trichlorophenol and the percent removal of chemical oxygen demand (C.O.D.) were 82%, 79%, and 58% respectively.

Knowing that chlorinated phenols are more objectionable than phenol itself, the addition of chloride salts to the electrolyte does not appear to be a good solution to the pollution problem even if the rate of phenol oxidation is higher than when using an inert support electrolyte such as sodium sulphate. The performance of a mixture of NaCl and Na_2SO_4 and pure Na_2SO_4 electrolytes have been compared (17) in terms of final C.O.D. after treatment. The results are also shown in Table 2 where it is observed that at the four current densities used, the final C.O.D. was always lower when the electrolyte contained NaCl than when the electrolyte was pure Na_2SO_4. However, an analysis of chlorinated phenols which

may have been produced was not provided, thus it is difficult to decide which electrolyte is more suitable.

Other electrolytes, such as $Na_2B_4O_7$, NH_3 and H_2SO_4 were tested using a packed bed graphite electrode (18). The results are shown in Table 3.

TABLE 3

EFFECT OF TYPE OF ELECTROLYTE ON PHENOL OXIDATION (18)

Electrolyte	pH	Electrolysis time (h)	Final phenol conc. (mg/l)
0.1 M sodium borate	9.7	3.5	420
0.1 M ammonia	10.0	5.5	400
0.1 M sulphuric acid	1.1	3.7	400
5% sodium chloride	5.7	20.0	10

Initial phenol conc. = 1000 mg/l
Volume of electrolyte = 700 ml
Current = 0.6 A (on graphite anode)

With the first three electrolytes phenol was removed from 1000 mg/l to about 400-420 mg/l in electrolysis times from 3 to 5 h. The final phenol concentration reached 10 mg/l only when using a sodium chloride electrolyte and at the excessively large time of 20 h. The different electrolysis times allowed makes the comparison between electrolyte performances difficult. In this case the current applied was relatively low and an estimation of the electrode area was not provided.

2.2.6 Effect of pH

The effect of pH on the oxidation potential of phenol has been reported (23). The results of this polarographic study are represented in Fig. 3.

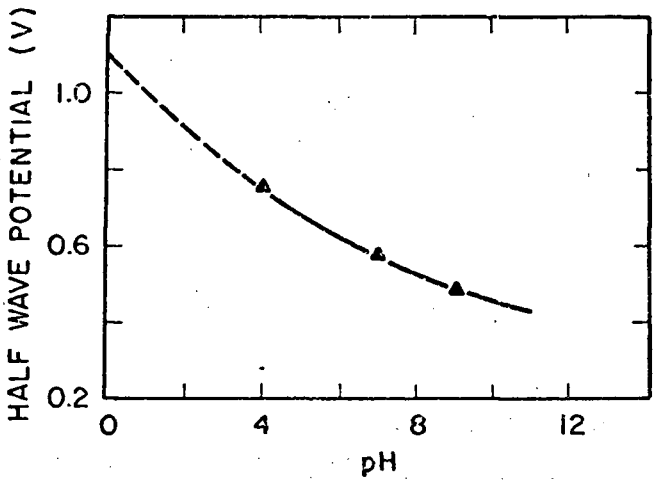

Fig. 3. Half-wave potential vs pH, for the oxidation of 4×10^{-4} M phenol (23).

The half wave potential is defined as the potential on a polarographic curve when the current is equal to one half the mass transfer limiting current (31).

It can be observed that the half wave potential decreases when going from acid to basic solutions and eventually stabilizes at a constant value for a pH equal to the pK_d (logarithmic of the dissociation constant of phenol). At pH = pK_d all the phenol will be in the ionized form, or in other words, protonation will be negligible. This means that a high pH makes the phenol more easily oxidizable as far as potential requirements are concerned.

The effect of pH on the rate of phenol oxidation is not well documented. In reference (17), it was concluded that the velocity of oxidation was practically independent of pH of the solution in the range

of pH 6 to 9, in absence of chloride ions. However, when the pH was changed to 11.9 a rapid increase in the optical density of the solution was reported, which was explained by an increase in the concentration of hydroquinone. However, phenol or C.O.D. analyses were not reported in this case.

In the study by Tarjanyi et al (18) the effect of pH can not be isolated from the data (Table 3). No definitive results could be found in the reviewed literature about the effect of pH on the further oxidation of intermediate products. Fichter (13) suggested that in alkaline solutions the primary products of the oxidation would probably be the same as in acid media, but that p-benzoquinone would be unstable at high pH and more easily oxidizable by the atomic oxygen.

2.3 The lead dioxide electrode

Two types of lead dioxide commonly exist. These differ according to the crystal structure. α-PbO_2 is orthorombic and β-PbO_2 is tetragonal. Each variety can be prepared substantially free from the other under carefully controlled conditions (32).

Lead dioxide never conforms exactly to the stoichiometric PbO_2 formula, an oxygen deficiency is always detected (33), with α-PbO_2 tending to show a lower oxygen content.

Contrary to most metal oxides, lead dioxide is a good electronic conductor, and is better in fact than lead itself (26). It is believed that the high electrical conductivity may be connected with the oxygen deficiency in the lead dioxide structure (32).

Potential-pH diagrams (or Pourbaix diagrams) show the regions of thermodynamic stability of lead and lead compounds (34). From thermodynamic predictions lead can be used as an anode at high electrode

potentials for pH values between 0 and 12 without appreciable corrosion. Under such conditions the metal will be covered with a layer of PbO_2.

Delahay et al (35) have constructed the potential-pH diagram for lead in the presence of sulfate ions (1 g-ion/l). Many electrode reactions are thermodynamically possible at different potentials and pHs. From these, the most studied reactions are those that form the basis of the universally used lead acid storage battery,

$$PbO_2 + 2e^- + 4H^+ + SO_4^{-2} \rightleftarrows PbSO_4 + 2\ H_2O \qquad V^\circ = 1.685 \qquad [R17]$$

$$Pb + SO_4^{-2} \rightleftarrows PbSO_4 + 2e^- \qquad V^\circ = -0.356 \qquad [R18]$$

The reactions occur in the indicated direction during discharge and in the opposite direction during charging (23). It is well known that the mechanism of discharge of PbO_2 in the presence of excess sulfate involves blocking of the PbO_2 surface with a deposit of $PbSO_4$ (32). These reactions may also be of importance in the oxidation of phenol in sulphuric acid media.

The suitability of lead dioxide as an anode material has been known for many years. It is clear that lead dioxide is able to withstand prolonged high anodic potentials more effectively than graphite (which undergoes degredation). Also, lead dioxide possesses a relatively high oxygen overvoltage (10,36) of the same order of magnitude as platinum and is much cheaper.

Preparation. Lead dioxide can be prepared as a coating on lead by anodization, or deposited onto other metals by electrodeposition.

a) Anodization. The most conventional anodization method is to put the lead in contact with an aqueous H_2SO_4 electrolyte and provide a flow of current until oxygen evolution is plainly visible, and the grey lead has acquired the characteristic black deposit of lead dioxide (26,33).

It is well known that oxygen is evolved from a lead anode only when a layer of lead dioxide has been laid down (32). After anodization, the electrode should not be left in contact with sulfate ions to avoid losses by reductive processes (Reaction R17) and should be used as soon as possible (26).

Some authors (37,38) have postulated that a shortcoming of the preparation of PbO_2 by anodization of Pb is that a solid phase reaction occurs between the PbO_2 and the underlying Pb to produce the less conductive PbO,

$$PbO_2 + Pb \rightleftarrows 2\ PbO \qquad [R19]$$

However, another study (39) reports that the only products of the anodization of lead in H_2SO_4 observed by x-ray diffraction, were α-PbO_2, β-PbO_2 and $PbSO_4$, but no PbO was detected, even after several weeks of storage of the electrode in the dry state. In the same study a mechanism is proposed for the anodization of lead. First, $PbSO_4$ is formed from Pb at the Pb/$PbSO_4$ potential, and later when the potential rises to the oxygen overpotential value, the $PbSO_4$ film transforms to β-PbO_2 and the underlying grid metal is converted directly to α-PbO_2.

It has been reported (36) that anodized lead can not tolerate the presence of chloride ions which cause it to disintegrate.

b) Electrodeposition. There are several methods for the electrodeposition of PbO_2 on inert metals from electrolytes containing lead. Some of the methods are summarized in reference (32).

PbO_2 has been deposited on nickel, tantalum, platinum, carbon, or graphite. Most other metals are unsuitable because of their inherently easy oxidation (26). Several types of electrolytes have been used for the deposition of PbO_2, and of these, lead nitrate has been found to give

the best deposits (40).

The largest producers of commercial electrodeposited lead dioxide anodes in the world are Pacific Engineering and Production Co. of Nevada and Sanwa Chemical Co. Ltd., of Tokyo, Japan.

Since the breakthrough by Pacific with a lead dioxide coated graphite anode, the greatest interest for PbO_2 formation has been shown in the electrodeposition process (36). The electrodeposition on graphite uses a lead nitrate electrolyte in acid media as described by Gibson (41).

The tetragonal β-PbO_2 is the form found in the commercial anodes produced from acid lead nitrate baths. The α-form is less common and can be deposited from alkaline solutions (26,36).

Unlike the anodized lead, the electrodeposited PbO_2 can operate effectively in chloride concentrations close to saturation. In fact the lead dioxide anodes produced by Pacific and Sanwa Co. are in use for perchlorate manufacture.

CHAPTER 3

OBJECTIVES

The aim of this work was to study the electrochemical oxidation of phenol for waste treatment applications. A packed bed anode was selected because it provides larger electrode surface areas per unit cell volume compared to a simple flat plate electrode. This is particularly important where dilute solutions are to be treated.

The research reported here includes the design and construction of equipment to carry out the process and an experimental study of the effect of important operating variables. These variables include type of lead dioxide anode (anodized lead versus electrodeposited lead dioxide), cell configuration (divided or undivided cell), type of ion-selective membrane (anionic or cationic), current applied, pH of the electrolyte, conductivity of the electrolyte, phenol concentration, flow-rate, and particle size. Lead dioxide was selected as the anode material to carry out this study for the reasons given in Chapter 2.

The performance of anodized lead and electrodeposited lead dioxide is compared in terms of phenol oxidation but also some tests were made to compare them in terms of corrosion resistance.

The use of a divided or undivided cell is of importance, since it may completely change the reaction mechanism for the further oxidation of intermediates. There is little information in the literature on such effects.

The electrolytes to be used for the oxidation of phenol consist of mixtures of Na_2SO_4 and H_2SO_4 or Na_2SO_4 and NaOH, to be able to vary independently pH and conductivity of the electrolytes.

From the point of view of waste treatment, it is of interest to determine what fraction of the phenol is converted to carbon dioxide, or how much organic carbon remains in solution after the electrochemical treatment. Therefore, the effect of the important variables is reported not only in terms of phenol oxidation but also on the total organic carbon (T.O.C.) oxidation. In the reviewed literature no T.O.C. analyses have been reported. In some cases chemical oxygen demand (C.O.D.) have been reported. But this is not an adequate technique of analysis in the case of aromatic compounds (42).

Relatively low phenol concentrations are used in this study (up to 1100 mg/l) in order to investigate the process until practically total phenol oxidation is achieved for the range of operating conditions of the experiments.

A batch-recirculation system was selected as the operating mode to study the effect of some of the variables. Once the system was better understood and controlled, some experiments were performed in the continuous mode.

Finally, the experimental fractional conversions of phenol are compared with the mass transfer model for a batch recirculation operation, and a simplified model including electrochemical reaction control is presented in order to analyze the data from the continuous experiments and compare the mass transfer and electrochemical reaction resistances.

CHAPTER 4

EXPERIMENTAL APPARATUS AND METHODS

4.1 Apparatus

4.1.1 Cell design

The electrolytic cell consists of a stack of elements arranged in series and compressed by a clamp mechanism. This flexible design is used because it permits the assembly of different arrangements (divided or undivided cell) and simplifies work with electrode materials.

a) Divided cell

A side view of the divided cell arrangement is shown in Fig. 4. Basically, the cell consists of two flat plates, the anode and cathode current feeders, which are in contact with the anodic and cathodic packings. Both packings are contained in 3 mm thick slotted neoprene gaskets and are separated from each other by an ion-selective membrane which prevents the mixing of the anolyte and catholyte. The cathodic packing is used to prevent the membrane from sagging due to the weight of the anodic packing.

The anolyte and catholyte inlets are located at the bottom of the cell and the outlets at the top, to facilitate the exit of the gases that will be produced during the electrolysis. Two different kinds of lead dioxide anode plates are used in this study: anodized lead sheet and electrodeposited lead dioxide on graphite plate.

In the case of the anodized lead electrode the current feeder plate

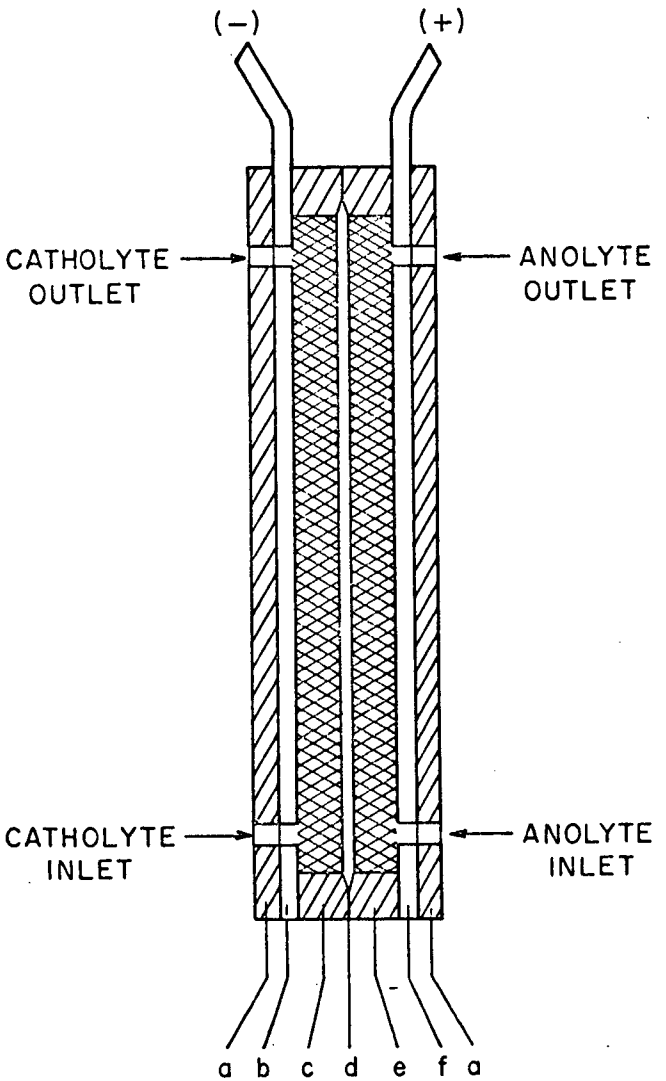

Legend

a = 1.6 mm thick neoprene insulator

b = 1.6 mm thick cathodic feeder plate (s.s. 316 plate)

c = 3 mm thick slotted neoprene gasket containing cathodic packing

d = ion selective membrane against protective plastic screen (variable thickness)

e = 3 mm thick slotted neoprene gasket containing anodic packing

f = anodic current feeder:
3 mm thick lead plate, or
lead dioxide coated graphite plate
3 cm thick

Fig. 4. Side view of the general divided-cell arrangement. (no scale)

was cut from a 0.3 cm thick lead sheet. The detailed front and side views of the anode chamber when using such electrode are shown in Fig. 5. A neoprene gasket determines the cross sectional area of the feeder plate that will be transporting the current. The side view shows that an extra stainless steel plate is used mainly to facilitate the welding of the inlet and outlet connectors to the cell and also to give more strength to the lead sheet. The front and side views of the cathode chamber are the same as the anode chamber, except that the thickness of the s.s. 316 cathode feeder was 0.16 cm.

The electrodeposited lead dioxide on graphite plate was obtained from Pacific Engineering Co. The total thickness of the plate is 3 cm and the thickness of the lead dioxide coating on each side of the graphite is 0.2 cm. Some modifications had to be made to the original commercial electrode to adapt it to the cell design being used. The final front and side views of the electrodedeposited PbO_2 anode are shown in Fig. 6. To avoid possible cracking of the PbO_2 coating, the electrode was left with its original width of 15 cm.

A modification had to be made in order to introduce the electrolyte flow through the graphite coated plate. A detail of the connection adapted is shown in Fig. 7. The electrolyte never comes in contact with the graphite base plate because the nylon connection was insulated by means of a neoprene washer. This type of connection prevents corrosion of the graphite base and eventual deterioration of the lead dioxide layer.

Some fundamental specifications of the different elements of the cell are given in Table 4. The dimensions of the anode and cathode chambers were never changed, but different sizes of anodic packings were used.

The cathodic packing consisted of several stainless steel-304 screens

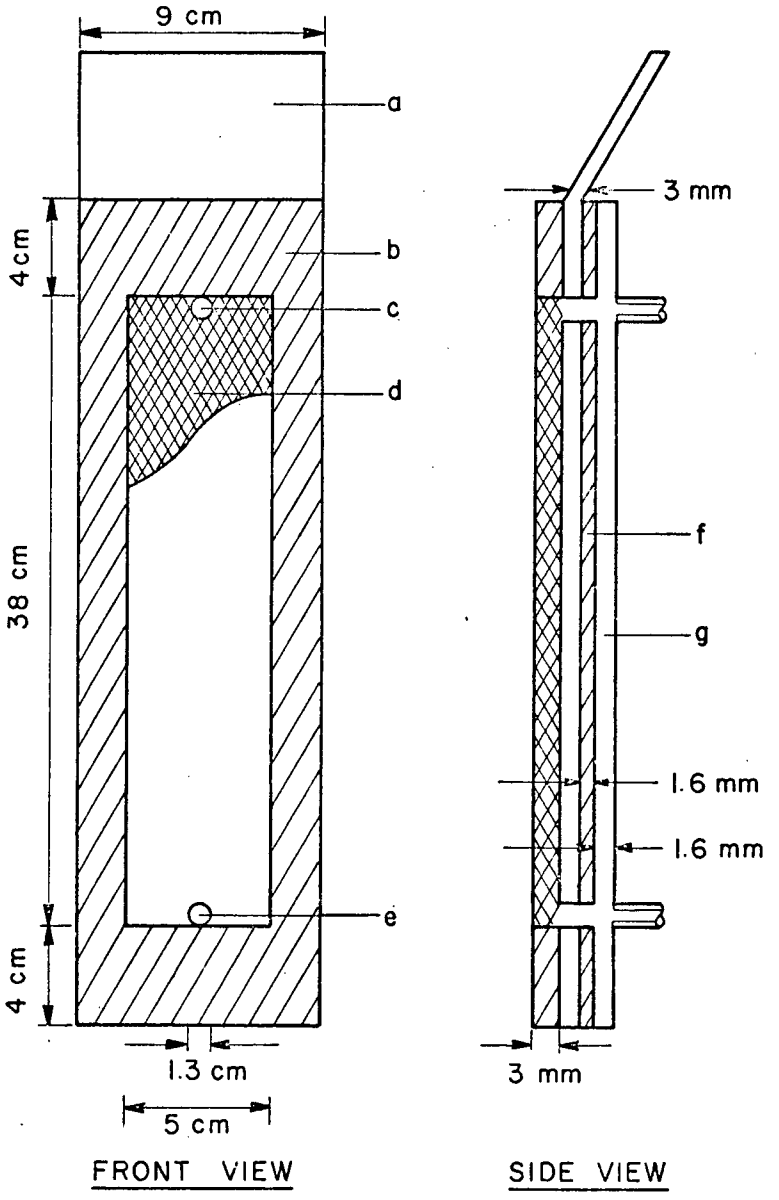

Legend

a = lead sheet anode feeder

b = slotted neoprene gasket

c = electrolyte outlet

d = anode packing (lead shot)

e = electrolyte inlet

f = neoprene insulator

g = stainless steel 316 plate (where connectors are welded)

Fig. 5. Front and side views of the anode chamber for the anodized lead electrode. (no scale).

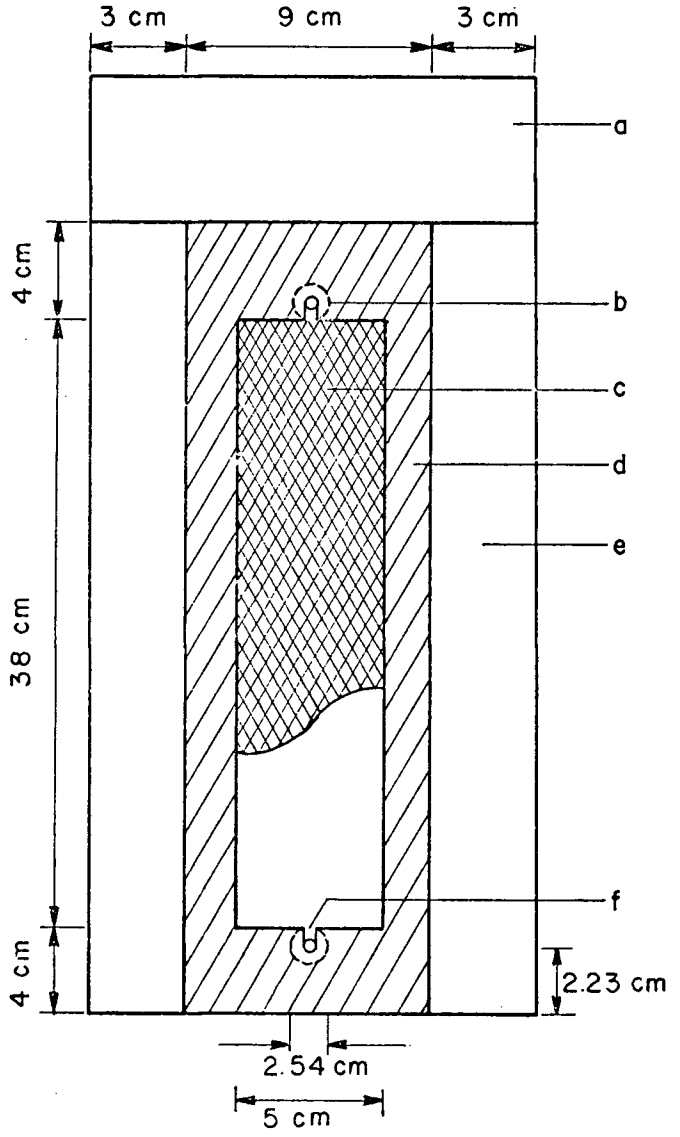

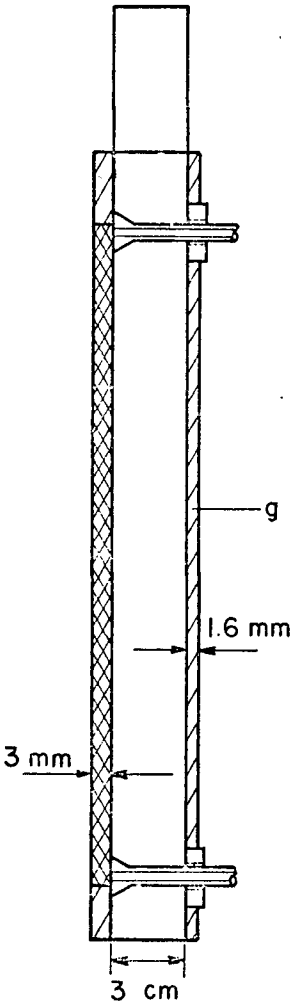

Legend

a = uncoated graphite section of the anode feeder

b = electrolyte outlet

c = anode packing

d = slotted neoprene gasket

e = electrodeposited PbO_2 section of the feeder plate

f = electrolyte inlet

g = neoprene insulator

Fig. 6. Front and side views of the anode chamber for the electrodeposited PbO_2 electrode. (no scale)

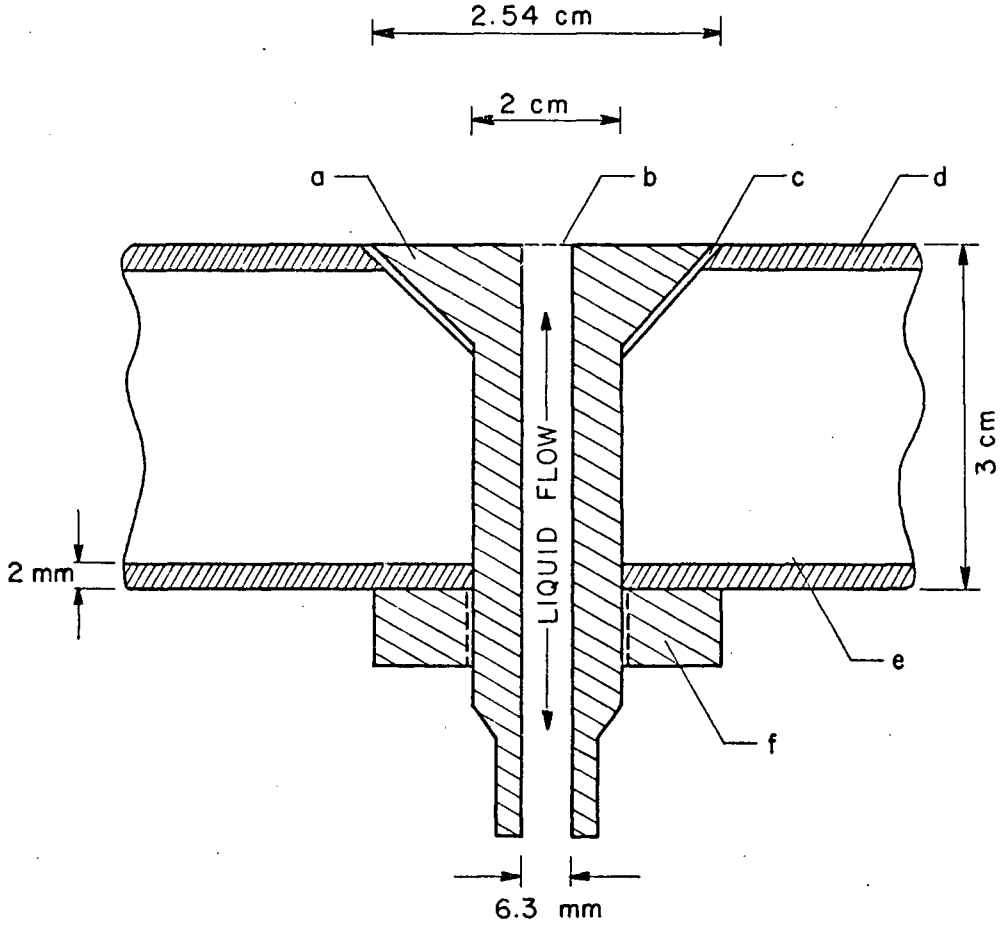

Legend

a = nylon connection

b = stainless steel mesh

c = neoprene washer

d = lead dioxide layer

e = graphite base plate

f = compressing nut (threaded)

Fig. 7. Detail of the inlet or outlet connection adapted on the electrodeposited PbO_2 on graphite anode. (no scale)

TABLE 4

FUNDAMENTAL SPECIFICATIONS OF THE ELECTROLYTIC CELL

Dimensions of the anode and cathode chambers:	
Length	= 38 cm
Width	= 5 cm
Thickness	= 3 mm
Anodic packings:	Particle size (mm)
lead shot (to anodize)	2
electrodeposited lead dioxide	1.7-2.00
	0.7-1.1
Cathodic packing:	
stainless steel-304 screens (20 × 20 mesh)	
cross sectional area of the screens (38 × 5) cm^2	
Membranes:	
cationic:	IONAC MC 3142
	IONAC MC 3470
	NAFION 127
anionic:	IONAC MA 3475
Protective screens:	
saran	
polypropylene	

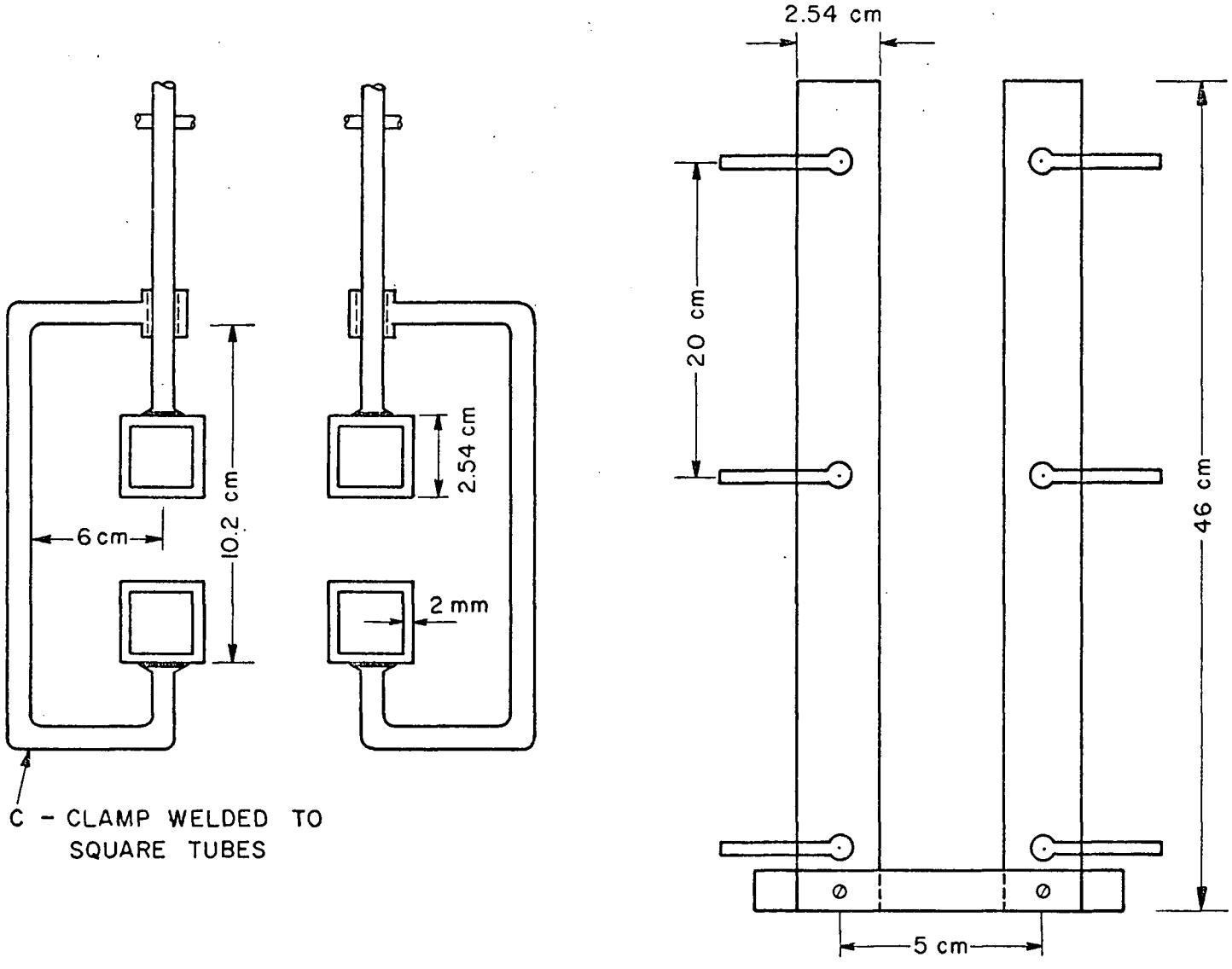

Fig. 8. Detail of the mechanism used to hold the cell. (no scale)

(20 mesh) cut to the size of the cathode chamber (5 × 38 cm^2) and joined so that the total thickness of the packing was 0.3 cm. The different ion selective membranes tested in this study are listed in Table 4, along with the protective plastic screens. The properties and characteristics of these materials as supplied by the manufacturers are given in Appendix 1.

A detail of the mechanism used to compress the various parts of the cell is given in Fig. 8. It consists of four mild steel square tubes which are welded to six C-clamps (Jorgensen, Style 81). The cell is introduced through the upper part of the press mechanism, and once the C-clamp screws are tightened, the four square tubes compress the neoprene gaskets, providing an effective seal for the cell. This versatile press design permits variations in the thickness and width of the cell materials within a certain range, and also can be rapidly opened and closed.

b) Undivided cell

A side view of the undivided cell arrangement is similar to that represented in Fig. 4, except that the ion selective membrane and the cathodic packing are eliminated and the inlet and outlet of the cathode side are closed by using a cathode feeder plate without holes. In this case, only a plastic screen (saran or polypropylene) is placed between the anodic bed and the cathodic feeder plate.

4.1.2 Flow diagram of the apparatus

Figure 9 is the schematic flow diagram. Equipment specifications are given in Appendix 1.

Two main flow circuits exist. At the right hand side of the electrolytic cell is the anolyte flow circuit. Pump PU-1 delivers the anolyte

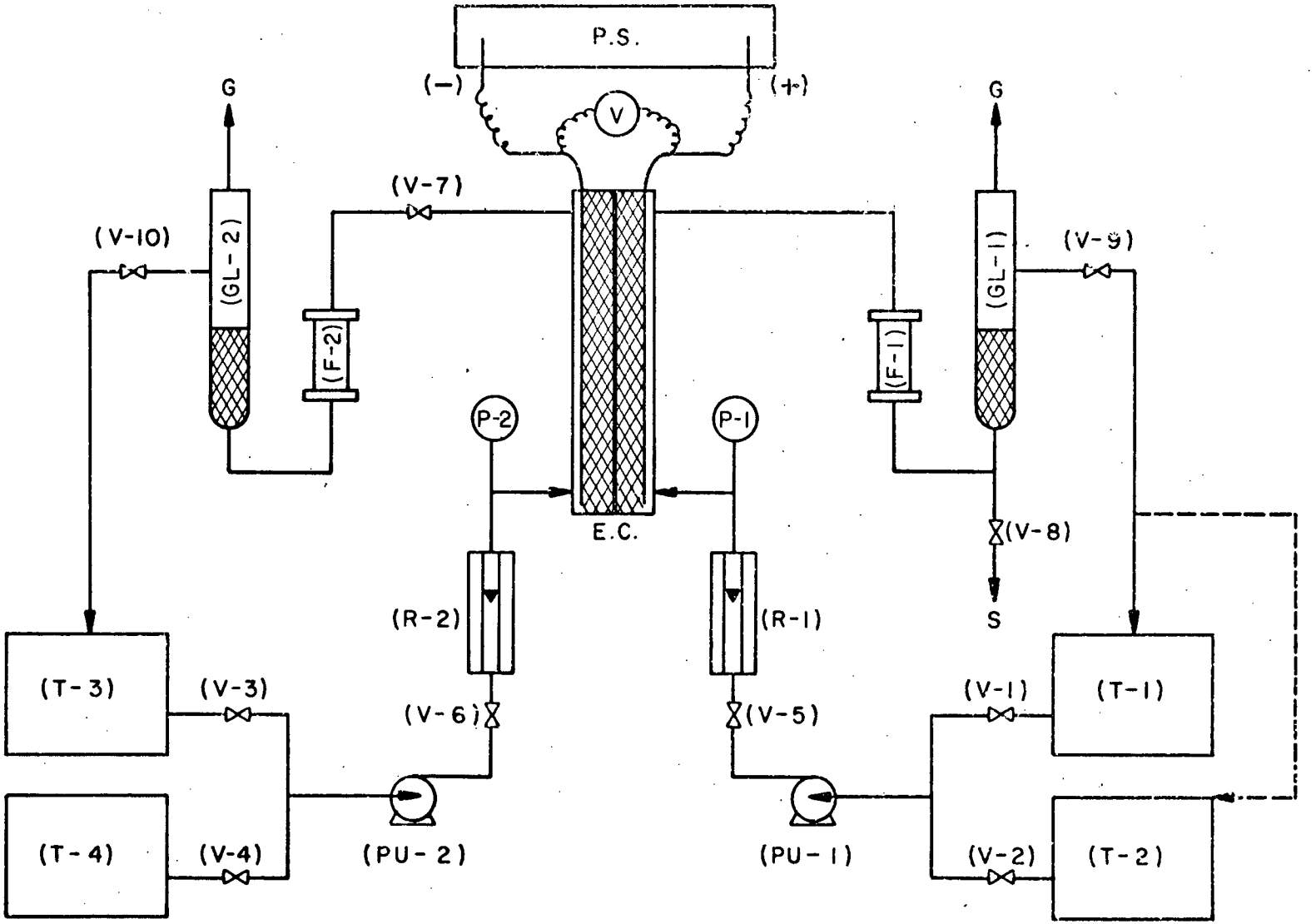

Fig. 9. Flow diagram of the apparatus.

Legend for Fig. 9.

(P.S.) Power supply (D.C.)

(V) Voltmeter

(E.C.) Electrolytic cell

(T-1) Anolyte tank (contains phenol solution)

(T-2) Anodization tank

(T-3) Catholyte tank

(T-4) Washing tank

(PU-1) Anolyte pump

(PU-2) Catholyte pump

(R-1) Anolyte rotameter

(R-2) Catholyte rotameter

(P-1) Anolyte pressure and temperature gauges

(P-2) Catholyte pressure and temperature gauges

(F-1) Anolyte filter

(F-2) Catholyte filter

(GL-1) Gas-liquid separator for the anolyte

(GL-2) Gas-liquid separator for the catholyte

(V-1) Anolyte tank shut-off valve

(V-2) Anodization tank shut-off valve

(V-3) Catholyte tank shut-off valve

(V-4) Washing tank shut-off valve

(V-5) Anolyte flow control valve

(V-6) Catholyte flow control valve

(V-7) Cathode chamber pressure-control valve

(V-8) Liquid sample valve

(V-9) Liquid level control valve in GL-1

(V-10) Liquid level control valve in GL-2

from tanks T-1 or T-2 to the anode chamber. The liquid flow rate is controlled by adjusting valve V-5 and is measured with rotameter R-1. Pressure and temperature of the anolyte at the entrance of the anolyte chamber are measured in P-1.

Filter F-1 is located at the outlet of the anode chamber, to collect small particles that might be withdrawn from the cell, thus protecting the pump from damage. This glass-wool filter serves also to agglomerate small gas bubbles produced in the electrolysis into bigger ones to facilitate the gas liquid separation in GL-1.

The gas-liquid mixture enters at the bottom of the gas-liquid separator GL-1 in which a bed of glass beads provides extra agglomeration surface for the gas bubbles. Valve V-9 controls the liquid level at the outlet of GL-1, to ensure that gas bubbles are not carried out with the liquid flow. This would result in a progressive accumulation of gas in the anolyte line which may affect the results of the experiments. The gas is then released at the top of GL-1 and the liquid flows towards the feed tanks (T-1 or T-2) to be recycled to the cell. The dotted line represents the recycle line when the anodization tank T-2 is in use. Valve V-8 serves to collect liquid samples after passage through the cell.

The flow diagram corresponding to the catholyte circuit is basically analogous to the anolyte circuit above described. Valve V-7 serves to control the pressure in the catholyte chamber, providing pressure equalization at both sides of the membrane, thus avoiding too high pressure differences between the anolyte and catholyte chambers that may result in membrane breaking.

When the cell was assembled with only one chamber, only the anolyte circuit was used. The catholyte circuit was eliminated by closing the

catholyte inlet and outlet to the cell.

The cell was powered by a 1 KVA D.C. power supply (Appendix 1). The cell current was read from the power-supply meter, and the voltage drop across the electrodes was measured independently.

4.2 Experimental methods

4.2.1 Batch experiments

The experimental procedure is described for the more complicated two chambers-cell operation, since the one-chamber cell operation can be considered as a particular case of the first.

a) Anodization process

Before each experiment, the lead electrode was anodized by electrolysis in 20% H_2SO_4 (43), to ensure that the anode was equally active before every run.

Valves V-1 and V-4 were shut off and tanks T-2 and T-3 were filled with a 20% H_2SO_4 solution. The D.C. power supply was turned on. Valves V-2 and V-3 were then opened and both pumps, PU-1 and PU-2, were activated at the same time. About 2 ℓ of solution coming out from the gas-liquid separators was withdrawn at each side to purge the system before the anolyte and catholyte flows were recycled to tanks T-2 and T-3 respectively. Five ℓ of H_2SO_4 solution remained in each tank for the anodization process. Immediately the current was adjusted to 10 A (c.d. $\simeq$ 526.3 A/m^2) and the liquid pressures in both chambers were equalized by adjusting valve V-7.

When lead was to be anodized for the first time, a 12 h anodization time was allowed, but for successive experiments the standard anodization time was 1 h. (Choice of the anodization time was justified experimentally, as shown in Chapter 5.) After anodization, both pumps were

simultaneously turned off and valves V-2 and V-3 were closed. Then, tanks T-1 and T-4 were filled with distilled water and connected to pumps PU-1 and PU-2 respectively. The cell was washed until the current dropped practically to zero and the potential difference through the cell increased indicating that essentially no electrolyte was contained in the cell.

b) Phenol electrochemical oxidation process

After the cell was thoroughly washed, 8 ℓ of anolyte solution were prepared in tank T-1. The concentration of phenol, the pH and the conductivity of the anolyte were set to the desired levels by adding the necessary volumes of stock solutions of phenol, NaOH or H_2SO_4, and Na_2SO_4, which had been previously prepared. The tank was well agitated before the initial sample was taken, and pH and conductivity were measured and readjusted if necessary.

An equal volume of catholyte solution was then prepared in tank T-3 and conductivity and pH were measured. Anolyte and catholyte data are recorded for each experiment in Appendix 2.

Tanks T-1 and T-3 were connected to the corresponding pumps and flow rates of anolyte and catholyte were set by adjusting valves V-5 and V-6 respectively. Pressure equalization was provided adjusting valve V-7. Immediately the current was set at the desired value.

As the operating conditions were being set 3 ℓ of the solutions coming out from the gas liquid separators were discarded in order to purge the system and also to provide some time for flows and current stabilization. At the moment the liquids were recycled to tanks T-1 and T-3, 5 ℓ of electrolyte remained in each tank. The electrolysis time was measured from the moment when the anolyte was recycled to tank T-1.

Thirty ml samples were taken in intervals of 15 min for phenol analysis by opening valve V-8. When the usual electrolysis time of 2 h was completed, the cell was washed with distilled water while the current was still flowing to avoid reduction of the PbO_2 anode.

The samples were first analyzed for phenol and T.O.C. and later pH and conductivity were measured, to avoid possible contamination of the samples when introducing the pH and conductivity probes.

4.2.2 Continuous experiments

Some experiments were carried out in the continuous mode (without recycle), to test the effect of varying flow on phenol oxidation in a single pass through the undivided cell.

The electrode pretreatment or anodization was carried out by the standard method of electrolysis with 20% H_2SO_4 at 10 A for 1 h. In this case the phenol solution to be treated was prepared in the same manner described previously but the total volume of the electrolyte in tank T-1 was 20 ℓ.

After the initial electrolyte sample was taken, and conductivity and pH were measured and adjusted to the desired values, the D.C. power supply was turned on, and the electrolyte was fed to the cell. A liquid flow rate was then fixed by adjusting valve V-5, and the desired current was set. Four ℓ of electrolyte were withdrawn at the outlet of GL-1 before the first sample was taken, to ensure stabilization of the process. A different flow rate was then set up and the same procedure repeated, until the liquid flow rate range provided by rotameter R-1 was covered.

In Appendix 2 the experiments are divided by groups according to cell assembly and operating mode.

4.3 Analytic techniques

The samples taken at the outlet of the cell were analyzed for concentrations of phenol, total organic carbon, and in some cases, lead.

4.3.1 Phenol analysis

Phenol concentrations in the samples were determined by gas chromatography using a flame ionization detector. The analytic equipment specifications and operating conditions used are given in Appendix 1.

Standard phenol solutions ranging from 0-116 mg/l were prepared by pipetting from the same phenol solution used to prepare the electrolyte for the experiments. Copper sulfate was added to the standards to an approximate concentration of 1 g/l to preserve them from possible biological degradation (42).

Phenol peaks were thin enough so that the estimation of the area below the peak was not necessary, and peak heights could be used. Before the analysis of the samples from each run, the phenol standards were always injected and the calibration curve of peak heights vs phenol concentration was constructed.

Standards and samples were injected until the variation in peak height was not more than 2-3%. This means that when the recorder full scale corresponded to about 100 mg/l the maximum allowed variation represented ± 2 mg/l, and the recorder detectability was 1 mg/l/division.

No peaks other than the solvent and phenol peaks were observed, in other words no interference of the phenol oxidation products was detected in the G.C. analysis. Phenol detention time was approximately 30 seconds.

All the samples were analyzed on the day of the experiment, even though it was shown that the concentration of phenol in the sample did

not vary after one week of storage.

For those experiments performed at phenol concentrations higher than 100 mg/l the samples were diluted by the necessary factor in order to work with the same standards and detectability.

4.3.2 Total organic carbon analysis

All total organic carbon analyses were carried out on a Beckman analyzer in the Civil Engineering Department. Basically, the total organic carbon analyzer consists of two furnaces: the total carbon furnace and the inorganic carbon furnace.

The total carbon furnace operates at a temperature of 1000°C to convert all the carbon contained in the sample to carbon dioxide. The inorganic carbon furnace operates at 150°C to convert only the inorganic carbon contained in the sample to carbon dioxide. The amount of carbon dioxide thus produced is detected in an infrared analyzer (44).

The total organic carbon (T.O.C.) in the sample is calculated by subtracting the inorganic carbon from the total carbon, therefore two different calibrations are required, one for each channel. The standards used for the total carbon analysis were the same phenol standards used to calibrate the chromatograph. Carbon content ranged between 0-90 mg/l. Before the analysis of the samples from each run, the total carbon standards were injected and the calibration curve peak height vs mg/l carbon constructed. Variations in peak height in successive injections of a certain sample never exceeded 2%.

The inorganic carbon standards were prepared from a stock solution of Na_2CO_3 and $NaHCO_3$ containing 1000 mg/l of carbon, so that the inorganic carbon in the standards also ranged between 0-90 mg/l. After the calibration curve of mg/l inorganic carbon vs peak height was constructed,

the samples were injected in the inorganic channel. Again maximum variations in peak height for a same sample were of the order of 2%.

Knowing that phenol contains 0.7657 g C/g phenol, it is possible to compare the phenol concentration obtained by gas chromatography with the concentration calculated from the T.O.C. analysis, for the initial sample. Deviations between both analysis were usually in the range of 2-3% which gives confidence in the analytical results.

All the specifications and operating conditions of the T.O.C. analysis are given in Appendix 1. The phenol standards for T.C. analysis showed no alteration after one month of storage when compared with fresh standards, and the samples from one experiment did not show variation in the T.O.C. analysis after one week.

4.3.3 Lead analysis

To test electrode corrosion, the samples from some of the experiments were analyzed for lead using atomic absorption spectrophotometry.

Lead standards were prepared by diluting a stock solution containing 1000 mg/l of lead. The range of concentrations of the standards was chosen according to the lead content of the samples.

The specifications of the atomic absorption apparatus used and its operating conditions are given in Appendix 1.

CHAPTER 5

RESULTS AND DISCUSSION

5.1 Electrode materials

Some preliminary experiments were performed to test possible electrode materials before starting to investigate other variables affecting the process. Results are given in the table for each run in Appendix 2.

The anodized lead electrode was tested in experiments group No. 1. Runs 1-1 and 1-2 were carried out to test the effect of anodization time on T.O.C. removal. The results showed that 1 h and 12 h anodization times produced approximately the same % T.O.C. removed vs time. This indicates that 1 h anodization time is probably sufficient to coat the lead shot with a layer of PbO_2. After each of these runs the electrode showed a fairly uniform brown coating. It is probable that the coating is thicker for the longer anodization time.

After the anodization period and while the cell was being washed with distilled water, the liquid at the outlet took on a brown colour as if some fine particles from the electrode surface were entering the water. Therefore it was considered necessary to test for lead concentration in solution. A series of tests were carried out to investigate what governed the presence of lead in the anolyte.

Experiments 1-4 to 1-8 were performed under different electrolyte concentrations and pHs. The results are summarized on p. 122. In all

these runs the concentration of lead in the anolyte tended to decrease with time, indicating that the corrosion rate is probably higher when the electrode first comes in contact with the solution. Also, the lead ions are able to pass to the catholyte chamber through the cation-membrane therefore reducing the lead content of the anolyte. (The pH changes in those runs occurred spontaneously as will be explained in the next section.)

In Run 1-4 the electrolyte (5 g/l NaOH) was recirculated through the cell without an applied current and it produced the highest maximum concentration of lead in solution (140 mg/l). Later this run was repeated, except that a potential difference was applied before the electrolyte was fed to the cell. The maximum amount of lead in solution was 2.7 mg/l. This observation is in agreement with the potential-pH diagram for lead which indicates that PbO_2 is thermodynamically stable at positive or anodic electrode potentials with respect to the normal hydrogen electrode. Runs 1-5 and 1-6 showed that at the same initial pH of 9.8 the maximum lead concentration was 4.2 mg/l when working at 30 g/l Na_2SO_4, and it was 1.7 mg/l when working with a 5 g/l Na_2SO_4 electrolyte.

At the same concentration of Na_2SO_4 (30 g/l) the amount of lead in solution was higher at higher initial pH (Runs 1-6, 1-7 and 1-8 respectively). An attempt was made to study the response of the anodized lead electrode under a 5 g/l NaCl electrolyte (Run 1-3). It was not possible to finish the experiment because the electrode coating began to dissolve rapidly, and as a result the anolyte pressure increased and the voltage drop decreased. When the cell was opened the electrode had lost its brown coating, showing the underlying grey lead, and the membrane was covered with a deposit of some lead compound.

The performances of anodized lead and electrodeposited PbO_2 can be compared from Runs 1-9 and 2-2 respectively. Both experiments were performed under the same experimental conditions, the same cationic membrane (IONAC MC-3470) and approximately equal voidage fraction (0.6). The results are represented in Fig. 10. The curve for % phenol oxidized vs time when using the electrodeposited PbO_2 electrode is above that curve corresponding to the anodized lead. The % T.O.C. removed vs time curves are practically coincidental for both electrodes, but the maximum concentration of lead in solution was about ten times higher in the case of the anodized lead.

Scanning electronmicrographs of the electrodeposited PbO_2 particles are shown in Fig. 11. Lead analyses are reported in many other experiments, (experiments Groups 2 and 3) where electrodeposited PbO_2 was used. In each case the maximum lead concentration was lower than 0.4 mg/1, and tended to zero towards the end of the run. The only exception was found in Run 2-3 where no current was applied and the lead concentration built up, reaching 2 mg/1 after 90 minutes.

Scanning electron micrographs of the anodized lead particles (Fig. 12) show that flaking of the PbO_2 film occurred. Once the electrode flakes are carried out from the cell they would dissolve more easily in the absence of the applied anodic potential.

The anodized lead electrode could become more resistant to corrosion after successive anodizations or after long periods of use. Also it is possible that its resistance to corrosion could be improved by anodizing the lead very slowly using more dilute H_2SO_4 solutions, lower current densities and longer anodization times. This might prevent the formation of cracks (where corrosion probably starts) that result from a

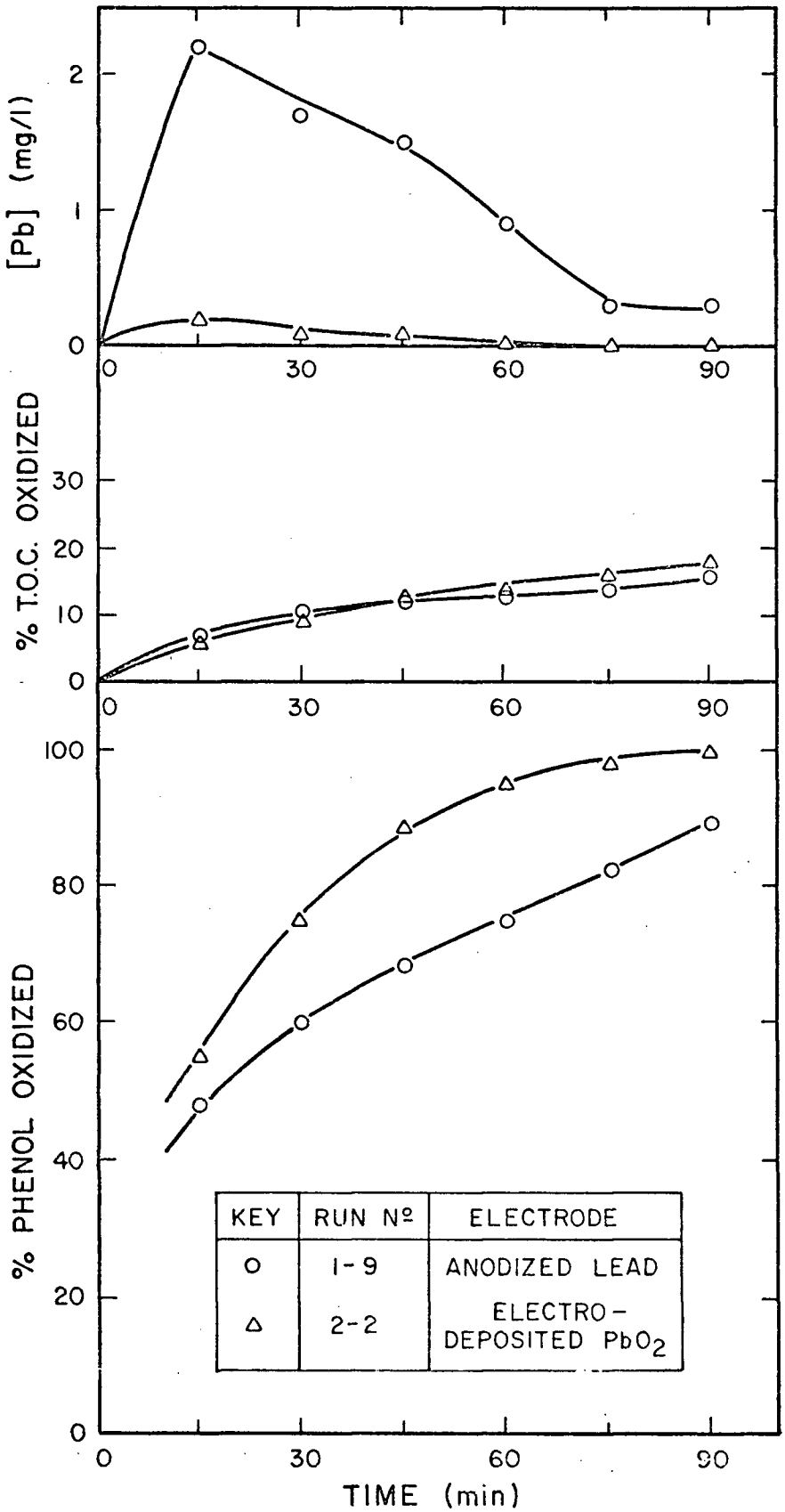

Fig. 10. Effect of type of lead dioxide electrode at 10 A and initial pH = 9.4 with IONAC MC-3470 membrane.

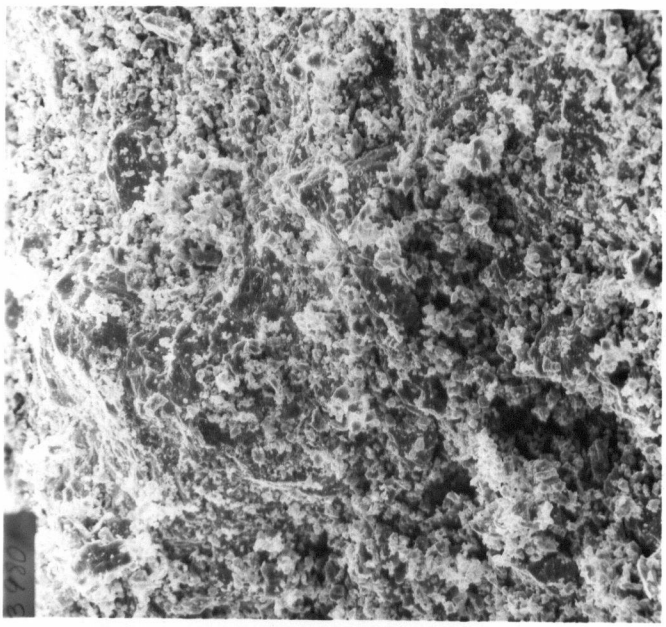

× 1000

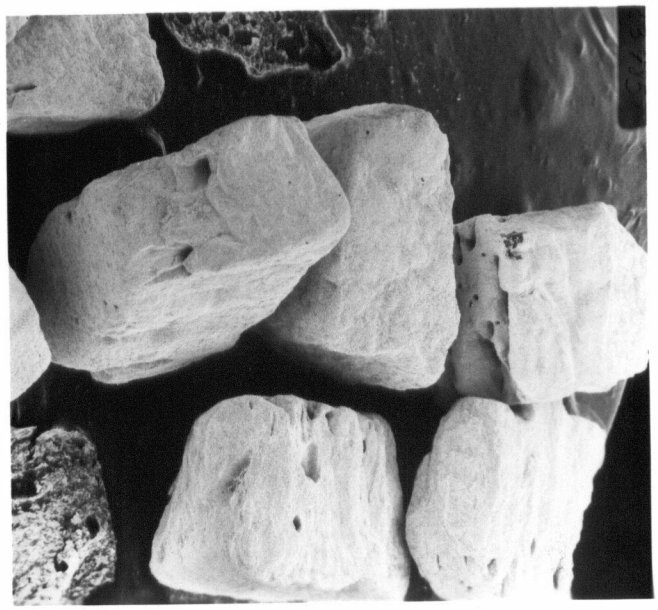

× 15

Fig. 11. Scanning electron-micrographs of the electrodeposited PbO_2 particles after use. (particle sizes between 1.7-2.00 mm)

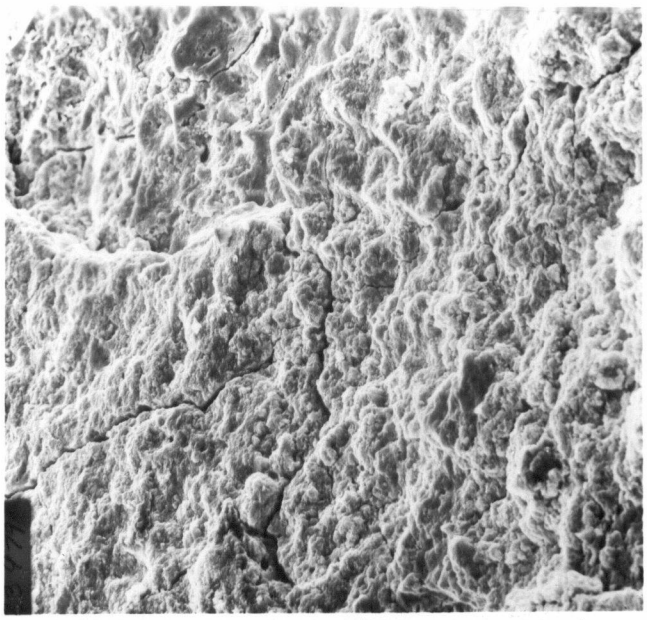

× 1000

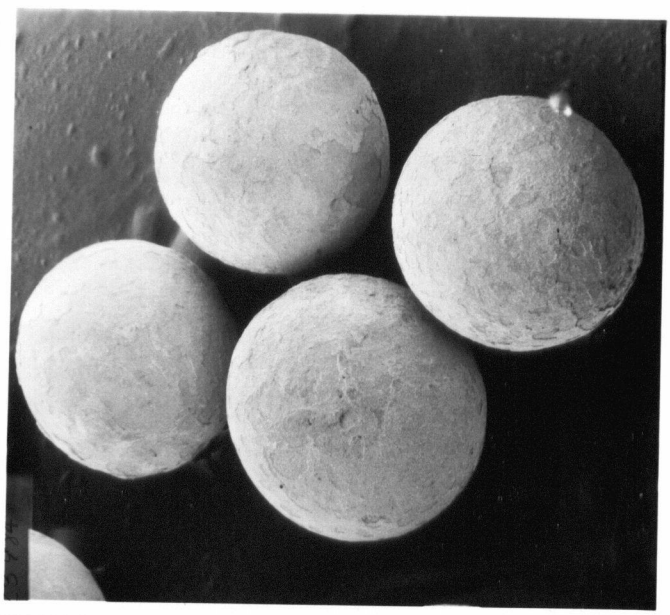

× 15

Fig. 12. Scanning electron-micrographs of the anodized lead particles, after use. (prepared from 2 mm lead shot)

perhaps too strong anodizing action.

An attempt was made to test a packed bed nickel electrode at pH = 12 and 10 A, but in two hours the voltage drop through the cell increased considerably and after opening the cell, it was observed that a precipitate was plugging the bed and covering the membrane.

Tungsten carbide (WC) particles were also tested at pH = 12 and 10 A. The anolyte took a grey colour indicating dissolution of the electrode and the total carbon test revealed increasing amount of carbon in solution.

From these preliminary tests it was concluded that the electrodeposited PbO_2 was the most convenient choice to carry out the remainder of the experiments because of its better corrosion resistance and its higher % phenol oxidation when compared to the anodized lead.

5.2 Effect of pH using the divided cell

Because of the lack of information in the literature about phenol electrooxidation in alkaline electrolytes, the effect of a basic pH range was investigated first using the divided cell. Before discussing the effect of pH on the electrooxidation of phenol, it is necessary to consider some important observations about the pH behaviour in the divided cell.

Using the cation membrane MC-3470 which is suitable for alkaline electrolytes, the anolyte phenol concentration was set at 100 mg/l and the pH was adjusted to 9.4. It was observed that after 15 min the pH of the sample at the outlet of the cell had dropped to about 3, when working at 10 A (Run 2-2, Fig. 13). Later, the same experimental conditions as in Run 2-2 were repeated but without phenol being present and

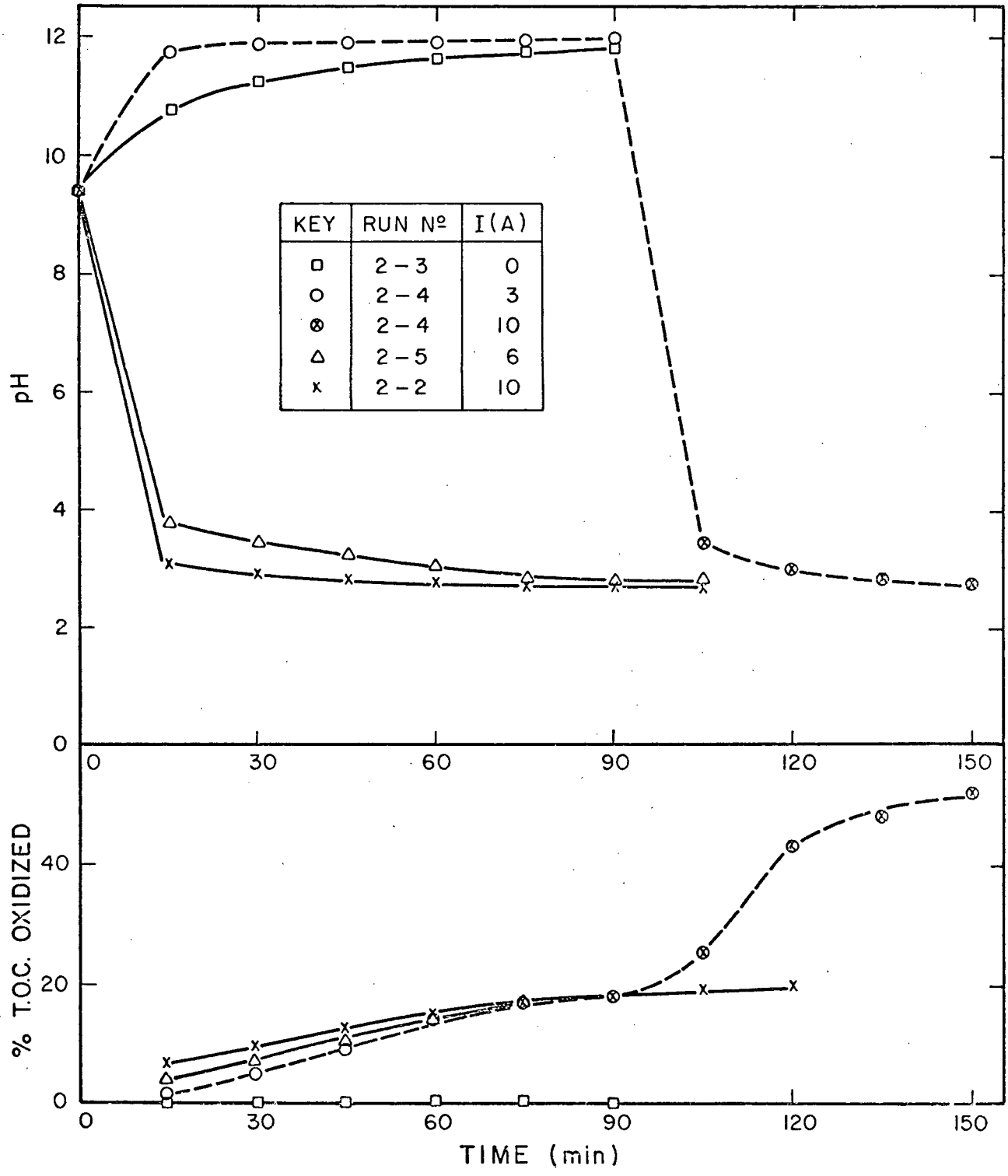

Fig. 13. Effect of current on pH and % T.O.C. oxidation with IONAC-MC3470 membrane

the same pH drop was observed. Thus, the pH drop appears to be due to side reactions of oxygen evolution, and not to production of an acid from phenol oxidation.

What probably happens is that the hydroxyl ions are discharged first at the electrode, and then the mechanism of oxygen evolution changes (Reactions R1 or R2) producing hydrogen ions. If the rate at which the hydrogen ions are produced is higher than the rate of transport through the membrane, the net effect is a progressive increase in the concentration of hydrogen ions, which would result in the observed pH drop. This would also explain why the electrolyte conductivity increases towards the end of the run and as a result the voltage drop through the cell decreases (Run 2-2).

If the side reactions of oxygen evolution are responsible for the observed pH behaviour, it follows that the pH response must be related to the current because the rate at which the side reactions occur will ultimately be determined by the current applied. The pH response was then compared at different currents (0, 3, 6, and 10 A) with all the other experimental conditions held constant. The pH vs time curves are also represented in Fig. 13. When working at 6 A (Run 2-5) the pH dropped from 9.4 to 3.7 in 15 min, showing the same tendency described previously for Run 2-2. A lower current of 3 A (Run 2-4) produced an unexpected result. In 15 min the pH of the sample at the outlet of the cell had increased from 9.4 to 11.7. The same behaviour was observed when the solution was recirculated without any current applied (Run 2-3).

Two possible explanations are proposed for this effect. Since the membrane used in these experiments was the cationic MC-3470, theoretically it only allows the transport of positive ions but as the ionic

selectivity is not 100%, it is possible that a certain amount of hydroxyl ions passed to the anolyte from the alkaline catholyte, therefore raising the pH. Another possibility is that the pH increase is associated with a lead dioxide reaction. This would explain why a potential difference was detected without an applied current (Run Table 2-3) and the lead concentration was building up during the run. In other words, the electrode may have behaved as in the lead battery where the PbO_2 reduces in the presence of sulphate ions generating a flow of current (Reaction R17).

In order to ensure that the different pH changes observed were associated with the applied current, during Run 2-4 the current was suddenly changed from 3 to 10 A, after 90 min and again the pH dropped from 11.8 to 3.8 during the next 15 min, following the same behaviour observed in Runs 2-2 and 2-5 (Fig. 13). The effect of pH-current changes on the rate of phenol oxidation is shown in Fig. 14.

When comparing the % T.O.C. removed in Runs 2-2, 2-4, and 2-5, it is observed that the three curves tended to a 17% T.O.C. removed in 90 min, but when the current was changed in Run 2-4 from 3 to 10 A, a higher percent of the carbon was oxidized in the interval from 90 to 120 min (Fig. 13). The most probable reason for this difference was the higher pH observed at 90 min in Run 2-4. This was the first indication of an enhancement of T.O.C. removal at high pH.

To investigate if there was any difference in the pH response when a different cation membrane was used, experiment 2-8 was carried out. Using the NAFION-127 membrane, starting at pH = 12 and 10 A the pH dropped even faster than in Run 2-2 (Fig. 15). After 15 min the pH had dropped from 12 to 2.

In Run 2-10 the pH was kept in the basic range for a longer period

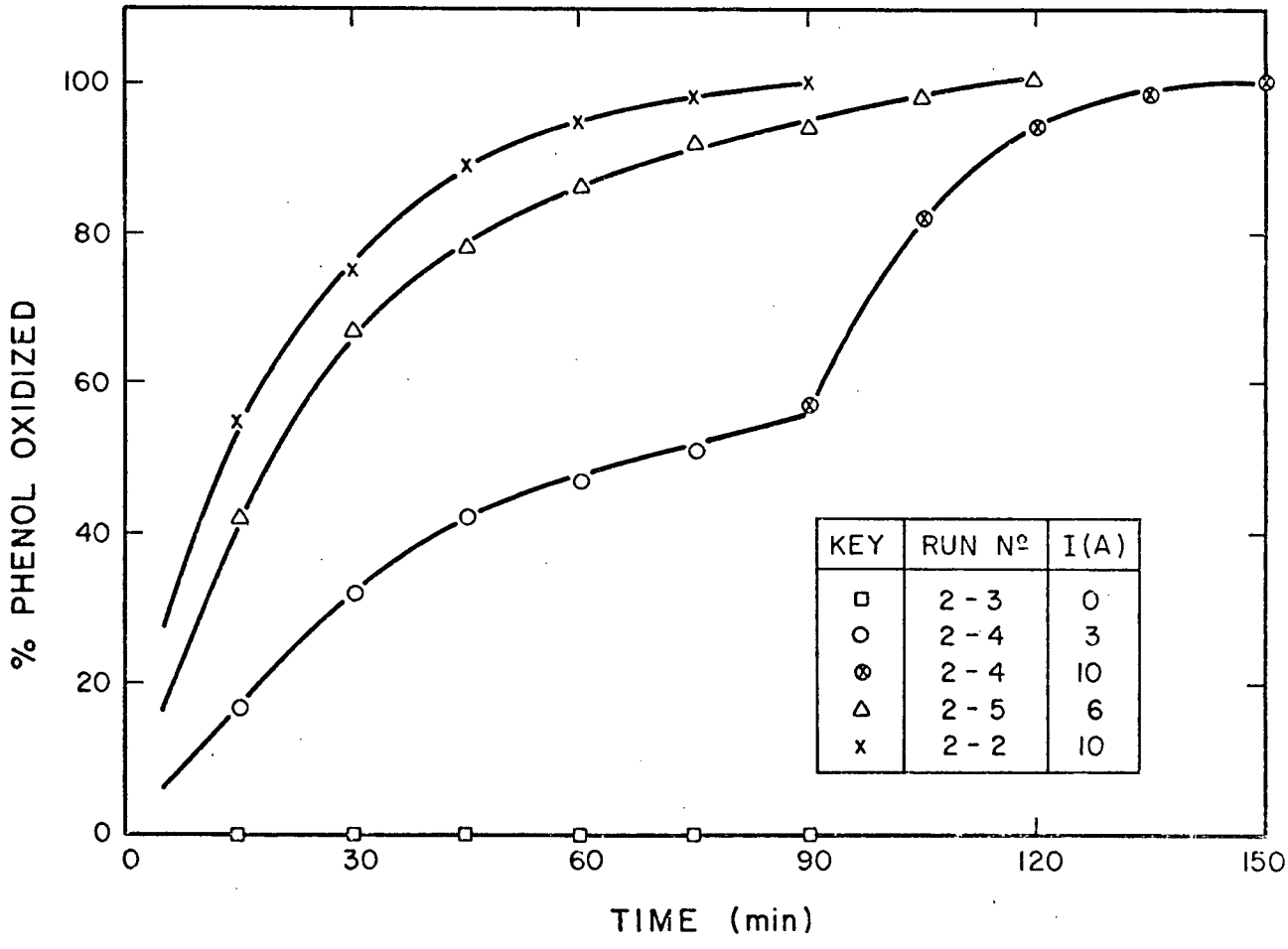

Fig. 14. Effect of current on % phenol oxidation at initial pH = 9.4 with IONAC MC-3470 membrane.

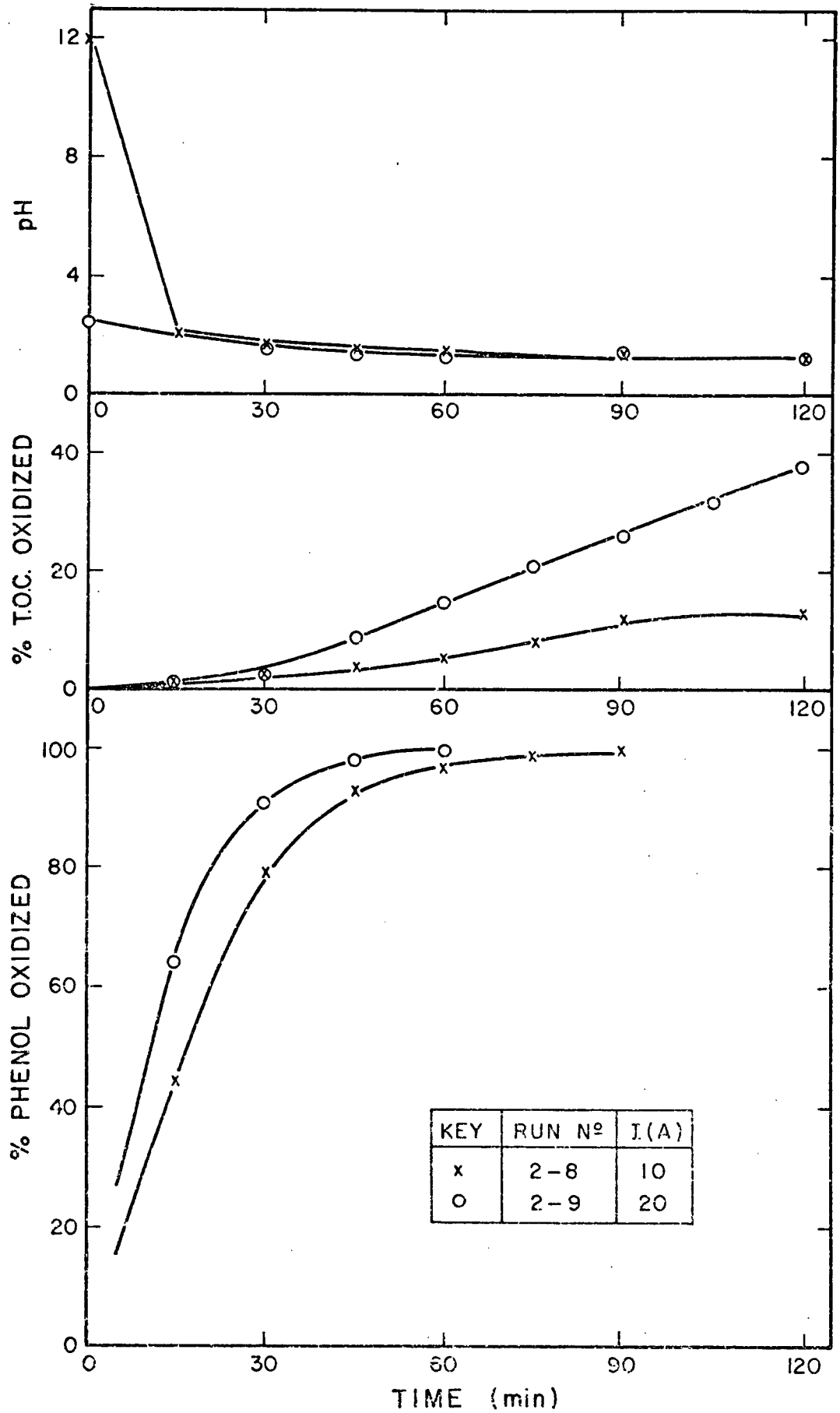

Fig. 15. Effect of current on pH, % T.O.C. oxidation and % phenol oxidation with NAFION-127 membrane.

of time, by starting at a pH of 12.8. As shown in Fig. 16 the pH started to drop after 45 min, and went from 12.2 to a value of 2.2 in the next 15 minutes.

In the same figure, it can also be observed that the oxidation of phenol is severely limited by a high pH. At 15 min and pH = 12.7 (Run 2-10) only a 10% of the phenol had been oxidized, whereas at pH ≃ 2, 65% of the phenol had already been oxidized after the same time (Run 2-9). On the other hand, the curve for % T.O.C. removed vs time corresponding to the high pH run is above the % T.O.C. curve corresponding to the low pH run.

It should be noted that the pH is measured at the outlet of the cell, and when the pH drop is recorded there must be a pH profile within the cell (higher pH at the entrance), and a variable pH in the recirculation tank. This makes the interpretation of the results more difficult, but still there is a definite enhancement in T.O.C. removal at high pH.

These experiments indicated that an optimum pH sequence would be a low pH at the beginning of the run, favouring phenol oxidation, and a high pH at the end, favouring T.O.C. removal. This idea suggested that an anion selective membrane could provide precisely such an optimum pH sequence. If the transport of hydroxyl ions from the NaOH catholyte, and through the membrane were sufficient to produce a pH increase from about 2 to 12, during the course of a run, at a given current, an optimum type of run could be possible.

With this objective, several preliminary tests were performed with the anionic membrane IONAC MA-3475. In Fig. 17, Run 2-11, it is observed that the desired increase in pH indeed occurs, and at 30 minutes 90% of

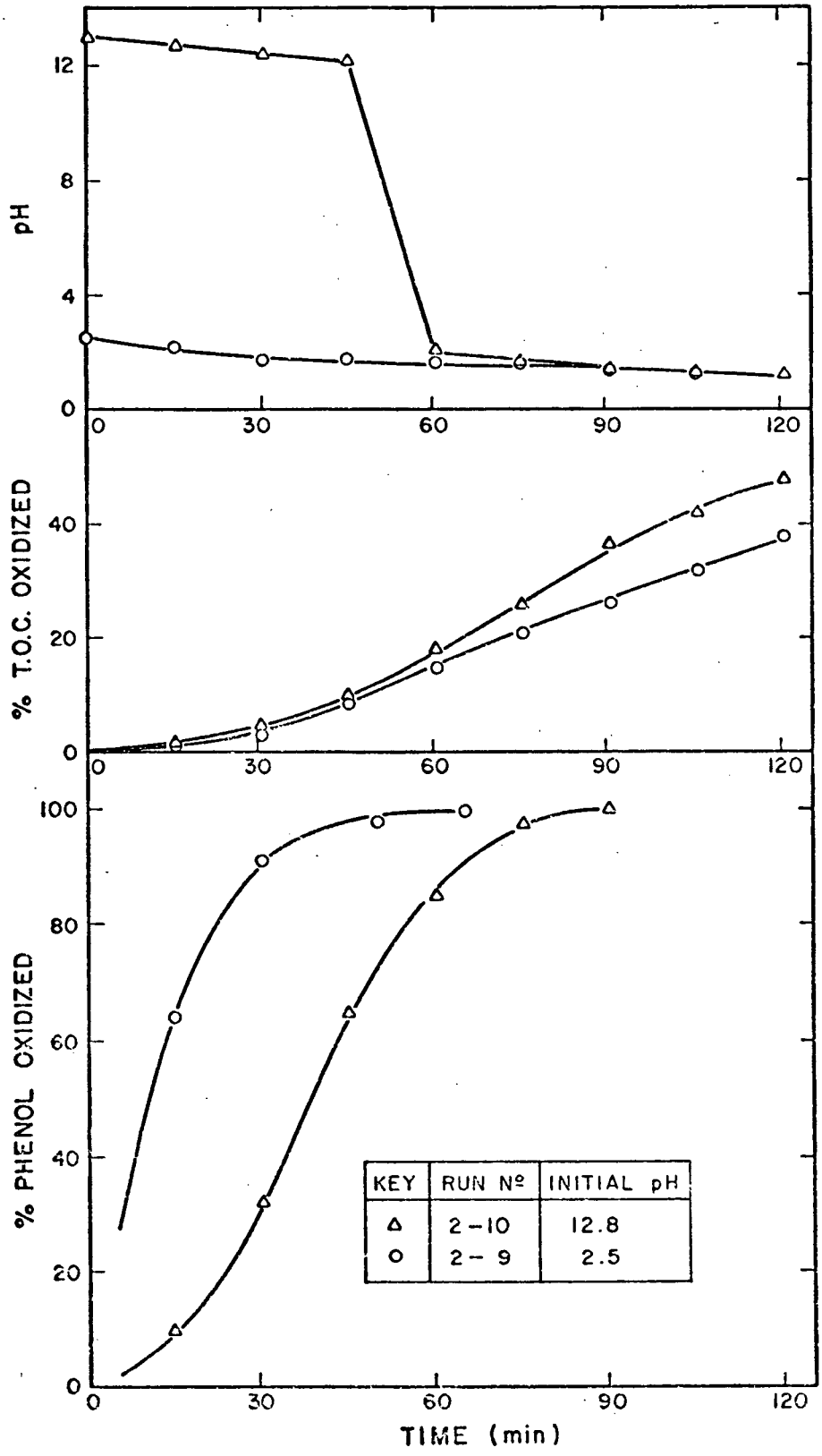

Fig. 16. Effect of pH on % T.O.C. and % phenol oxidation at 20 A with NAFION 127 membrane.

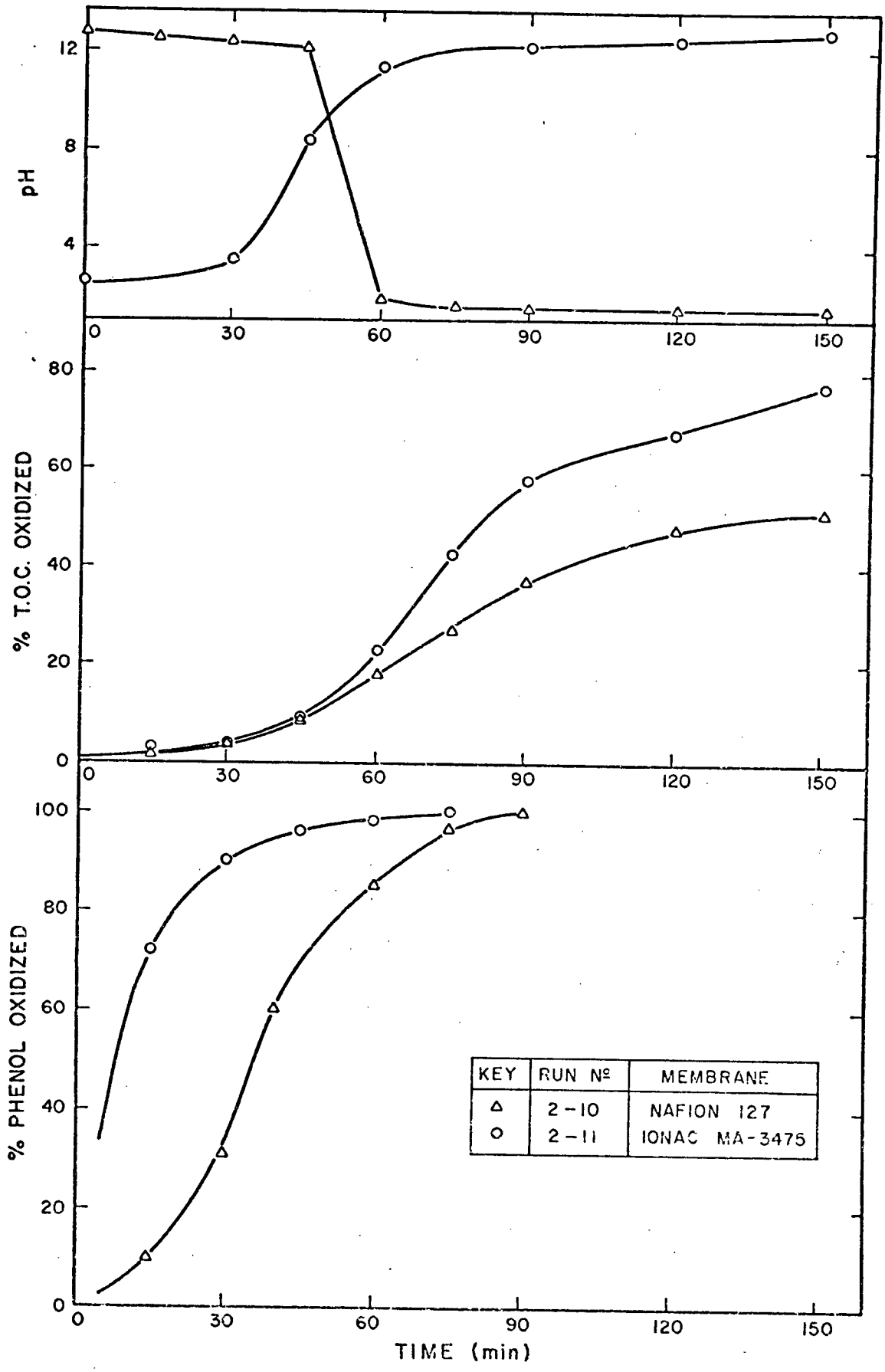

Fig. 17. Type of membrane-pH effect on % T.O.C. and % phenol oxidation at 20 A.

the phenol had been oxidized, before the pH started to increase. When the pH increase was produced, the T.O.C. started to be oxidized at a higher rate than in Run 2-10.

It should be noted that in the high pH range the oxidized organic carbon remains in solution in the form of inorganic carbon (e.g., Run 2-11) probably carbonates, due to the higher solubility of carbon dioxide in alkaline solutions.

Particularly interesting colour changes were observed during these experiments. The electrolyte at the outlet of the cell showed a brown-reddish colour when the pH was alkaline (higher than 9.4), and in those runs where the pH dropped spontaneously, the colour changed to light yellow. For example, in Run 2-10 the electrolyte took a deep brown-reddish colour until 60 min and when the pH drop was produced, the outlet showed the light yellow colour while tank was still brown. These colour reactions, when the pH was changed, were also observed in a pure benzoquinone solution, prepared for comparison.

5.3 Effect of current using the divided cell

In experiments 2-3, 2-4, and 2-5, current and pH were dependent variables and therefore the unique effect of the current can not be analyzed separately. However, in Fig. 13 it can be seen that the runs at 6 and 10 A showed approximately similar pH drops and therefore the current effect can be compared. The % T.O.C. removed vs time curves for those two runs are practically coincidental.

From Fig. 14 it is observed that at 10 A and 15 min, 12% more of the phenol had been oxidized than at 6 A. At 10 A, total phenol conversion was achieved in 90 min, but at 6 A, 120 min were necessary to oxidize the

phenol completely.

Two runs were carried out with the cationic membrane MC-3470 to study the effect of the current without significant pH changes (Runs 2-6, 2-7). The results are plotted in Fig. 18, where it is observed that the % phenol oxidized vs time curves are very close and total phenol conversion is achieved at 75 min for both currents. However, the T.O.C. analyses revealed that at 20 A, 47% of the carbon had been oxidized to carbon dioxide in 120 min, whereas at 10 A only a 12% had been oxidized during the same time.

5.4 Comparisons of membrane performances

The performances of cationic membranes IONAC MC-3470 and NAFION 127 can be compared from Runs 2-6 and 2-9, both at 20 A and pH = 2. The results are plotted in Fig. 19. The % phenol oxidized vs time curves showed that when using the IONAC MC-3470, about 77% of the phenol had been oxidized in 15 min versus 65% when using NAFION-127. But at 75 min total phenol conversion had been achieved with both membranes. The % T.O.C. removed vs time curves are very close but not exactly coincidental. At 120 min, 10% more carbon was oxidized in the run with IONAC MC-3470.

The anionic membrane MA-3475 gave the best performance as far as T.O.C. removal is concerned, because it provides the favourable pH increase as described previously (Fig. 17). In 15 min, phenol oxidation was 70%, and total phenol oxidation was also achieved in 75 min. However, the membrane was found to be changed in colour from yellow to brown, when the cell was opened after Run 2-11. The actual reason for this is unknown, but it is possible that the polymer structure of the membrane experienced oxidation, or that it interacted in some way with the phenol

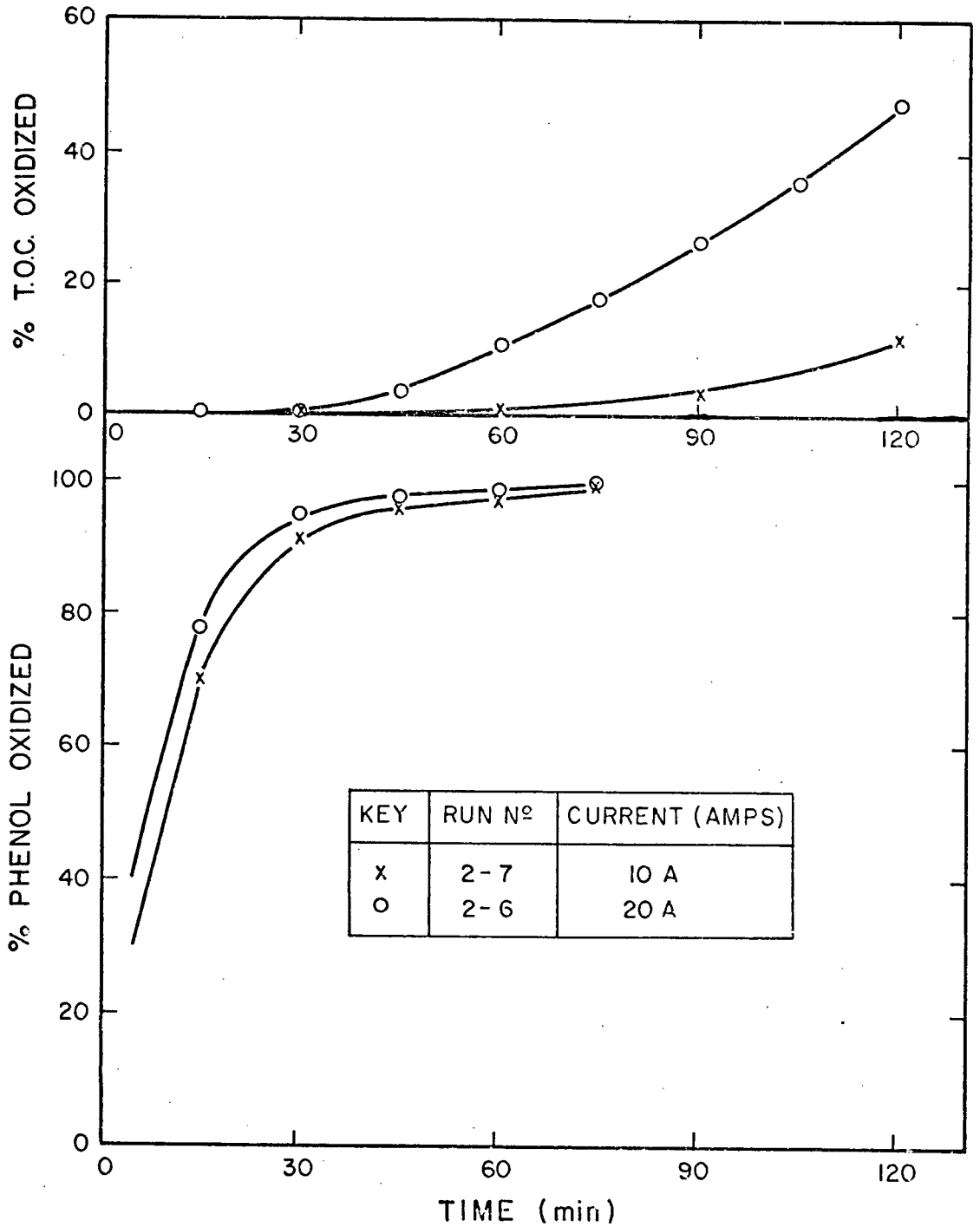

Fig. 18. Current effect on % T.O.C. and % phenol oxidation at pH = 2.5 with IONAC MC-3470.

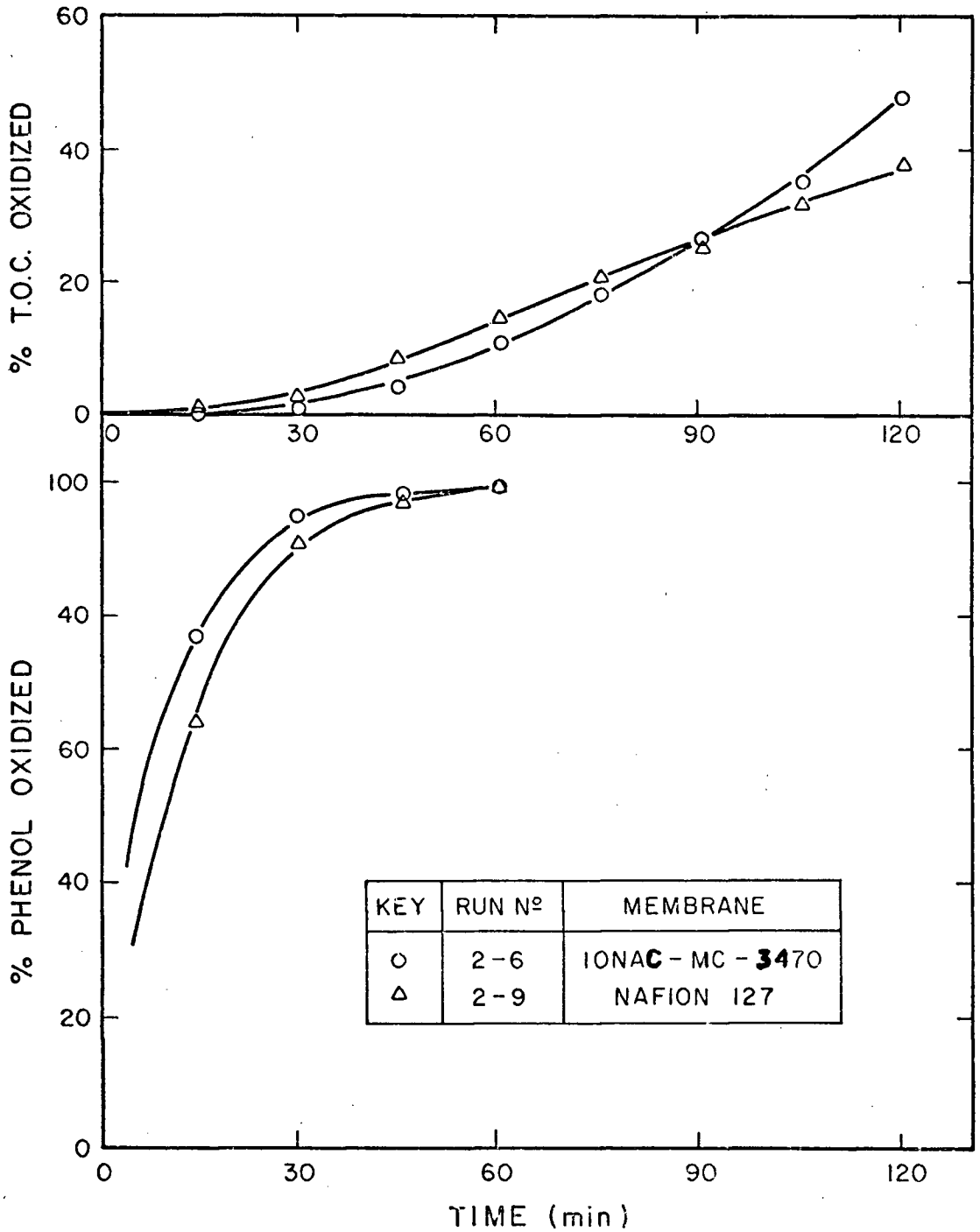

Fig. 19. Type of cationic membrane effect on % T.O.C. and % phenol oxidation at 20 A and pH = 2.5.

oxidation products. These changes may affect the lifetime of the membrane.

The cationic membrane MC-3142 was only tested during the preliminary experiments with anodized lead. On several occasions the membrane was perforated by protruding particles, which resulted in short circuits. For this reason, a plastic screen was introduced between the membrane and the particles. Another disadvantage of the IONAC MC-3142 membrane is that its nylon support will deteriorate with use in NaOH solutions.

In terms of mechanical resistance, the IONAC membranes MC3470 and MA3475 were stronger than the NAFION-127 and IONAC MC3142. Problems of breaking never occurred with the first two owing to their different support materials and thicknesses (Appendix 1).

The polypropylene screen, used in Run 2-1, produces much higher potential drops than the saran cloth used in Run 2-2, probably due to its closely packed screen structure. These experiments show that the use of the different plastic screens does not affect the results as far as phenol and T.O.C. removal is concerned.

5.5 Effect of pH using the undivided cell

From the pH vs time curve in Fig. 20, it can be seen that when working with only one chamber the pH does not drop as fast as in the divided cell. In Run 3-2 the pH only dropped from 12 to 11.5 in two hours whereas in corresponding Run 2-8 (Fig. 15) the pH dropped from 12 to 2 in 15 min. The reason for this different pH behaviour is that in the case of the undivided cell, the reaction of hydrogen evolution taking place at the cathode changes the hydroxyl ion balance in the electrolyte.

When starting at pH = 9.5 the pH dropped to 3.8 which also represents a smaller drop than in the case of the divided cell, and when starting at pH = 2.5, the pH was held practically constant.

As was found in experiments with the divided cell, the % phenol oxidized vs time curves at 10 A for the undivided cell (Fig. 20), show that phenol is oxidized much faster at a low pH than at a high pH. In 15 min, 70% of the phenol was oxidized when the pH was 2.5, compared with only a 33% when the pH was 12. On the other hand, more T.O.C. was oxidized at the high pH. At 120 min, 19% of the carbon was oxidized at pH = 2.5, whereas at pH = 12, a 32% of the carbon had been oxidized but remained in solution as inorganic carbon (e.g., Run 3-2).

The pH effect was also studied when working at 20 and 30 A (Figs. 21 and 22) and the results showed the same tendency. Phenol oxidation is favoured by a low pH whereas the further oxidation of intermediates is improved at a high pH. When comparing Figs. 20, 21 and 22 it is also observed that as the current increases, the pH has a greater effect on T.O.C. oxidation than on phenol oxidation.

5.6 Effect of current using the undivided cell

Figure 23 describes the effect of 10, 20, and 30 A currents at constant low pH (2.5), and Fig. 24 at a high pH (12). It should be noted that during the runs at 10 A, the temperature of the electrolyte remains constant at room temperature. At 20 A slight heating occurs, and a 4°C temperature increase can be detected in the recirculation tank after 120 min operation. When working at 30 A, approximately a 12°C temperature increase is registered (e.g., Runs 3-6 and 3-7). These temperature increases are small and the side effects due to temperature variations

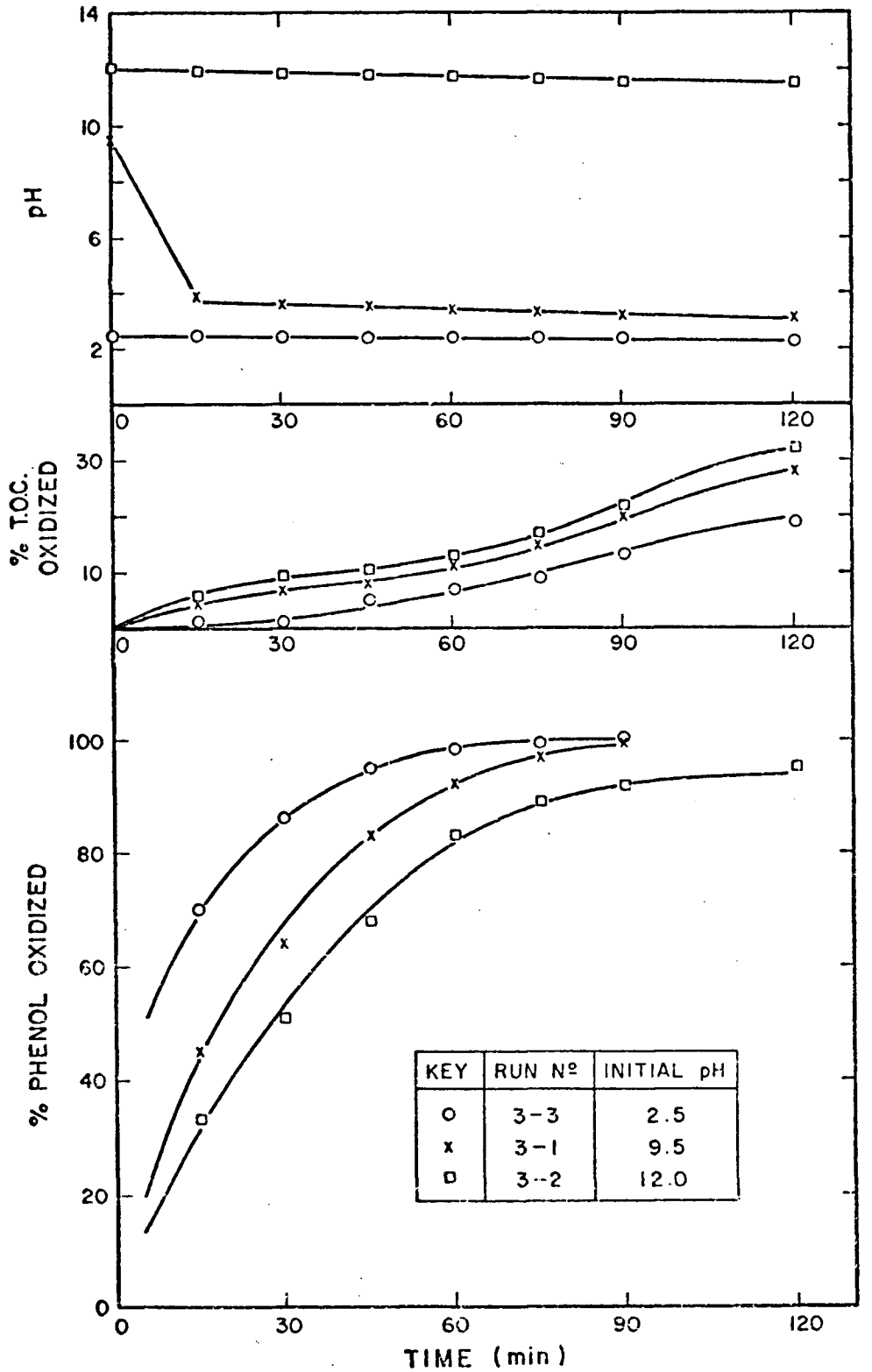

Fig. 20. pH effect on % T.O.C. and % phenol oxidation at 10 A in an undivided cell.

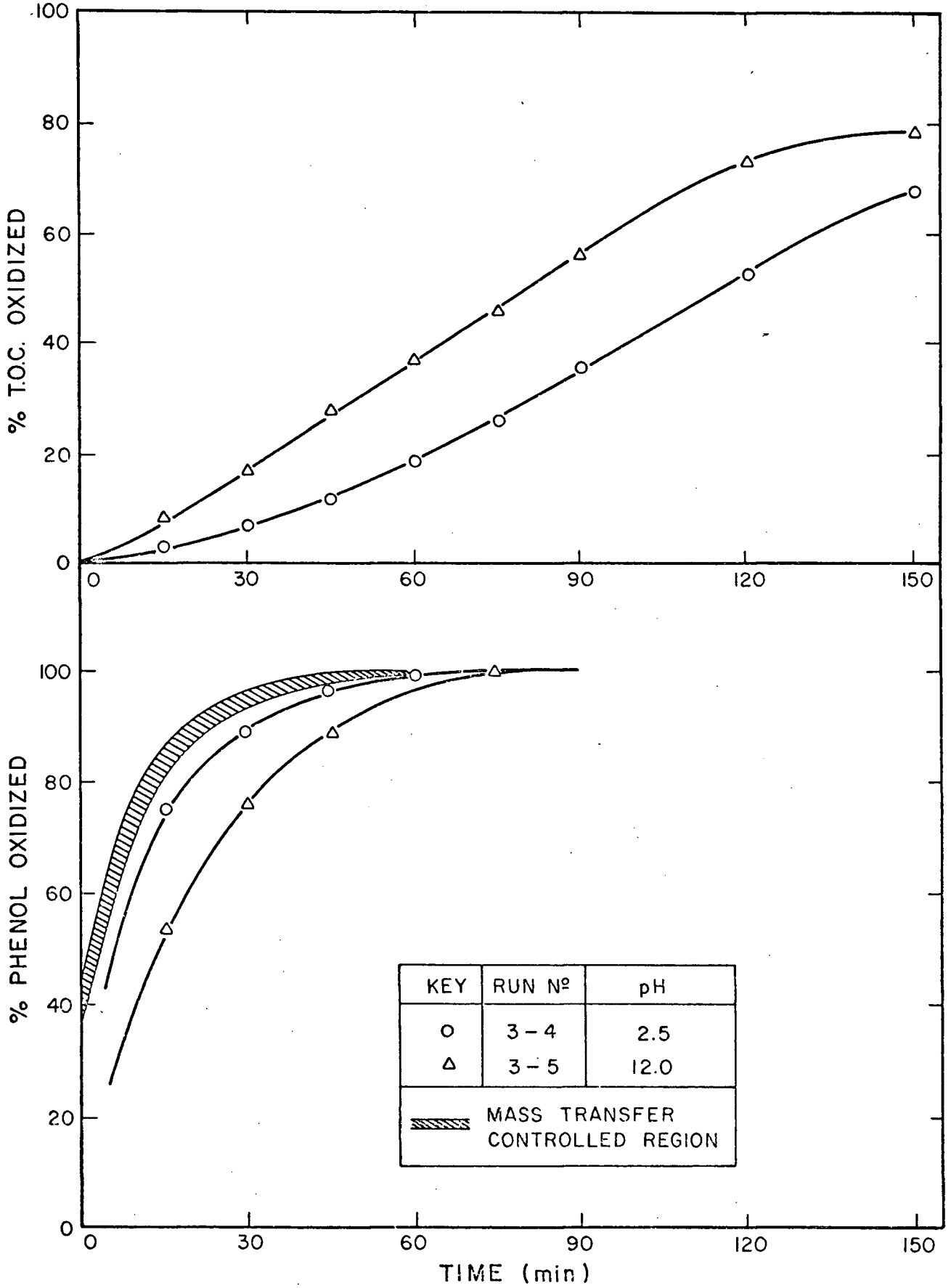

Fig. 21. pH effect on % T.O.C. and % phenol oxidation at 20 A in an undivided cell.

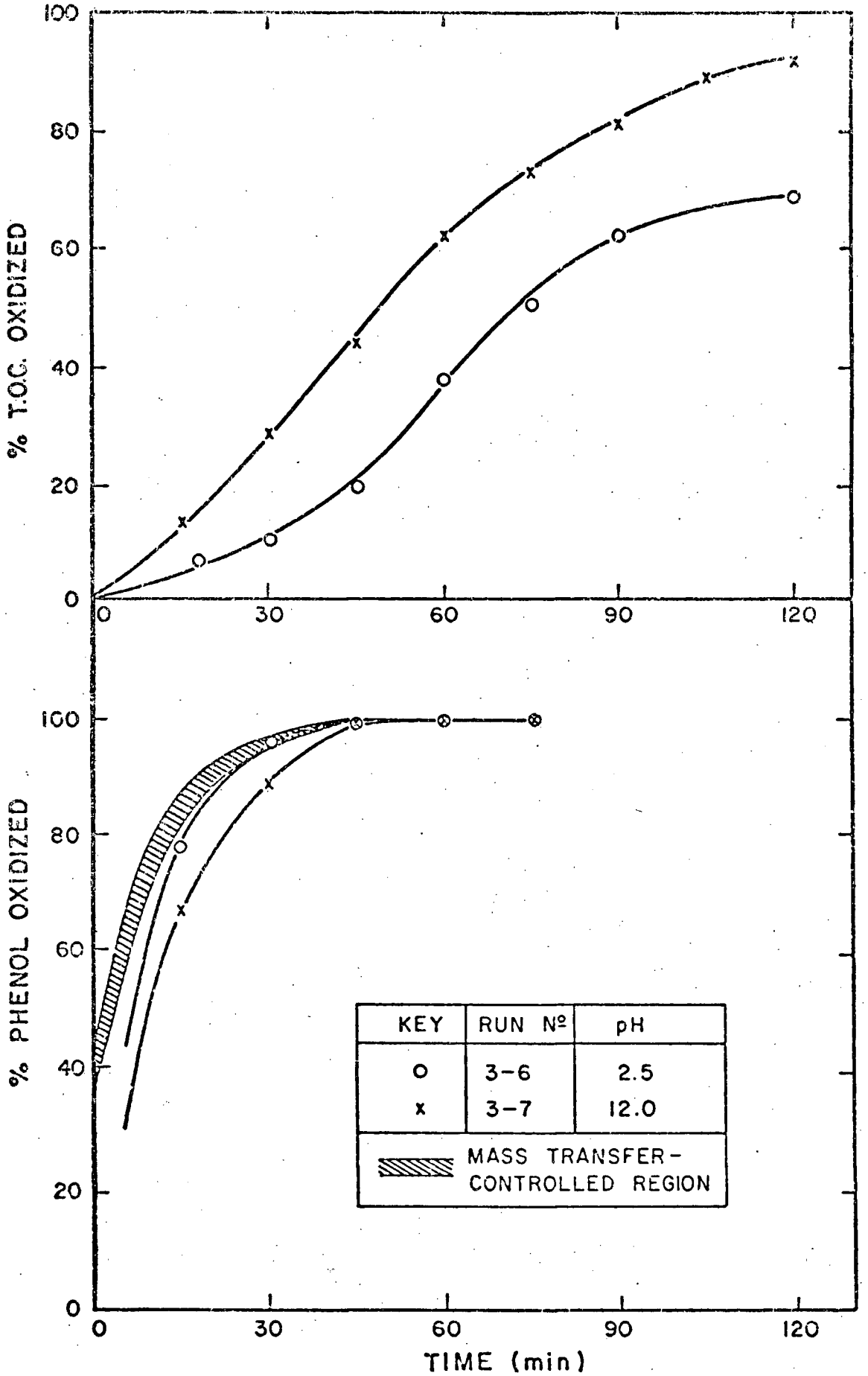

Fig. 22. Effect of pH on % T.O.C. and % phenol oxidation at 30 A in an undivided cell.

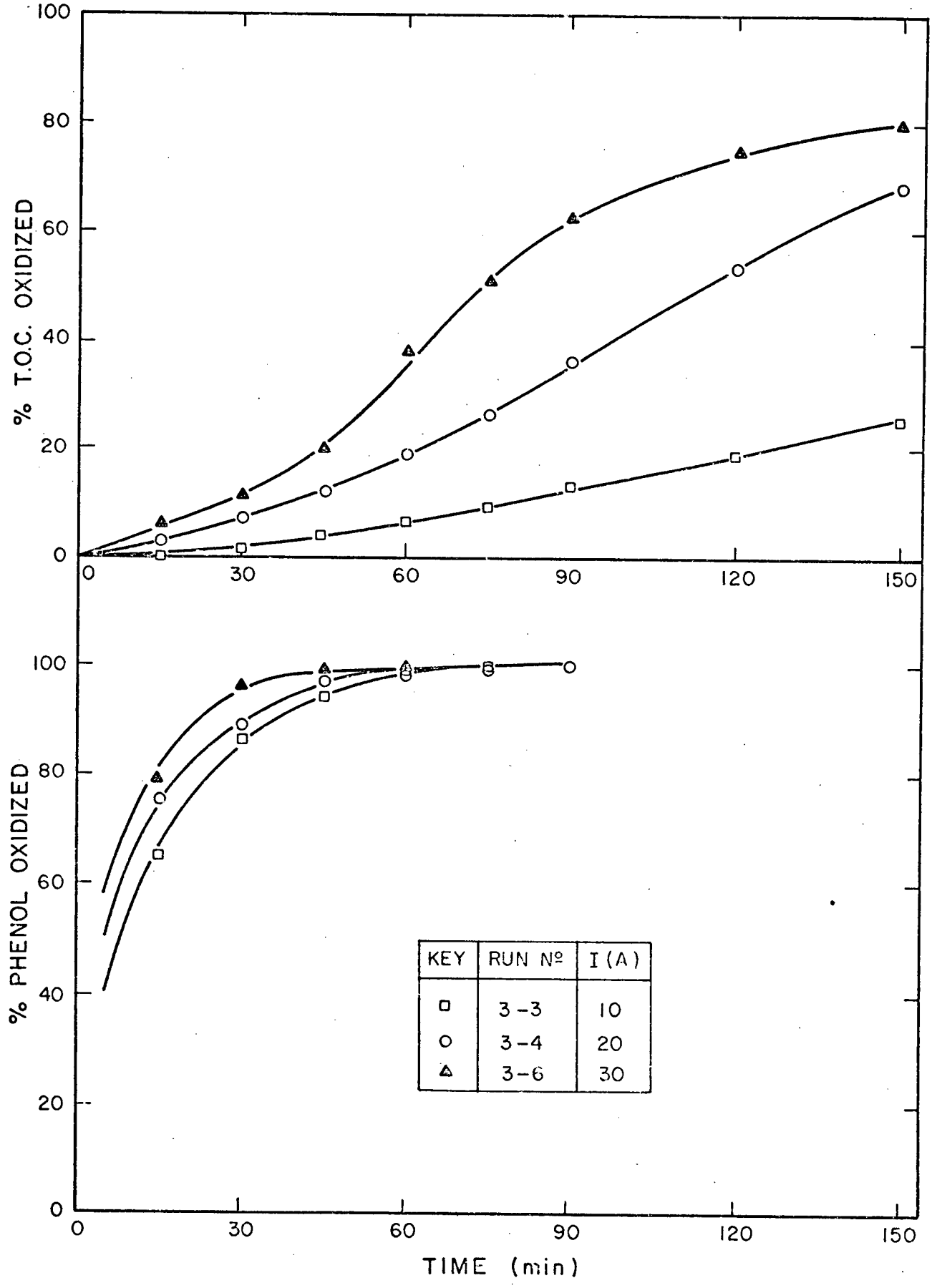

Fig. 23. Current effect on % T.O.C. and % phenol oxidation at pH ≈ 2.5 in an undivided cell.

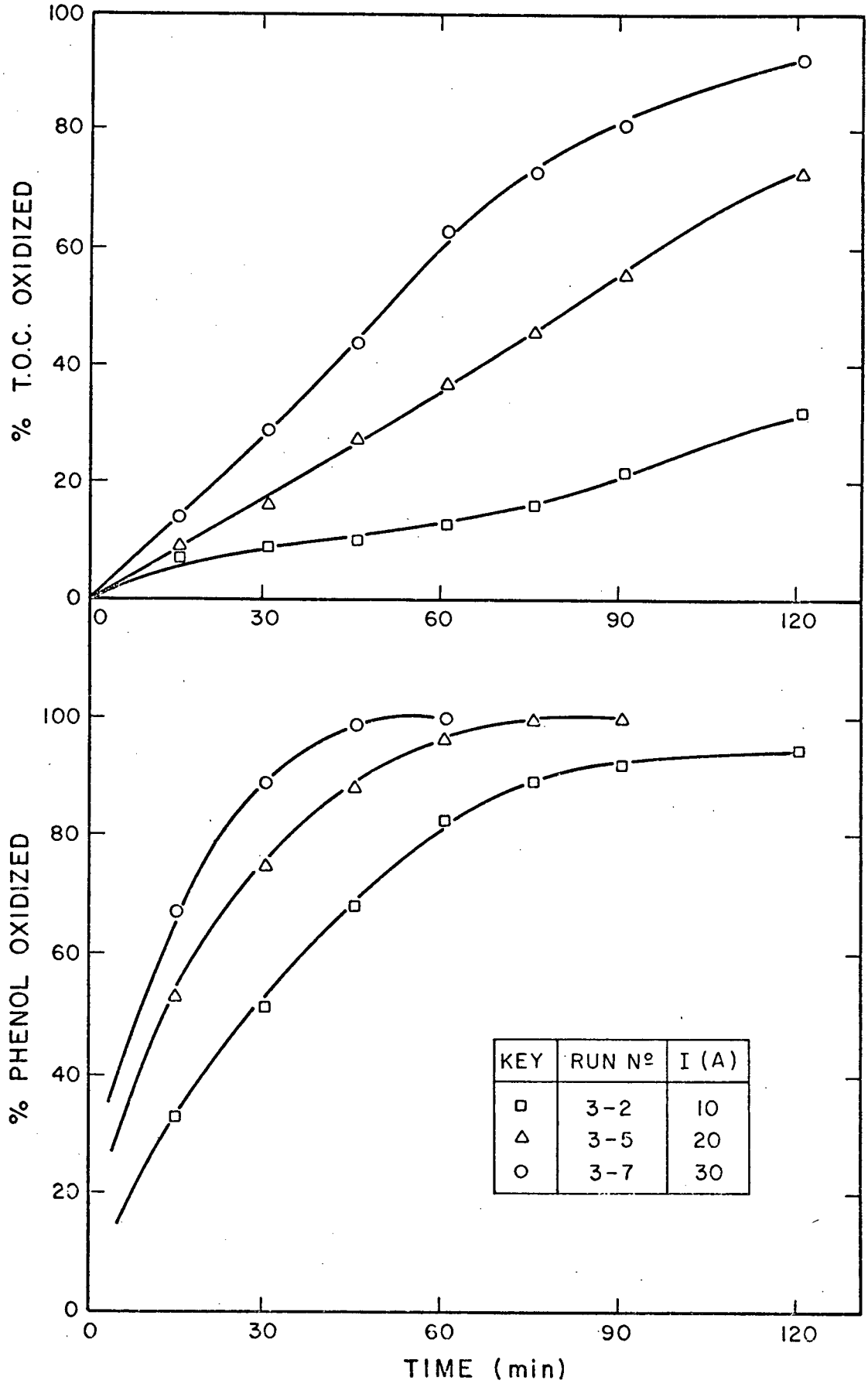

Fig. 24. Effect of current on % T.O.C. and % phenol oxidation at initial pH = 12, in an undivided cell.

can probably be neglected.

In Fig. 23 and Fig. 24 the effect of increasing current is to substantially raise the initial rate of phenol oxidation, thus decreasing the time to complete oxidation and to increase the % of T.O.C. removed. These effects are not proportional to the current since there is a bigger increase in T.O.C. removal and in the rate of phenol oxidation in going from 10 A to 20 A than in going from 20 A to 30 A (i.e., Fig. 24).

It can also be observed that in Fig. 23 the % phenol oxidized vs time curves are closer together than in Fig. 24, which indicates that at high pH the current has a greater effect on phenol oxidation than at low pH.

The maximum % T.O.C. oxidation is encountered in Run 3-7, for the highest current and alkaline pH, where 92% of the carbon was oxidized in 120 minutes.

5.7 Comparisons of divided and undivided cells

It is possible to evaluate the performances of divided and undivided cells under similar conditions. Table 5 shows the operating condition and results of three comparisons.

Cationic membranes IONAC MC-3470 and NAFION 127 gave similar performances to the undivided cells in terms of phenol oxidation. Considering that 2% error arises in the determinations of phenol and T.O.C. it can be said that the results seem to favour the undivided cell slightly in terms of T.O.C. removal.

Run 2-11, with anionic membrane MA-3475, can be either compared with Run 3-4 or with Run 3-5. Because in Run 2-11 the pH increased from 2.4 to 12, higher % T.O.C. oxidation was achieved than in Run 3-4, but

TABLE 5

COMPARISONS OF DIVIDED AND UNDIVIDED CELLS

Run No. (cell configuration)	% Phenol ox. at 15 min	% T.O.C. ox. at 120 min	Conditions I(A)	pH
Run 2-7 (IONAC MC-3470)	70	11	10	2.5
Run 3-3 (undivided)	70	19	10	2.5
Run 2-9 (NAFION 127)	77	47	20	2.5
Run 3-4 (undivided)	75	53	20	2.5
Run 2-11 (IONAC MA 3475)	72	67	20	2.4 to 12
Run 3-5 (undivided)	53	73	20	12

similar % phenol oxidation. When comparing Run 2-11 with Run 3-5 (at a constant pH of 12) it is observed that higher T.O.C. oxidation was achieved in Run 3-5, even if the % phenol oxidized at 15 min was lower due to the higher pH.

On the basis of these results and because the undivided cell is simpler to operate, it was decided to perform the rest of the experiments with the undivided cell.

5.8 Effect of conductivity of the electrolyte

Figure 25 shows the effect of electrolyte conductivity when working at 20 A. At a pH of 12, in Runs 3-5 and 3-11, the electrolyte conductivity was changed from 8×10^{-3} to 32×10^{-3} $(\Omega.cm)^{-1}$, by adding 5 g/l and 30 g/l of Na_2SO_4, respectively. The results showed that the increase

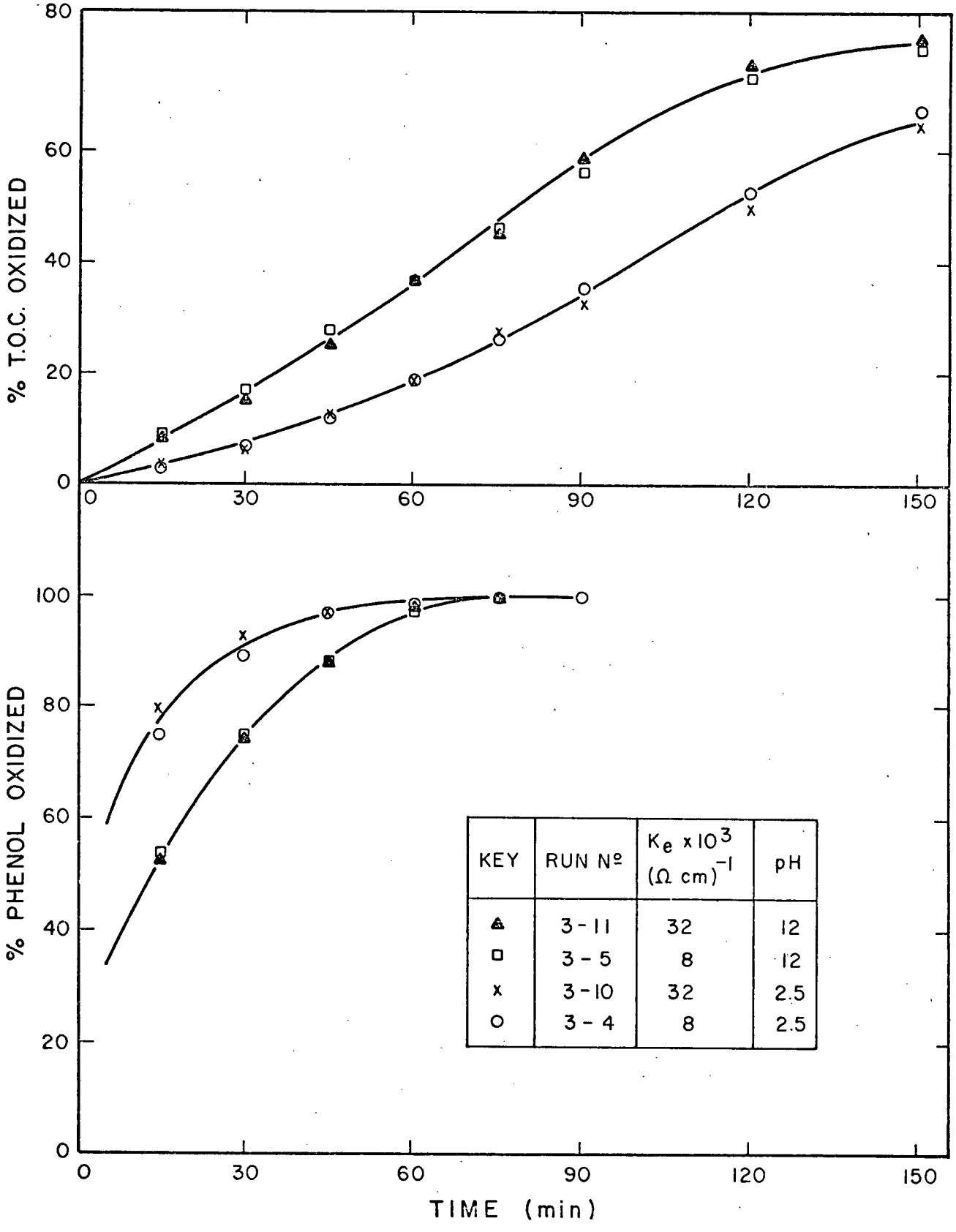

Fig. 25. Effect of electrolyte conductivity at 20 A (in alkaline and acid media).

in conductivity did not affect the phenol oxidation, nor the T.O.C. removal. Both experiments gave almost perfectly coincidental curves of % phenol oxidized vs time and of % T.O.C. vs time. The same result was obtained when the conductivity was changed, at pH = 2.5 in Runs 3-4 and 3-10.

However, when working at 10 A, and pH = 12, the same increase in conductivity produced an extra 20% carbon oxidized after 120 min, but the % phenol oxidized vs time curve remained practically unchanged (Fig. 26). Similarly, at 10 A, and pH = 2.5 (Fig. 27) about 8% more carbon was oxidized after 120 min when conductivity was changed from 8.4×10^{-3} to 30×10^{-3} $(\Omega.cm)^{-1}$, but again, the % phenol oxidized vs time curve showed no variation.

An explanation can be proposed for these observations. An increase in conductivity of the electrolyte produces a lower solution potential, and therefore a higher electrode potential. At 10 A, such an increase in electrode potential results in an appreciable change in the rate of further oxidation of intermediates to CO_2. But at 20 A, the metal potential is much higher so that the decrease in solution potential did not change the net electrode potential appreciably, and therefore no change is detected in the % of T.O.C. removed.

5.9 Effect of initial phenol concentration

Figure 28 represents the % phenol oxidized vs time for three different initial concentrations of phenol (Runs 3-3, 3-12, and 3-13). As the initial phenol concentration was increased from 93 mg/l to 525 mg/l to 1100 mg/l, the % phenol oxidized after 15 min decreased from 70% to 38% and to 27%. However, in Fig. 29 it is possible to see that a given

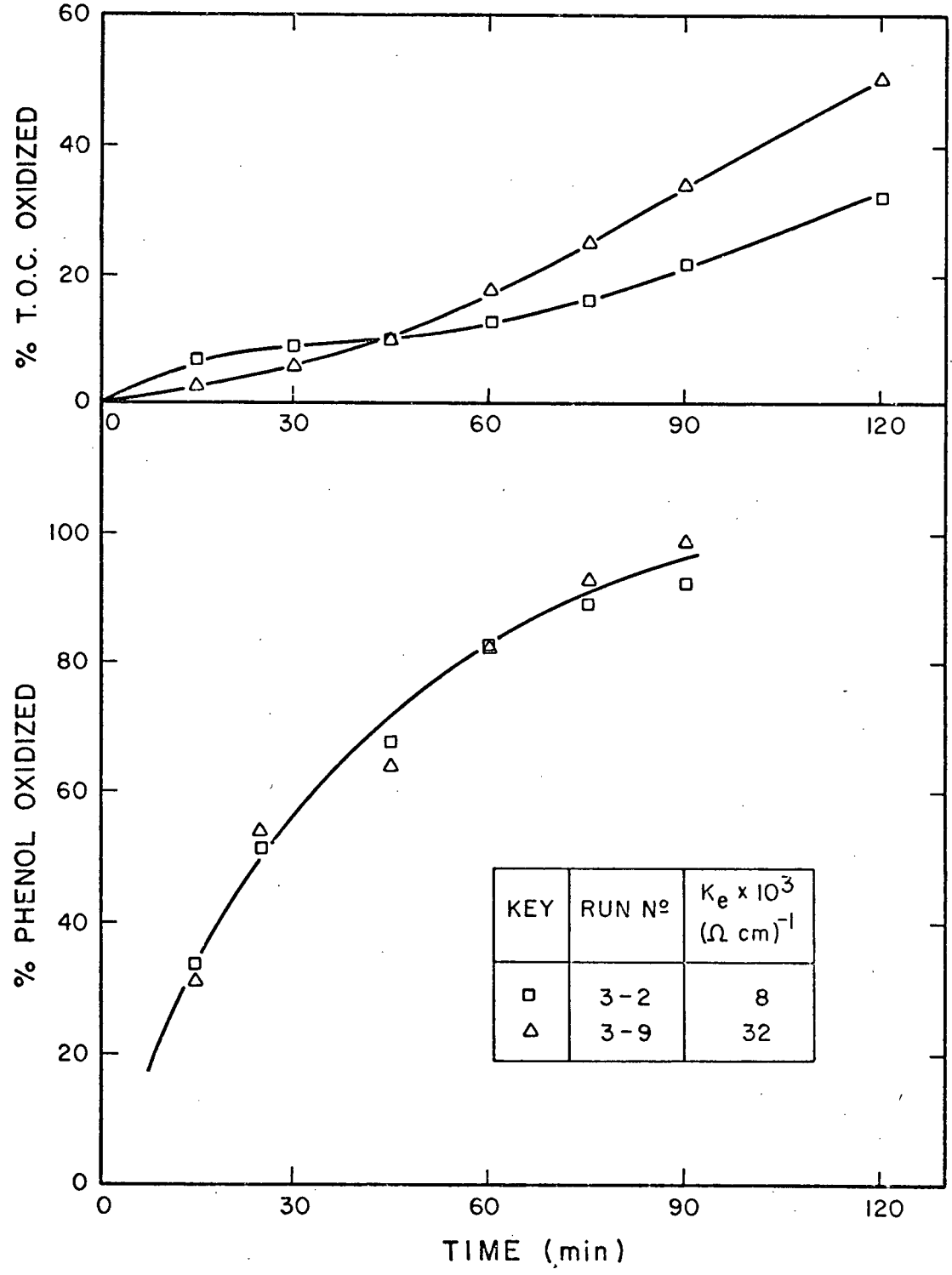

Fig. 26. Effect of electrolyte conductivity at 10 A and initial pH = 12.

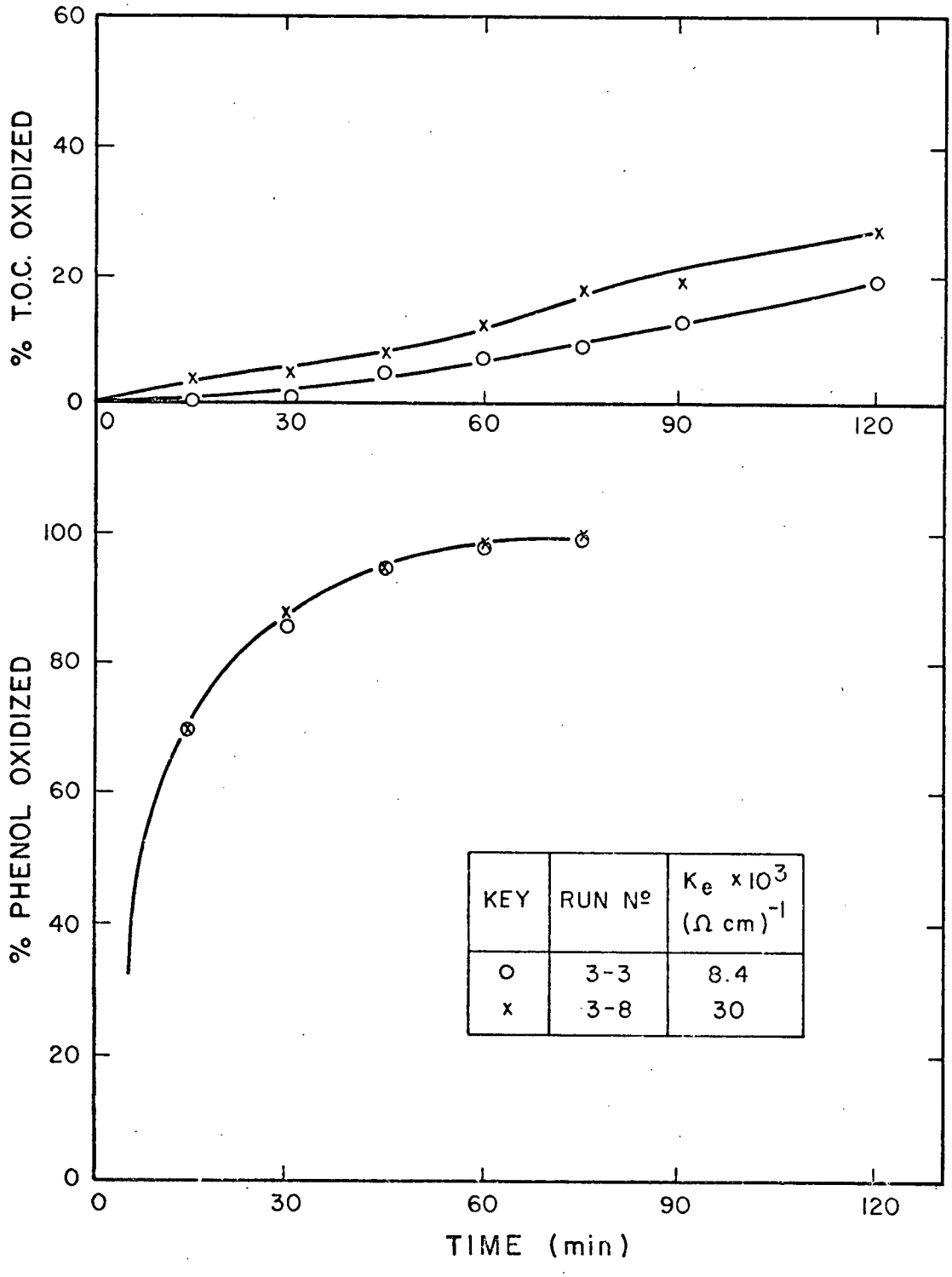

Fig. 27. Effect of electrolyte conductivity at 10 A and initial pH ≈ 2.5

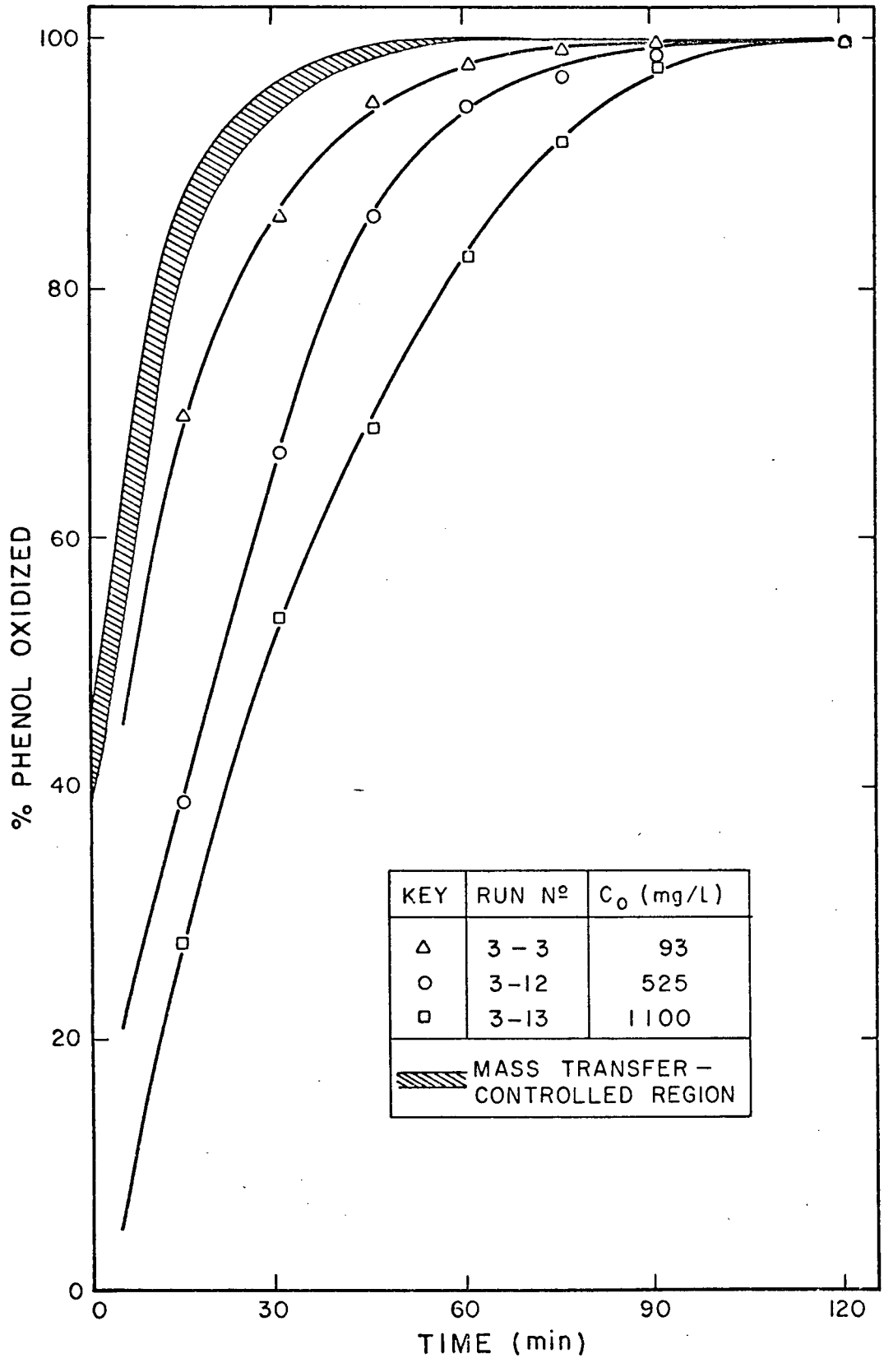

Fig. 28. % phenol oxidized vs time for various initial phenol concentration at 10 A and pH = 2.5.

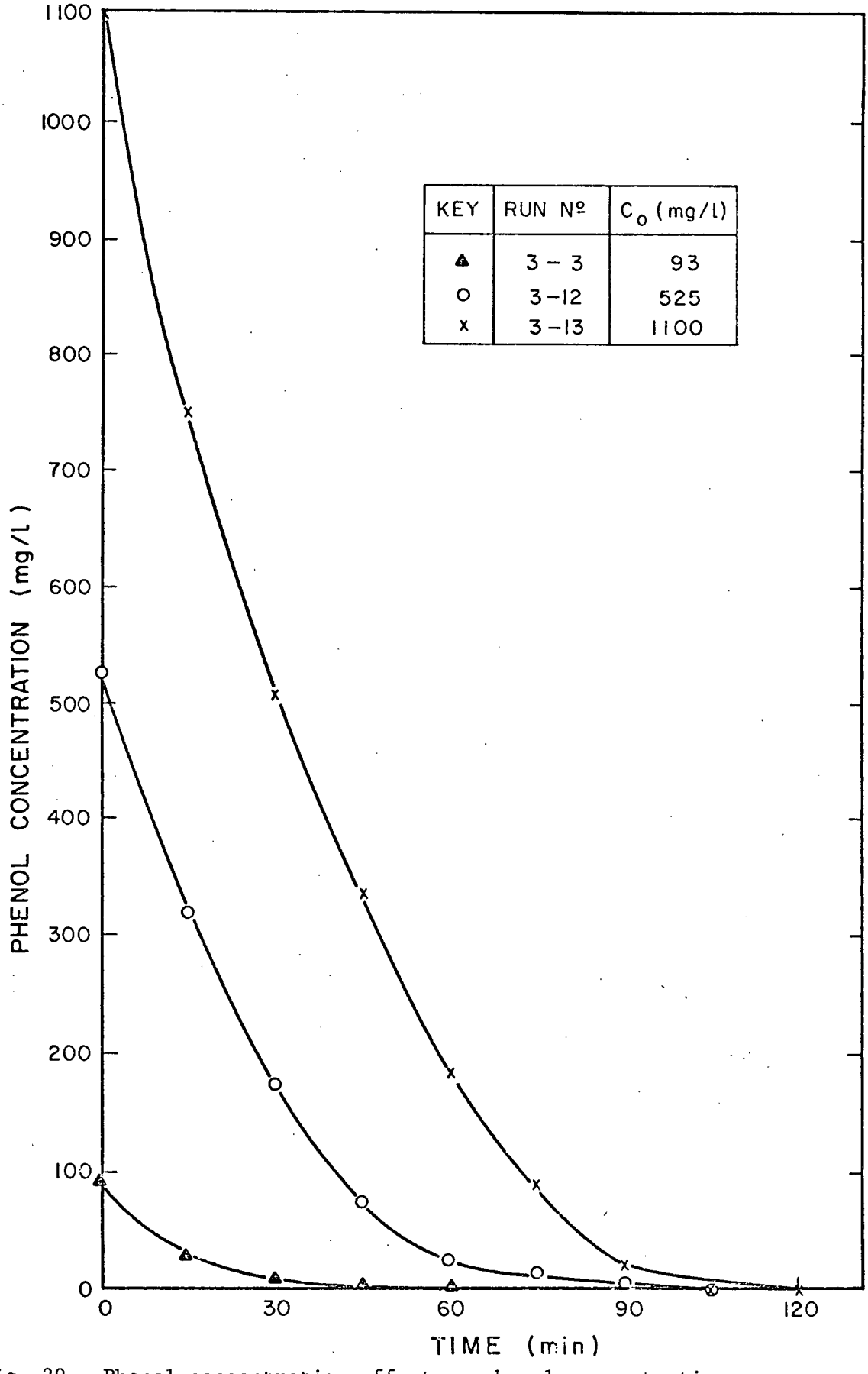

Fig. 29. Phenol concentration effect on phenol concentration vs time at 10 A and 2.5 pH.

time the net amount of phenol oxidized is higher as the concentration increases. Thus, 350 mg/l of phenol were oxidized in 15 min in Run 3-13 compared to 200 mg/l in Run 3-12 and only 75 mg/l in Run 3-3. In this figure it is easier to observe the parallelism between the three curves. For example, if the curve for Run 3-12 was displaced along the time axis until it matched the curve corresponding to Run 3-13, both curves would be practically coincidental. In other words, after 30 min of Run 3-13, the same results would be observed as in Run 3-12 from time zero.

As these runs were performed at 10 A and pH = 2.5, the T.O.C. removal is relatively low. When the initial concentration was 93 mg/l, 25% of the carbon was removed in 2 h versus 11% when the initial concentration was 525 mg/l. But for the initial concentration of 1100 mg/l of phenol, the net change in T.O.C. was practically undetectable due to the higher concentration of carbon present in solution.

5.10 Effect of electrolyte flow rate

Run 3-15 was performed at a flow rate of 0.55 ℓ/min. A comparison of the results with those from Run 3-4 where the flow was 1.12 ℓ/min, under otherwise equal operating conditions, shows that at both flow rates practically the same % phenol vs time and % T.O.C. oxidized vs time were obtained. Thus, phenol was 75% oxidized after 15 min in Run 3-4 and about 73% in Run 3-15. The % T.O.C. oxidized after 120 min were 53% and 54% respectively. (Refer to Run tables in Appendix 2.)

The effect of the flow rate is masked by the presence of the relatively large recirculation tank. In a single pass experiment, a higher conversion would be expected at a lower flow rate. With recirculation, a lower flow rate means it takes more time for a given

effect to be detected in the recirculation tank analysis. The effect of both inlet concentration and flow rate, is more easily examined in single pass experiments where the cell operates in steady state. Thus some single pass experiments were carried out.

Figure 30 represents the % phenol oxidized in a single pass through the cell vs flow rate, at different initial concentrations, when operating at 10 A and pH = 2.5. Runs 4-1, 4-2, and 4-3 were carried out at essentially the same phenol concentration of 100 ± 5 mg/1 to check reproducibility. They produced practically coincidental % phenol oxidized vs flow rate curves. About 90% of the phenol was oxidized at a flow rate of 0.11 ℓ/min, and as the flow rate was increased the % of phenol oxidized dropped, reaching a 20% at a flow rate of 1.1 ℓ/min.

Run 4-4 was performed under the same conditions (pH = 2.5, I = 10 A) but starting at the higher phenol concentration of 580 mg/1. The phenol analysis showed that about 70% was oxidized when the liquid flow rate was 0.11 ℓ/min and that the % phenol oxidized decreased with increasing flow rate, to about 8% when the flow rate reached 1.1 ℓ/min.

Similar effects were observed when operating at a current of 20 A, for initial concentrations of 110 and 510 mg/1.

The table for Run 4-1 shows that when the flow rate was 0.11 ℓ/min at 10 A, the temperature of the electrolyte was raised from 24°C at the inlet to 32°C at the outlet of the cell. But when the flow was increased to 0.25 ℓ/min the outlet temperature increased only 4°C above the inlet temperature. The operation can be considered practically isothermal for all flows equal or higher than 0.25 ℓ/min.

At 20 A (i.e., Run 4-5) the temperature at the outlet increased more than at 10 A, as could be expected, but the operation can be

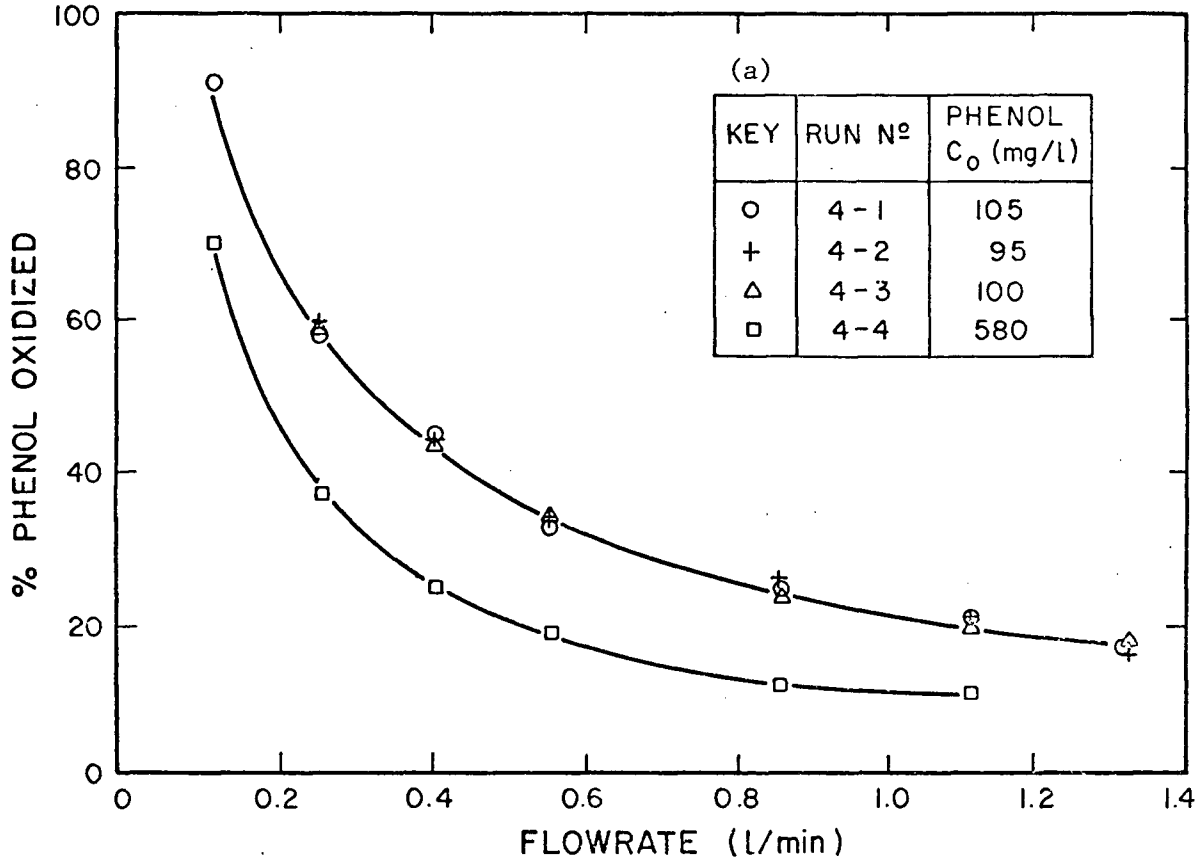

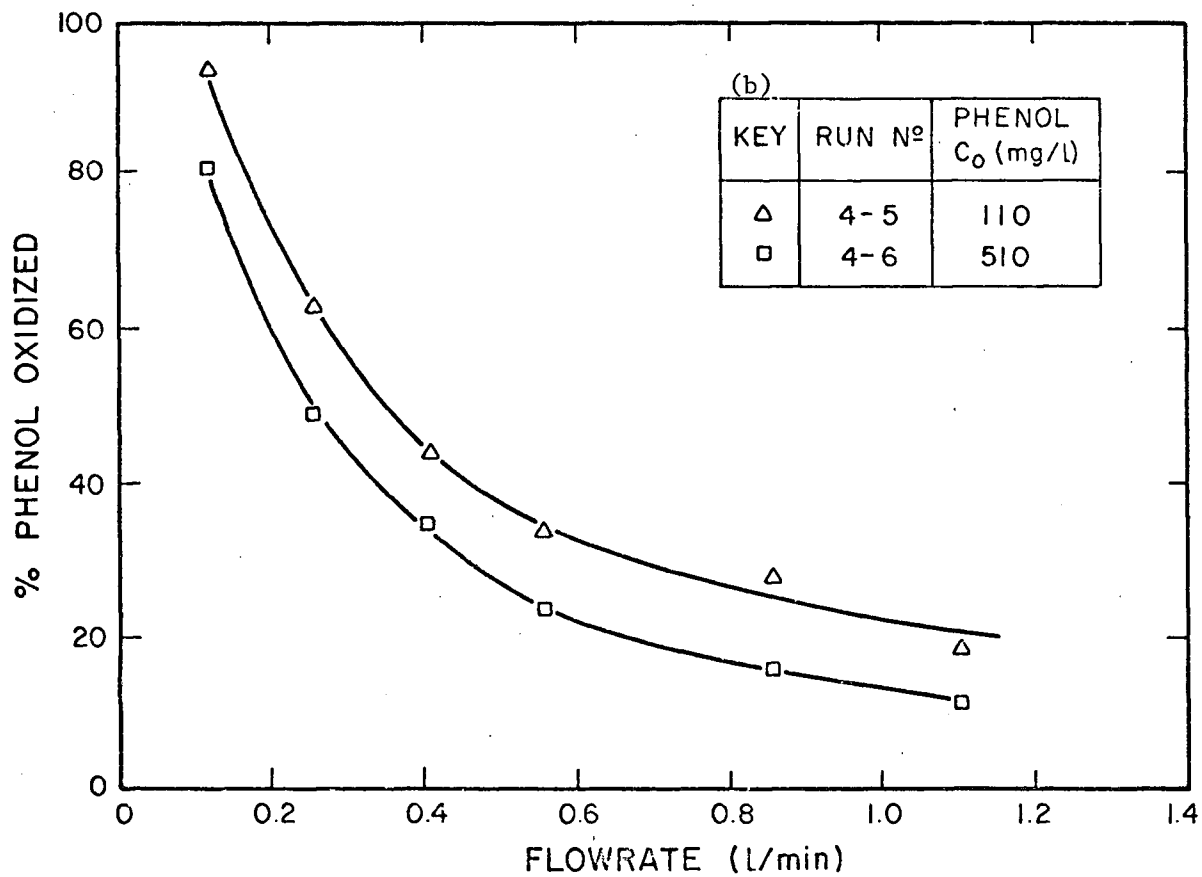

Fig. 30. Effect of flow rate on the single pass % phenol oxidation at (a) 10 A, (b) 20 A.

considered practically isothermal for flows above or equal to 0.55 ℓ/min.

In retrospect, it would have been better to report all the results under constant room temperature to eliminate any possible side effect due to temperature variations. However, this would require the design of a totally different cell with a built-in heat exchanger to remove the heat released by the current.

5.11 Effect of particle size

Figure 31 shows the % of phenol oxidized vs flow using three different anode surface areas. The lower curve corresponds to experiment 4-8, where no particles were present and the anode was just the lead dioxide on graphite plate. The intermediate curve corresponds to the average % phenol oxidized from Runs 4-1, 4-2, and 4-3 where a particle size between 1.7 and 2.0 mm was used and the upper curve was obtained when working with particle sizes between 0.7 and 1.1 mm.

Taking as a reference the flow of 0.4 ℓ/min, where the operation is practically isothermal, it is observed that when working without particles the specific area was 3.3 cm^{-1} and only 20% of the phenol was oxidized, whereas for a specific area of 20.6 cm^{-1} using the larger particles, about a 59% oxidation was achieved. With the smaller particles (sizes = 0.7-1.1 mm) about a 67% of the phenol was oxidized and the specific area was 41.5 cm^{-1}. (Calculations of the specific electrode areas are found in Appendix 4.)

These effects will be discussed in the next section based on mathematical models for the process.

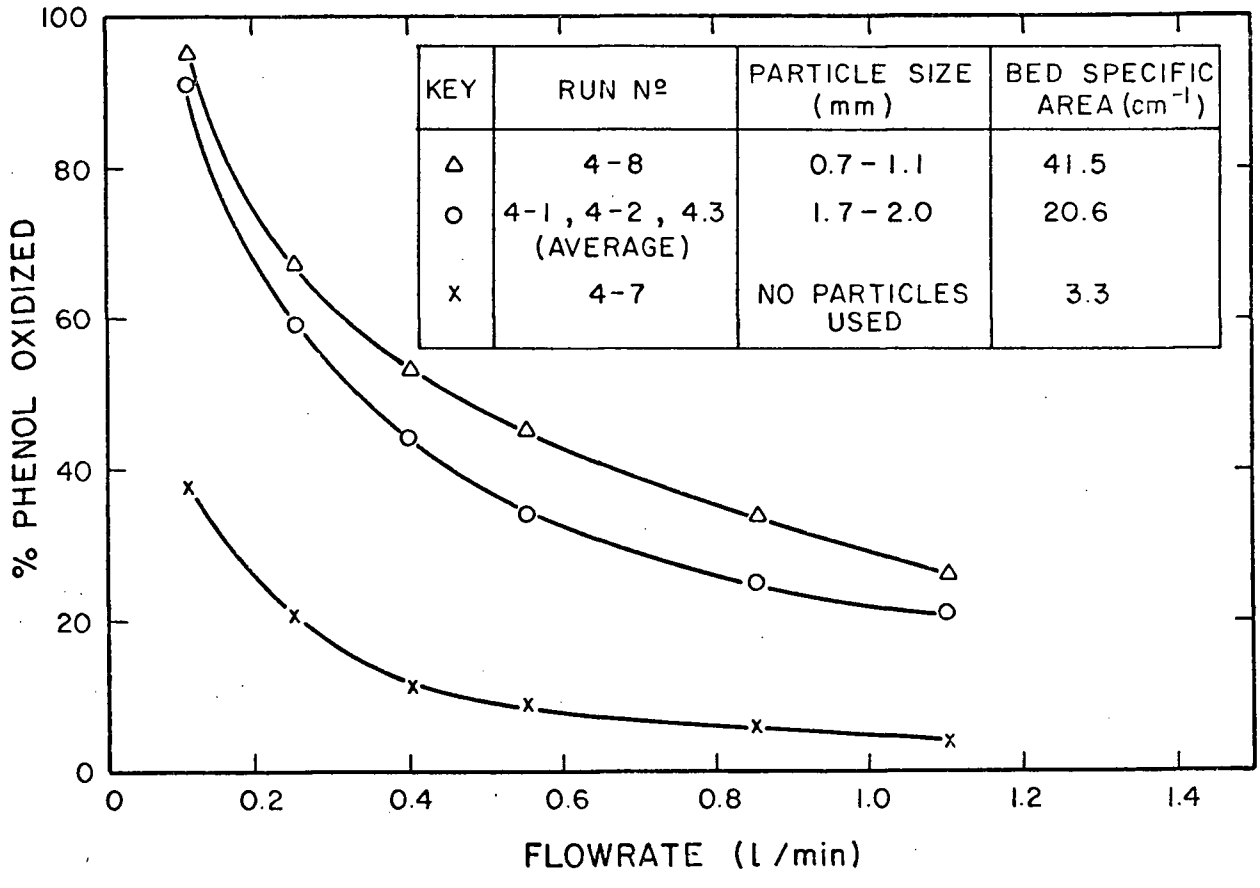

Fig. 31. Effect of anode surface area-particle size on the % phenol oxidized in a single-pass vs flow rate.

5.12 Comparisons of experimental results with mathematical models

5.12.1 Batch experiments

If the rate of phenol disappearance is controlled by mass transfer of phenol from the bulk electrolyte to the surface of the electrode, then for a batch recirculation system, the following equation relates the phenol fractional conversion with dimensionless time and mass transfer groups (Appendix 3).

$$X = 1 - \exp\left[(\exp\left(\frac{-K_m\ a\ L}{u}\right) - 1)\frac{t}{t_m} - \frac{K_m\ a\ L}{u}\right]$$

Here, t_m is the time the electrolyte spends in the mixing tank, a the specific surface area of the electrode, L the electrode height, and u the superficial electrolyte velocity.

The model calculations are represented as a band or region of conversion vs time, taking into account that a 10% error can be expected from the empirical equation for the mass transfer coefficient. As well, the correlation chosen may underestimate the mass transfer coefficient for this particular case, as discussed in Appendix 3, page 160. Calculations of X vs t are presented in Appendix 4, Table A-2.

Figure 28 shows the deviations of the experimental results from the mass transfer model when operating at 10 A. As expected, the curve corresponding to the lowest initial phenol concentration (93 mg/l) is closest to the mass transfer-controlled region with a 15 min conversion approximately 15% lower than predicted by the mass transfer model.

Where the initial concentration of phenol was 1100 mg/l (Run 3-13) the experimental % phenol oxidized after 15 min is about 55% below that predicted by the mass transfer model. This implies that the electrochemical reaction kinetics controls the rate of phenol oxidation under

such conditions. However, as the phenol concentration drops during the course of the experiments, the curves approach that of the mass transfer model. In other words, the process is controlled by reaction kinetics at the beginning and as phenol depletes, mass transfer becomes the controlling mechanism.

Figures 21 and 22 show that as the current is increased at an initial phenol concentration of the order of 100 mg/l (Runs 3-4, 3-6) the experimental % phenol oxidized vs time curve moves closer to the mass transfer region as might be expected. At 20 A, the experimental curve is still below the mass transfer region until about 75 min when the conversion was complete. But at 30 A the mass transfer band encloses the experimental curve from Run 3-6, at 30 min time.

For both 20 and 30 A currents, the curve at low pH is closer to the mass transfer model than the curve corresponding to the high pH run.

It should be noted that the experimental curves obtained with either the divided or the undivided cell are never above the mass transfer region. The closest experimental curve to the mass transfer model is that of Run 3-6 at 30 A and pH = 2.5.

5.12.2 Continuous experiments

For a single pass through the packed bed reactor where phenol disappears, by a rate process first order in phenol concentration, the assumption of plug flow yields (Appendix 3)

$$- \ell n(1 - X) = K a L/u$$

where X is the fraction of phenol oxidized and K is the overall rate constant, which can be related to the mass transfer and electrochemical rate constants by using the concept of additive mass transfer and electrochemical resistances as,

$$\frac{1}{K} = \frac{1}{K_m} + \frac{1}{K_r}$$

Using the data from those experiments performed in the continuous mode, it is possible to evaluate an experimental rate constant. When $-\ln(1 - X)$ is plotted vs $\frac{1}{u}$ a straight line is obtained (Fig. 32) and the experimental rate constant K can be determined from the slope. Thus, using available correlations for K_m, K_r can be determined.

The nature of the electrochemical rate constant K_r was alluded to in Chapter 2. Unlike a chemical reaction rate constant, it is dependent on electrode potential. As discussed in Appendix 3, when operating at a fixed current rather than at a fixed potential, changes in phenol concentration, flow rate, surface area, etc. will result in changes in potential and hence in K_r. Therefore, the analysis of results in terms of K_r to be presented here, is of limited usefulness except to indicate what resistance (mass transfer or electrochemical kinetics) is more important under determined conditions. However, considerations of the effects of the process variables on K_r does show qualitative agreement with what is expected from the simple model, as will be shown with the following examples.

Taking the average fractional conversion from experiments 4-1, 4-2, 4-3, performed at 10 A and initial concentrations of phenol of 100 ± 5 mg/l, with particle sizes between 1.7 and 2.00 mm, the experimental rate constant is obtained from the corresponding straight line represented in Fig. 32. The resulting value of K is 3.1×10^{-3} cm/s. Using the correlation by Pickett and Stanmore (45) for mass transfer coefficient in electrochemical packed bed reactors K_m and K_r are calculated at various flows (Table A-3).

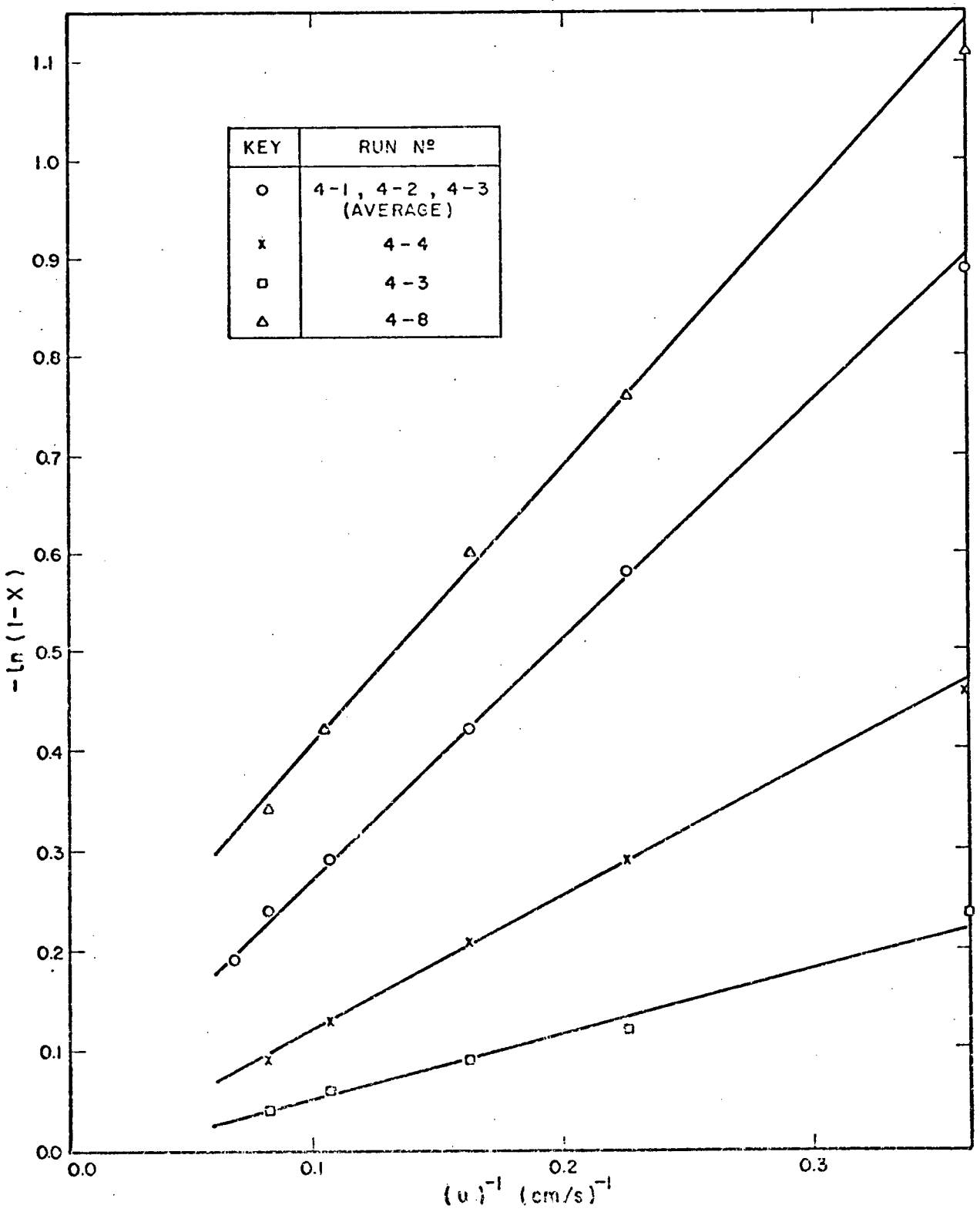

Fig. 32. $-\ell n(1 - X)$ vs $(u)^{-1}$ for the calculation of experimental rate constants in single pass experiments.

For example,

at 0.25 ℓ/min : $K_m = 3.9 \times 10^{-3}$ cm/s, $K_r = 15.7 \times 10^{-3}$ cm/s, and

at 1.10 ℓ/min : $K_m = 8.8 \times 10^{-3}$ cm/s, $K_r = 4.8 \times 10^{-3}$ cm/s.

This implies that at the low flow rate, mass transfer controls the phenol oxidation because the mass transfer resistance $(\frac{1}{K_m})$ represents about an 80% of the overall resistance. On the other hand, at the high flow rate, the resistance to reaction $(\frac{1}{K_r})$ represents a 65% of the overall resistance $(\frac{1}{K})$.

The same calculation procedure was applied to the data from Run 4-4 when the initial concentration was 580 mg/l, working under otherwise equal conditions as in the previous example. The resulting experimental rate constant was 1.4×10^{-3} cm/s. In this case the electrochemical reaction resistance was higher than the mass transfer resistance at all flows (Table A-4)

i.e., at 0.25 ℓ/min : $K_m = 3.8 \times 10^{-3}$ cm/s, $K_r = 2.21 \times 10^{-3}$ cm/s

at 1.10 ℓ/min : $K_m = 8.8 \times 10^{-3}$ cm/s, $K_r = 1.67 \times 10^{-3}$ cm/s.

The results from both examples are in qualitative agreement with the predictions of the model, since at a constant initial concentration, K_r should decrease when the flow rate increases, and at a constant flow rate, K_r should also decrease when the initial concentration increases as described in Appendix 3.

The experimental rate constant was also evaluated for the smaller particle size (0.7-1.1 mm). Using the results from Run 4-8, the experimental rate constant is $K = 1.8 \times 10^{-3}$ cm/sec (Table A-5), and the mass transfer and reaction coefficients at the extreme flows are,

at 0.25 ℓ/min : $K_m = 5.3 \times 10^{-3}$ cm/s, $K_r = 2.68 \times 10^{-3}$ cm/s

1.10 ℓ/min : $K_m = 12.1 \times 10^{-3}$ cm/s, $K_r = 2.09 \times 10^{-3}$ cm/s.

These data indicate that the reaction offered a higher resistance than mass transfer. In this case, the initial concentration of phenol was 100 mg/l and all the experimental conditions except for particle size, were equal to those in the first example. The mass transfer coefficients K_m are higher at a given flow rate than in the first example, due to the dependance of the empirical mass transfer coefficient on particle size, but lower reaction coefficients K_r are obtained with the smaller particles.

This result is also in qualitative agreement with the theoretical model, since for a higher specific surface area of the bed (smaller particles), the electrode potential will be lower for the same input current applied to the cell, and thus lower values of K_r are expected.

Even though a lower value of the overall rate constant K is obtained with the smaller particles, the net effect is that higher conversions are achieved at a given flow rate than with the larger particles (Fig. 31), due to the increase of the specific surface area of the bed, from 20.6 to 41.5 cm^{-1}. This is expected from the plug flow equation:

$$X = 1 - \exp\left(-\frac{K\,a\,L}{u}\right)$$

It should be emphasized that the values reported here for the reaction rate constants are particular for the set of conditions used in each experiment, and therefore should not be used in a scale-up, since for a larger cell even with the same particle sizes than used in this study, the average electrode potential (or the average K_r value) will be different for the same net current input, according to the model.

Using the data from Run 4-7 where the anode was the electrodeposited PbO_2 on graphite feeder plate (without particles), the experimental rate constant obtained from the slope of the straight line on Fig. 32 is

$K = 5 \times 10^{-3}$ cm/sec. For the ranges of flows used in the experiments the Re numbers referred to the hydraulic diameter, de = 2SW/(S + W) are lower than 700. For $Re_{de} < 2000$, an applicable correlation for the mass transfer coefficient in a parallel plate reactor is (page 133, Ref. 10)

$$\frac{K_m de}{D} = 1.47 \left(Re_{de}\ Sc\ \frac{de}{L}\ \frac{de}{S}\right)^{1/3}$$

For liquid flow rates between 0.25 and 0.11 ℓ/min, this correlation results in mass transfer coefficient values between 4×10^{-4} and 7×10^{-4} cm/sec which are about ten times lower than the calculated experimental constant. Since the overall rate constant can never be higher than the mass transfer coefficient, it means that the values of the mass transfer coefficient obtained by the correlation are an underestimation of the real situation. It could be suggested that in practice there is an enhancement in the mass transfer coefficient due to gas evolution, which is not taken into account by the correlation.

Most of the correlations for mass transfer coefficients in gas evolving parallel plate electrodes have been developed for the case of stationary solution where mixing of the electrolyte is only provided by the gas bubbles. It is known that mass transfer coefficients under gas evolution are between four or five times greater than the mass transfer coefficients from conventional free-convection correlations in flat plates (10).

But for the case of forced convection and gas evolving electrodes, an empirical correlation could not be found in the literature. However, the results seem to indicate that mass transfer controls the rate of phenol oxidation on the flat plate, since even if the mass transfer coefficients were increased by a factor of five, the resulting K_m values

would still be lower than the experimental rate constant.

5.13 Current efficiencies, energy requirements and energy costs for phenol oxidation

5.13.1 Batch experiments

Typical current efficiencies, energy requirements, and costs are estimated for batch experiments nos. 3-3, 3-12, 3-13, after recirculation times of 15 and 90 min. A sample calculation is given in Appendix 4, page 178. For the estimation of the % C.E. it was assumed that four electrons are transferred from the phenol molecule as proposed by Covitz (Reaction R9). Energy per g mol phenol oxidized is calculated taking \$0.02/Kw-h as a basis.

Table 6 shows that for lower initial concentrations of phenol or higher recirculation times, the % C.E. are relatively lower and the energy costs are higher.

TABLE 6

TYPICAL CURRENT EFFICIENCIES, ENERGY REQUIREMENTS AND ENERGY COSTS IN BATCH EXPERIMENTS WITH UNDIVIDED CELL (Q=1.12 ℓ/min)

Run No.	C_{A_0} (mg/l)	ΔV (volts)	t (min)	C_{A_2} (mg/l)	X (%)	C.E. (%)	Energy $\left(\frac{\text{Kw-h}}{\text{g mol}}\right)$	Electrical costs (\$/g mol)
3-3	93	8.6	15	28	70	11	6.7	0.14
			90	0	100	3	22.6	0.45
3-12	525	8.3	15	320	39	36	2.5	0.05
			90	5	99	19	4.8	0.10
3-13	1100	8.5	15	792	28	54	1.7	0.03
			90	22	98	35	2.4	0.05

Run 3-3 at C_{A_0} = 93 mg/l, yields the maximum energy cost of \$0.45/g mol oxidized for the 90 min operation, where practically no phenol was present after treatment.

5.13.2 Continuous experiments

Using the data from Runs 4-3 and 4-4, it is possible to estimate % C.E. and energy costs for various flows in a single pass through the cell. A sample calculation is given in Appendix 4, page 180, and the results are presented in Table 7.

TABLE 7

TYPICAL CURRENT EFFICIENCIES, ENERGY REQUIREMENTS AND ENERGY COSTS IN CONTINUOUS EXPERIMENTS WITH UNDIVIDED CELL

Run No.	C_{A_1} (mg/l)	Q (ℓ/min)	ΔV (V)	C_{A_2} (mg/l)	X (%)	C.E. (%)	Energy ($\frac{Kw\text{-}h}{g\ mol}$)	Electrical costs (\$/g mol)
4-3	95	0.25	8.7	39	59	9.6	9.7	0.195
		0.55	8.3	63	34	12.2	7.4	0.148
		1.1	7.4	76	20	14.3	5.6	0.110
4-4	580	0.25	8.6	365	37	36.7	2.5	0.050
		0.55	7.9	470	19	41.5	2.0	0.041
		1.10	7.0	526	9	39.3	1.9	0.037

The electrical cost of treatment decreases as the initial phenol concentration and electrolyte flows are increased. Comparing the results from Run 3-12 after 15 min (Table 6) with those from Run 4-4 at 0.25 ℓ/min, it can be seen that in terms of current efficiences and energy requirements, both situations are practically equivalent.

5.13.3 Cost comparisons

It is of interest to compare the estimated electrical costs with the operating costs for other treatments given by Katzer (8). Table 8

TABLE 8

OPERATING COSTS OF VARIOUS TREATMENT METHODS, ESTIMATED FOR 1974 FOR A CATALYTIC CRACKER EFFLUENT CONTAINING 700 mg/1 PHENOL (8)

Process	Treatment costs ($/1000 gal)	($/g mol)[5]
Oxidation pond[1]	0.14-0.51	0.005-0.018
Activated sludge[1]	0.24	0.009
Activated sludge with dilution[2]	2.4	0.090
Carbon adsorption[3]	0.86	0.031
Catalytic oxidation[4]	0.57	0.020
Electrochemical oxidation	2.00[I]	0.08[II]

[1] $0.38/$10^3$ gal in 1967; operating costs of biological oxidation ponds at Billing Montana Oil Refinery; extrapolation to 1974 gives $0.51/$10^3$ gal. Capital investments not included.

[2] Extrapolated from 1968 to 1974 using a factor of 1.34; if dilution of effluent is required cost of treatment will increase; 10:1 dilution factor results in $2.4/$10^3$ gal.

[3] 10^6 gal/day design for treating unfiltered activated sludge plant effluent to produce water with 8 mg/1 C.O.D.

[4] Calculated for a 99% phenol removal by catalytic oxidation.

[5] Calculated from the original paper (Ref. 8) assuming that total phenol conversion was achieved in all the examples.

[I] Calculated in this study for treating a 5ℓ volume with 99% removal (Appendix 4).

[II] Calculated in this study by interpolating from Table 6 for 700 mg/1 phenol initial conc., using a factor of $0.02/Kw-h for electrical energy cost.

shows the 1974 costs for treating a catalytic cracker effluent containing 700 mg/l phenol. For the electrochemical process, electrical energy costs are interpolated from Table 6 using the data from Run 3-12 (525 mg/l phenol) and Run 3-13 (1100 mg/l phenol) at 90 min, when phenol conversions are 98-99%. To treat an effluent with 700 mg/l phenol, approximately $0.08/g mol phenol would be necessary. In Appendix 4 is estimated the electrical cost per volume of waste in about $2.00/$10^3$ gal, to compare with the data by Katzer. Electrical energy cost is about ten times higher than the activated sludge cost in normal conditions, but of the order of the activated sludge cost if dilution is required. The cost of other processes appear to be lower than the estimated electrical cost; for example, carbon adsorption operating costs would be less than a half ($0.03/g mol).

It should be noted that the electrical cost ($0.08/g mol) has been estimated for the arbitrary cell characteristics and operating conditions used in the experiments. To draw firm conclusions about feasibility of the process would require an optimization of operating costs and a capital cost estimate of this and the other processes. Some recommendations for the former are given in Chapter 7.

CHAPTER 6

CONCLUSIONS

An investigation was made of the electrochemical oxidation of phenol on lead dioxide packed bed anodes. In all the experiments performed, phenol oxidation occurred more easily than the further oxidation of intermediate organics to carbon dioxide or carbonates.

The conclusions of this study are summarized below.

1. Electrodeposited lead dioxide was found to be a better anode than the anodized lead shot in terms of phenol oxidation and corrosion resistance.
2. The oxidation of phenol was more rapid under acidic conditions but the removal of oxidized products (measured by the total organic carbon) was favoured by alkaline conditions. In divided cells, operated with recirculation of solution, the electrolyte pH depended on the type of ion selective membrane used. An anionic membrane which provided a pH increase from acidic to alkaline proved to be superior to a cationic membrane in terms of T.O.C. removal.
3. The rates of phenol oxidation in divided and undivided cells were similar. In terms of T.O.C. removal no improvement was obtained with the divided cell even under optimum pH controlled conditions provided by the anionic membrane.
4. The extents of phenol and T.O.C. oxidation increased with applied current density at high or low pH. But at high pH, current density

changes affected the rate of phenol oxidation more strongly than at low pH.

5. An increase in electrolyte conductivity from 8×10^{-3} to 32×10^{-3} $(\Omega.cm)^{-1}$ had no effect on the rates of phenol or T.O.C. oxidation at high or low pH at c.d. = 1052.6 A/m^2, but at 526.3 A/m^2 c.d., the same increase in conductivity produced higher T.O.C. oxidation rates, even though the phenol oxidation rates remained constant.
6. The effect of increasing the initial phenol concentration in a single pass was to reduce the % phenol oxidized at a given time or in a single pass. However, the current efficiency for phenol oxidation increased.
7. Increasing electrolyte flow rate reduced the single pass phenol conversion at a given inlet phenol concentration in continuous experiments.
8. Increasing the specific surface area of the anode in the range of 3.3 to 41.5 cm^2/cm^3 produced higher single-pass phenol conversions at a given flow rate and inlet phenol concentration of the electrolyte.
9. Comparisons of the experimental results from batch experiments with the mass transfer model indicated that the oxidation of phenol is controlled by the electrochemical reaction at the beginning and as phenol depletes, the experimental % phenol oxidized vs time approach that of the mass transfer model. Continuous experiments showed that the electrochemical reaction resistance becomes more important at higher electrolyte flow rates, higher inlet phenol concentrations and smaller particle sizes.
10. Electric energy costs estimated were generally higher than operating costs of other processes. However, power costs can likely be reduced with further work.

CHAPTER 7

RECOMMENDATIONS

Investigation of other factors regarding the electrochemical oxidation of phenol could possibly raise the prospective feasibility of the process. Improvements to the model would lend confidence to the feasibility calculations.

On the basis of this study, the following recommendations are made, to yield a more complete knowledge of the process.

1. Analysis of the phenol oxidation products:

   Routine analysis of the phenol oxidation products, (benzoquinone, hydroquinone and possibly maleic acid) should be attempted, to draw definite conclusions about effluent quality under different operating conditions. The T.O.C. analysis would permit one to determine what fraction of the carbon is in the form of each compound.

2. Measurements of electrode potential:

   Reference electrodes should be located at certain points on the bed, to determine electrode potential variations. It would be of interest to determine the effect of electrode potential on the kind of oxidation products under different operating conditions. Also electrode potential measurements are of interest for the process modelling.

3. Control of the electrolyte temperature:

   A heat exchanger built in the electrolytic cell would permit

temperature control within the cell in single pass experiments. However, the construction of a cell equipped with such a heat exchanger might be difficult.

4. Analysis of the gases produced during electrolysis:
   A gas analysis technique could be assessed for complete monitoring of the process. It would permit a total carbon balance. Also a measurement of the rate of gas production would be of interest to include the effect of gas evolution in the process modeling.

After these experimental improvements were assessed, the effect of some of the other important factors on the electrochemical oxidation of phenol might be studied, e.g., the effect of different anode materials on the kind of oxidation products, and the effect of temperature and electrode potential on the rates of oxidation of phenol and intermediates.

The following recommendations would allow improvements to the mathematical modeling of the process in addition to furthering general understanding.

5. The effect of gas evolution on the mass transfer coefficient should be studied. Another electrochemical reaction that is purely mass transfer controlled could be used for this purpose (45).
6. Cell length, width, and thickness of the bed should be varied. Measurements of electrode potential at different points on the bed would permit one to determine under which conditions the assumption of a uniform or average electrode potential is reasonable.
7. Experiments could be set up to determine the relationship between electrode potential and electrochemical rate constant under different operating conditions.
8. The effect of gas evolution and electrolyte conductivity on the

electrode potential could be studied to include these effects in the mathematical models.

9. Computer methods could be used to correlate all the variables affecting the process, and determine costs of energy under different operating conditions to optimize operating costs.

NOMENCLATURE

		Typical units
a	specific surface area of the bed	cm^2/cm^2
a_j, b_j	constants of the Tafel equation for the reaction j	V
c.d.	current density referred to the surface area of the feeder plate	A/m^2
C.E.	current efficiency	
C_{A_0}	initial phenol concentration in batch experiments	mg/l
C_{A_1}	inlet phenol concentration	mg/l
C_{A_2}	outlet phenol concentration	mg/l
C_{A_b}	phenol concentration in the bulk of solution	mg/l
C_{A_s}	phenol concentration at the surface of the electrode	mg/l
C_w	concentration associated with a water electrolysis reaction	mg/l
dp	average particle diameter	mm
D	diffusivity of phenol in water	cm^2/s
F	Faraday's constant	coul/g equiv.
i_A	local current density for phenol oxidation	A/m^2
i_s	local current density carried by the solution	A/m^2
i_m	local current density carried by the metal	A/m^2
$\bar{i}_A$	average current density for phenol oxidation	A/m^2
$\bar{i}_w$	average current density for water electrolysis	A/m^2
$\bar{i}$	total average current density	A/m^2
I	applied current	A

K_{e_a}	electrical conductivity of the anolyte	$(\Omega\ cm)^{-1}$
K_{e_c}	electrical conductivity of the catholyte	$(\Omega\ cm)^{-1}$
K_{e_m}	electrical conductivity of the metal	$(\Omega\ cm)^{-1}$
K_{e_s}	electrical conductivity of the solution	$(\Omega\ cm)^{-1}$
K_r	electrochemical reaction rate constant	cm/s
K_m	mass transfer coefficient	cm/s
K	overall or experimental rate constant	cm/s
L	length of the cell	cm
P	pressure	kPa
Q	electrolyte flow rate	ℓ/min
R	universal gas constant	kJ/k mol°K
Re	Reynolds number	
Sc	Schmidt number	
S	thickness of the bed (in the direction of current)	cm
T	temperature	°C
t	time of electrolysis	(min)
t*	dimensionless time	
tm	residence time in the mixing tank	min
u	superficial velocity	cm/s
V_a*	anode potential	V
V_c*	cathode potential	V
V_j	reversible equilibrium potential for the reaction j	V
V_j°	standard reduction potential for the reaction j	V
ΔV	total voltage drop through the cell	V
V_m	volume of the mixing tank	ℓ

W	width of the bed	cm
X	phenol fractional conversion	
y	variable length of the bed	cm
z	number of electrons associated with phenol oxidation	

Greek letters

α	transfer coefficient	
ε	voidage of the bed	
η_j	overpotential for the reaction j	V
ξ	shape factor for the particles	
θ	K_m a L/u dimensionless mass transfer group	
ν	kinematic viscosity of water	(cm^2/s)
ϕ_{ma}	metal potential of the anode	V
ϕ_{sa}	solution potential of the anolyte	V
ϕ_{mc}	metal potential of the cathode	V
ϕ_{sc}	solution potential of the catholyte	V

BIBLIOGRAPHY

1. Throop, M. W. "Alternative methods of phenol waste water control." Journal of Hazardous Materials 1, 319 (1975/77).

2. Siegerman, H. "Applications of electrochemistry to environmental problems." Chem. Tech. 675 (Nov. 1971).

3. Lanouette, K. "Treatment of phenolic wastes." Chem. Eng. 84, 99 (Oct. 1977).

4. Hardsity, D. M., and Bishop, H. E. "Waste water treatment experience at organic chemical plants using a pure oxygen system." A.I. Ch. E. Symposium Series 73, No. 167, 140 (1976).

5. Dunlap, R., and McMichael, F. C. "Reducing coke plant effluent." Env. Sci. & Tech. 10, No. 7, 654 (1976).

6. Kostenbader, P. D., and Flecksteiner, J. W. "Biological oxidation of coke plant weak ammonia liquor." J. Water Pollution Control Federation 41, No. 2, (Feb. 1969).

7. Kazuo, S., Kazuto, T., and Satoru, T. "Degradation of aqueous phenol solutions by gamma irradiation." Am. Chem. Soc. 12, No. 9, 1043 (1978).

8. Katzer, J., Sadana, A., and Ficke, H. "Aqueous phase catalytic oxidation as a waste water treatment technique." Eng. Ext. Series 145, 29 (1974).

9. Zeff, J. "Uv. ox. process for the effective removal of organics in waste water." A.I. Ch. E. Symposium Series 73, No. 167, 206 (1976).

10. Pickett, D. J. Electrochemical reactor design. Elsevier, Amsterdam (1977).

11. Allen, M. J. Organic electrode processes. Reinhold, New York, (1958).

12. Sherwood, T. K., Pigford, R. L., and Wilke, C. R. Mass Transfer. McGraw Hill, New York (1975).

13. Fichter, F. "Electrochemical oxidation of aromatic hydrocarbons." Trans. Amer. Electrochem. Soc. 45, 107 (1924).

14. Fichter, F., and Stocker, R. "Electrochemical oxidation of aromatic hydrocarbons and phenols." Chem. Abstr. 8, 3037 (1914).

15. Fichter, F., and Brunner, E. "New products of the electrochemical oxidation of phenol." Chem. Abstr. 10, 2873 (1916).

16. Clarke, J. S., Ehigamusoe, R. E., and Kuhn, A. T. "The anodic oxidation of benzene, toluene, and anisole." Electroanalytical Chem. and Interfacial Electrochem. 70, No. 3, 336 (1976).

17. Gladisheva, A. I., and Lavrenchuck, V. I. "Electrochemical oxidation of phenol," (original title in Russian). Uch. Zap. Tsent. Nauch. Issled. Inst. Olovyan. Prom, No. 1, 68 (1966); Chem. Abstr. 67, 28639X (1967).

18. Tarjanji, M., et al. "Decreasing the phenolic content of liquids by an electrochemical technique." U.S. Pat. 3,730,864. (May 1, 1973).

19. Covitz, F. "Electrochemical oxidation of phenol." U.S. Pat. 3,509,031. (Apr. 28, 1970).

20. Jones, G. C., et al. "Electrolytic oxidation of phenol at lead thalium anodes." U.S. Pat. 4,035,253. (July 12, 1977).

21. Jones, G. C., and Payne, D. A. "Electrochemical oxidation of phenol." U.S. Pat. 3,994,788. (Nov. 30, 1976).

22. Fioshin, M. Y., et al. "Electrochemical oxidation of phenol to quinone." Electrokhimiya 13, No. 3, 381 (1977).

23. Ronlan, A. "Phenols." Encyclopedia of electrochemistry of the elements. M. Dekker, New York, Vol. XI, 242 (1978).

24. Nilsson, A., Ronlan, A., and Parker, V. "Anodic oxidation of phenolic compounds. Journal Chem. Soc. Perkin trans. 1 20, 2337 (1973; Chem. Abstr. 80 115431k (1974).

25. Surfleet, B. "Electrolytic destruction of industrial effluents." The Electricity Council Research Centre. Report No. 204, (Oct. 1969).

26. Rifi, M. R., and Covitz, F. H. Introduction to organic electrochemistry. M. Dekker, New York (1974).

27. Kempf, R. "Electrolytic oxidation of P.Benzoquinone." Chem. Abstr. 5, 2815 (1911).

28. Lure, Y. Y., and Genkim, V. E. "The use of anodic oxidation and cathodic reduction methods for the purification of industrial waste waters." Chem. Abstr. 57, 8371c (1962).

29. Shakarnov, A. V. "Dephenolization of wastes by electrochemical oxidation." Chem. Abstr. 56,13978b (1962).

30. Mieluch, J., et al. "Electrochemical oxidation of phenol compounds in an aqueous solution." Chem. Abstr. 84, 10275a (1976).

31. Antropov, L. Theoretical electrochemistry. Mir, Moscow (1972), p. 396.

32. Carr, J. P., and Hampson, N. A. "The lead dioxide electrode." Chem. Rev. 72, No. 6, 679 (1972).

33. Ruetschi, P., and Cahan, B. "Electrochemical properties of PbO_2 and the anodic corrosion of lead and lead alloys." J. of Electrochem. Soc. 105, No. 7, 369 (1958).

34. Pourbaix, M. "Atlas of electrochemical equilibria in aqueous solutions." Houston, Texas. National Association of Corrosion Engineers, (1974), p. 489.

35. Delahay, P., Pourbaix, M., and Van Rysselberghe, P. "Potential pH diagram of lead and its applications to the study of lead corrosion and to the lead storage battery." J. Electrochem. Soc. 98, No. 2, 57 (1951).

36. Kuhn, A. T., and Wright, P. M. Industrial electrochemical processes. North Holland Publ. Co. (1971), p. 525.

37. Burbank, J. J. "Anodization of lead and lead alloys in sulfuric acid." J. of Electrochem. Soc. 104, 693 (1957).

38. Lander, J. J. "Further studies on the anodic corrosion of lead in H_2SO_4 solutions." J. of Electrochem. Soc. 103, 1 (1956).

39. Rüetschi, P., and Cahan, B. D. "Anodic corrosion and hydrogen and oxygen overvoltage on lead and lead antimony alloys." J. of Electrochem. Soc. 104, No. 7, 406 (1957).

40. Grigger, J. C., Miller, H. C., and Loomis, F. D. "Lead dioxide anode for commercial use." J. Electrochem. Soc. 105, 100 (1958).

41. Gibson, F. D. "Inert lead dioxide anode and process of production." U.S. Pat. 893,823. (April 11, 1962).

42. Standard methods for the examination of water and waste water. American Public Health Association, 12th ed. (1955) pp. 516, 511.

43. Shields, J. R., and Coull, J. "Rate studies in the electrochemical oxidation of phenol." Trans. Am. Electrochem. Soc. 80, 113 (1941).

44. Wesley, W. Water quality engineering for practicing engineers. Barnes & Noble, New York (1970), p. 25.

45. Pickett, D. J., and Stanmore, B. R. "An experimental study of a single layer packed bed cathode in an electrochemical flow reactor." J. App. Electrochem. 5, 95 (1957).

46. Grot, W. G. F., Munn, G. E., and Walmsley, P. N. "Perfluorinated ion exchange membranes." 141st meeting of the Electrochemical Soc. Houston, Texas, May 7, 1972.

47. Sedahmed, G. H. "Mass transfer behaviour of gas evolving particulate-bed electrode." J. of Appl. Electrochem. 9, 37 (1979).

48. Alkire, R. "Two dimensional current distribution within a packed bed electrochemical flow reactor." J. Electrochem. Soc. 121, No. 1, 95 (1974).

49. Perry, R. H., and Chilton, C. H. Chemical engineers handbook. Fifth edition, McGraw Hill, New York (1973).

50. Bird, R. B., Stewart, W. E., and Lightfoot, E. N. Transport phenomena. John Wiley & Sons, Inc., New York (1960) p. 515.

51. Weast, R. Handbook of chemistry and physics. The Chemical Rubber Co. 53rd edition (1972/73).

APPENDIX 1

Specification of Auxiliary Equipment and Materials

Power supply

Sorenson DCR 40-25B
  Voltmeter range: 0-40V
  Am meter range: 0-25A

Voltmeter

Central Scientific Co., D.C. Voltmeter
  Scales: 0-1.5 volts
          0-15 volts

Rotameters

a) Anolyte:

Brooks, full view indicating rotameter
  Type: 7-1110
  Tube No.: R-7M-25-1
  Float: 316 stainless steel
  Max. flow: 1400 cc/min (s.g. = 1)
  Scale: 0-100% linear

b) Catholyte:

Brooks, full view indicating rotameter
  Type: 8-1110
  Tube No.: R-8M-25-2
  Float type: 8-RS-8
  Max. flow: 1 U.S. G.P.M. (s.g. = 1)
  Scale: 0-250 mm linear

Gas liquid separators

2.5 cm I.D. and 60 cm long glass tube. Liquid outlet located at 40 cm from the bottom. Packed to approximately 20 cm depth with 2 mm diameter glass beads.

Filters

3.0 cm I.D. and 15 cm long glass tube filled with glass wool (Merck).

Pressure gauges

Marsh-type 3-100-SS with 316 stainless steel tube
Scale: 0-30 psi (1/4 psi/div).

Pumps

Barrish Pumps Co., N.Y.
Model type: 12A-60-316
Flow data: 21 6.P.H. at 40 psid, 29 6.P.H. at 0 psid. (psid indicates outlet pressure minus inlet pressure.) Pumps are preset at 45 psid but are adjustable to 65 psid max.

pH meter

Corning, Model 101 (accuracy ± 0.001 pH)
Electrode: Fisher, plastic body-protected bulb type
Model No. 13-639-97

Conductivity meter

Seibold, Model LTA. Provided with adjustable maximum ranges (from 1 mmho cm^{-1} to 100 mmho cm^{-1} maximum)
Conductivity cell constant = 0.88 cm^{-1}

Tubing

Imperial Eastman "Poly Flo" 66-P-3/8"

Valves

Whitey, forged body regulating
316 stainless steel. 3/8" connections

Fittings

Swagelok compression tube fittings
316 stainless steel 3/8"

Membranes

a) IONAC membranes
The IONAC membranes are supplied by Ionac Chemical Sybron Corporation, Birmingham, N.J.
Table A-1 includes some of the specification sent by the manufacturer.

b) NAFION 127 membrane
Supplied by duPont de Nemours & Co., Delaware.
NAFION 127 consists of an homogeneous film of 1200 equivalent weight polymer, 7 mils thick (perfluorosulfonic acid polymer). Supports are made from teflon.
Details of membrane properties such as strength, ionic transport, water permeability etc., are available in a publication supplied by the manufacturer (46).

TABLE A-1

SUMMARY OF TYPICAL PROPERTIES OF IONAC MEMBRANES

Property	Cation Exchange Membranes MC-3142	MC-3470	Anion Exchange Membranes MA-3475
Electrical Resistance (ohm-cm^2, A.C. measurement)			
0.1N NaCl	14	12	17
1.0N NaCl	5	6	8
% Perselectivity			
(0.5N NaCl/1.0N NaCl)	94.1	96.2	99.0
(0.2N NaCl/0.1N NaCl)	99.0		
Water Permeability (ml/hr/$ft.^2$/5 psi)	negligible	(less than 30)	(less than 30)
Mullen Burst Strength (minimum psi.)	175	200	200
Membrane Thickness (mils)	7	15	15
Approx. Density			
Net as shipped $oz./yd^2$	6	12	12
g/m^2	202	405	405
Capacity meq/g	1.08	1.22	0.70
Dimensional Stability (ability to rewet after drying)	good	good	good
Chemical Stability	up to 60°C	up to 125°C	up to 125°C
H_2SO_4	up to 5%	up to 35%	Superior to
HCl	up to 4%	conc. HCl	MC-3470 in low
NaOH	NR*	50% NaOH	and high pH
Salt	OK at all conc.	OK at all conc.	media
Size			
Available nominal sheet sizes (inches	40 × 120	40 × 120 30 × 96	40 × 120

*Not recommended

Plastic screens

Supplied by Chicopee Manufacturing Co., Georgia
Saran type
Max. operating temperature = 125°F
Chemical resistance: good resistance to acids and most alkalis
Style: 6100900
Weight/sq.yd. = 7 oz.
Polypropylene type
Max. operating temperature: 180°F
Chemical resistance: excellent resistance to most acids and alkalis with exception of chlorosulfonic acids and oxidizing agents
Style: 60070XX
Weight/sq.yd. = 8.7 oz.
Cathode chamber packing material
Stainless steel 304 - 20 × 20 mesh

Analytic equipment and operating conditions specifications

a) Gas chromatography specifications
Gas chromatograph
Manufacturer: Varian Aerograph
Model: 1440 series, single column model
Detector: H_2 flame ionization detector
Chromatographic column
Supplier: Western Chromatography Supplies, New Westminster, B.C.
Material: glass
Dimensions: 2mm I.D., 6.4 mm O.D., 6 ft long
Packing: 10% SP-2100 ON 100/120 Supelcoport (details of the packing are given in Bulletin 742D by Supelco, Inc.)
Operating conditions
Injector port temperature 150°C
Column temperature 120°C
Detector temperature 175°C
Carrier gas N_2
Carrier gas flow 30 ml/min
Air flow 300 ml/min
H_2 flow 30 ml/min
Attenuation setting 4×10^{-10}
Recorder
Model: Corning 840 series
Response 1 mv full scale
Chart speed: 1 cm/min
Syringe
Supplier: Unimetrics
Sample size: 1 µℓ

b) T.O.C. analysis specifications

Model: Beckman 915 total organic carron
Analyzer: Beckman 865 infrared analyzer

Operating conditions

Temperature of the total carbon channel 1000°C
Temperature of the inorganic carbon channel 150°C
Oxygen flow in each channel 250 ml/min

Syringe

Hamilton with automatic plunger
Sample size 50 µℓ

Recorder

Model: Hewlett Packard 7127A
Response: 1 mv full scale
Chart speed: 1 cm/min

c) Atomic absorption specifications

Manufacturer: Jarrel Ash, Division of Fisher Sci. Co.
Model: 810 Atomic absorption spectrophotometer
Lead lamp: Westinghouse hollow lead cathode
Wave length: 2170 A
Flame: rich (air-acetylene)

Recorder

Hewlett Packard 7127A
Speed: variable
Range: 1 or 2 mv full scale

Reagents

Phenol--liquified reagent
Matheson Coleman & Bell Manuf. Chem.
Code: PX 511-CB-1040
Assay: min 88% phenol, max 12% H_2O

NaOH--pellets, reagent
American Scientific Chemical
Code: SS 350
Assay: NaOH min 98%

H_2SO_4--reagent A.C.S.
Allied Chemical
Code: 001180-009580
Assay: 95.5-96.5%

Na_2SO_4--anhydrous reagent grade
American Scientific and Chemical SS 530

Buffers: Fisher Scientific (2 ± 0.02)
American Scientific and Chemical (10 ± 0.01)

Lead standard solution for atomic absorption:
Fisher Scientific, 1000 ppm

Water for solutions: single distilled water

APPENDIX 2

Experimental Data

1. Characteristics of each group of experiments

Group No. 1

a) Mode of operation:
Batch experiments using the divided cell and the anodized lead electrode

b) Cell description:
Cathode: Stainless steel 316 plate and mesh
Anode: Fresh lead feeder plate and particles
Particles: lead spheres
Size: dp = 2 mm
Weight: 250 g
Volume: $\frac{250\ g}{11.337\ g/cc} = 22\ cm^3$ (ref 49)
Void fraction: $\varepsilon = (57 - 22)/57 = 0.61$
Membranes tested:
IONAC MC-3142 or IONAC MC-3470 protected by saran screen

Group No. 2

a) Mode of operation:
Batch experiments using the divided cell and the electrodeposited PbO_2 electrode

b) Cell description:
Cathode: Stainless steel 316 feeder plate and mesh
Anode: PbO_2 electrodeposited on graphite feeder plate
Particles: electrodeposited PbO_2 crushed and sized
Size: $1.7 < dp < 2.0$ mm
Weight: 215 g
Volume: 23 cm^3
Void fraction (ε) = 0.6
Membranes tested:
Cationic membranes: IONAC MC-3470
NAFION 127
Anionic membrane: IONAC MA 3475
In all runs, a saran screen was located between particles and membrane to prevent membrane breaking and short circuit. The only exception was Run 2-1 where a polypropylene screen was used.

Group No. 3

a) Mode of operation:
Batch experiments using the undivided cell (only one chamber) and the electrodeposited PbO2 electrode

b) Cell description:
Cathode: stainless steel 316 plate (no packing mesh used to avoid by-passing of the liquid)
Anode: feeder and particles are the same as described in group No. 2.
Separator: two pieces of saran screen between cathodic plate and PbO_2 particles

Group No. 4

a) Mode of operation:
Continuous experiments (single pass) using the undivided cell and electrodeposited PbO_2 anode
b) Cell description:
The same as in group No. 3 with exceptions of Runs 4-7 and 4-8.
In Run 4-7: the anode was the feeder plate only (without particles)
In Run 4-8: the particles had the following characteristics:
Size: $0.7 < dp < 1.1$ mm
Weight: 230 g
Volume: 24.5 cm
Void fraction (ε) :$(57 - 24.5)/57 = 0.57$

2. Volume, flow pressure and temperature of the electrolytes

For groups No. 1 and No. 2 (unless otherwise stated)

Electrolyte	Volume (ℓ)	Flows (ℓ/min)	P^+ (kPa)
Anolyte	5	1.12	2.40
Catholyte	5	1.54	2.40

+Pressures may vary ± 20 kPa due to gas evolution.

Note: The symbol (*) which appears in each Run table (Groups 1 and 2) indicates that the catholyte pH and electrical conductivity reported were measured on sample diluted by a factor of ten.

For group No. 3 the electrolyte volume flow and pressure are the same given for the anolyte in groups No. 1 and 2 with exception of Run 3-15 where data are recorded.

In experiments group No. 4 the electrolyte flow was varied and therefore the pressure, too. Data are then reported in each particular Run table.

Temperatures

All the experiments were set up at room temperature (22 to 24°C). During the batch experiments (groups 1,2,3) at currents below or equal to 10 A the electrolyte temperatures remained constant. But for all those experiments performed at 20 A (i.e., Runs 3-4, 3-5) a temperature increase of 4°C was always detected in the recirculation tank (after the 120 min run). Also, when working at 30 A the electrolyte temperature rose about 12°C (i.e., Runs 3-6 and 3-7).

For the continuous experiments (group No. 4) the temperature variations at a given current are a function of the flow and will be reported in each experiment table.

3. Anodization

Before each experiment the anode was treated with 20% H_2SO_4 at 10 A for 1 hour. (Refer to experimental method section.) Any exception to the standard procedure is given in the particular run table.

RUN 1-1

Membrane: IONAC MC-3142

Anodization: Starting from the fresh lead particles for 1 h (at the specified conditions)

Electrolytes	Approx. Conc.	pH
Anolyte	1% H_2SO_4	1.5
Catholyte	10% H_2SO_4	1.0*

I = 20 A c.d. = 1052.6 A/m^2

t (min)	ΔV (V)	T.O.C. (mg/l)	% T.O.C.
0	7.3	72	0
15	6.8	68	6
30	6.5	62	14
60	5.7	59	17
90	5.7	57	21
120	5.6	52	28

Comments: Particles showed an homogeneous brown colour after the 1 h anodization.

*Indicates that the pH was measured on a sample diluted by a factor of 10.

RUN 1-2

Membrane: MC-3142

Anodization: Starting from fresh lead particles for 12 h (at the specified conditions)

Electrolytes	Approx. Conc.	pH
Anolyte	1% H_2SO_4	1.5
Catholyte	10% H_2SO_4	1.1*

I = 20 A c.d. = 1052.6 A/m^2

t (min)	ΔV (V)	T.O.C. (mg/l)	% T.O.C.	(Pb) (mg/l)
0	7.3	80	0	0
15	6.9	75	6	
30	6.4	72	11	0.8
60	5.8	66	18	0.7
90	5.6	61	24	0.6
120	5.5	5	30	0.4

Comments: Particles showed homogeneous brown coating (with the same appearance than after Run 2-1)

RUN 1-3

Membrane: IONAC MC-3142

Anodization: The bed was originally anodized for 12 h and then was reanodized for 1 h before the run

Electrolyte	Conc.	pH
Anolyte	5 g/l NaCl	5.4
Catholyte	10% H_2SO_4	1.0*

I = 10 A c.d. = 526.3 A/m^2

t (min)	ΔV (V)	T.O.C. mg/l	T.O.C. (%)
0	10	73	0
15	5	55	24
30	3	52	28

Comments: It was observed that the glass wool filter collected small fragments that had flaked off the electrode, and the solution took a dark grey colour, indicating that the electrode was rapidly dissolving. When the cell was opened the electrode had lost the brown oxide coating showing the underlaying grey lead. The membrane was fouled with deposits.

RUNS 1-4 to 1-8

(Corrosion studies on anodized lead)

Membrane: IONAC MC3142
Anodization time: 12 h starting from fresh lead, and 1 h prior to each run
I = 10 A c.d. = 526.3 A/m^2
Catholyte: 25 g/l NaOH (pH_c^* = 12.7 $K_{e_c}^*$ = 14 × 10^{-3} $(\Omega\ cm)^{-1}$)

Run No.	1-4			1-5		1-6		1-7		1-8	
Anolyte	5 g/l NaOH			5 g/l Na_2SO_4 NaOH to adj. pH		30 g/l Na_2SO_4 NaOH to adj. pH		30 g/l Na_2SO_4 NaOH to adj. pH		30 g/l Na_2SO_4 NaOH to adj. pH	
t (min)	pH	(Pb)[1] (mg/l)	(Pb)[2] (mg/l)	pH	(Pb) (mg/l)	pH	(Pb) (mg/l)	pH	(Pb) (mg/l)	pH	(Pb) (mg/l)
0	12.7	140	0.0	9.8	0.0	9.8	0.0	12.0	0.0	7.0	0.0
15	12.6	36	2.7	2.9	1.7	3.2	4.2	3.4	5.0	2.5	3.4
30	12.5	24	1.7	2.7	1.6	2.9	3.5	2.9	5.0	2.2	3.0
45	12.4	13	1.7	2.6	1.4	2.8	2.7	2.6	4.3	2.0	2.3
60	11.8	3	0.7	2.5	1.3	2.7	2.0	2.5	3.3	1.9	2.2
75				2.4	1.1	2.6	1.7	2.4	3.0	1.8	2.0
90				2.3	0.8	2.5	1.4	2.3	2.3		

[1]The electrolytes were recirculated without a potential applied.
[2]A potential was applied before the electrolytes entered the cell.
*Measured on a sample diluted by a factor of 10.

RUN 1-9

Membrane: IONAC MC-3470
I = 10 A c.d. = 526.3 A/m^2

Electrolytes	Concentration	$K_e \times 10^3$ $(\Omega\ cm)^{-1}$	pH
Anolyte	5 g/1 Na_2SO_4 NaOH to adjust pH	6.4	9.41
Catholyte	25 g/1 NaOH	16*	12.6*

t (min)	ΔV (V)	$K_{e_a} \times 10^3$ $(\Omega\ cm)^{-1}$	pH_a	Phenol (mg/1)	Phenol (%)	T.O.C. (mg/1)	T.O.C. (%)	(Pb) (mg/1)
0	6.0	6.4	9.41	104		80		
15	6.0	7.9	3.00	55	47	74	8	2.2
30	5.7	9.0	2.80	42	60	72	11	1.7
45	5.4	10.5	2.70	33	68	71	13	1.5
60	5.2	11.5	2.63	27	74	70	14	0.9
75	5.0	12.0	2.58	19	82	68	15	0.3
90	5.0	12.7	2.54	11	89	67	16	0.3

RUN 2-1

Membrane: IONAC MC-3470 against polypropylene screen
I = 10 A c.d. = 526.3 A/m^2

Electrolyte	Concentration	$K_e \times 10^3$ $(\Omega\ cm)^{-1}$	pH
Anolyte	5 g/l Na_2SO_4 NaOH to adjust pH	6.4	9.44
Catholyte	25 g/l NaOH	14*	12.7*

t (min)	ΔV (V)	$K_{e_a} \times 10^3$ $(\Omega\ cm)^{-1}$	pH_a	Phenol (mg/l)	Phenol (%)	T.O.C. (mg/l)	T.O.C. (%)	(Pb) (mg/l)
0	12.9	6.4	9.44	102.0	-	78	0	0.0
15	15.0	8.1	3.04	51.0	50			0.2
30	16.0	9.4	2.80	29.0	71	72	8	0.1
45	16.0	11.0	2.67	9.0	91			
60	15.0	12.0	2.58	1.0	99	67	14	0.1
75	14.0	12.5	2.52	0.0	100			
90	14.0	13.0				65	16	0.1
105	13.5	13.5	2.48					
120	13.5	14.0	2.42			62	21	0.0

Comments: The polypropylene screen produces a higher potential drop compared with the saran screen.

RUN 2-2

Membrane: IONAC MC-3470 against saran screen
I = 10 A c.d. = 526.3 A/m^2

Electrolyte	Concentration	$K_e \times 10^3$ $(\Omega\ cm)^{-1}$	pH
Anolyte	5 g/l Na_2SO_4 NaOH to adjust pH	6.5	9.42
Catholyte	25 g/l NaOH	14*	12.6*

t (min)	ΔV (V)	$K_{e_a} \times 10^3$ $(\Omega\ cm)^{-1}$	pH_a	Phenol (mg/l)	Phenol (%)	T.O.C. (mg/l)	T.O.C. (%)	(Pb) (mg/l)
0	8.0	6.5	9.42	100	-	77		0.0
15	8.0	7.8	3.12	45	55	72	6	0.2
30	8.0	8.8	2.9	25	75	70	9	0.1
45	7.9	9.5	2.82	11	89	68	13	0.1
60	7.5	10.5	2.75	5	95	66	14	0.0
75	7.3	11.0	2.68	2	98	65	16	0.0
90	7.1	11.5	2.60	0	100	64	17	0.0
105	7.0	12.0	2.58			63	18	
120	7.0	12.0	2.56			61	21	

RUN 2-3

Membrane: IONAC MC-3470
I = 0 (no current applied)

Electrolyte	Concentration	$K_e \times 10^3$ $(\Omega\ cm)^{-1}$	pH
Anolyte	5 g/l Na_2SO_4 NaOH to adjust pH	6.5	9.47
Catholyte	25 g/l NaOH	14*	12.7*

t (min)	ΔV (V)	$K_{e_a} \times 10^3$ $(\Omega\ cm)^{-1}$	pH_a	Phenol (mg/l)	T.O.C. (mg/l)	(Pb) (mg/l)
0	0.8	6.5	9.47	95	73	0.0
15	0.75	5.7	10.74	95	73	0.5
30	0.7	6.1	11.22	95	73	0.7
45	0.01	6.3	11.47	95	73	1.0
60		6.6	11.64	95	73	1.2
75		6.6	11.8	95	73	1.5
90		6.6	11.9			2.0

Comments: No appreciable change in phenol or T.O.C. concentration was detected, but while the first 3ℓ were withdrawn (to purge the system), the solution showed the brownish colour characteristic of the oxidation of phenol.

RUN 2-4

Membrance: IONAC MC-3470
I = 3 A c.d. = 157.9 A/m^2

Electrolyte	Concentration	$K_e \times 10^3$ $(\Omega\ cm)^{-1}$	pH
Anolyte	5 g/l Na_2SO_4 NaOH to adjust pH	6.2	9.44
Catholyte	25 g/l NaOH	15*	12.6*

t (min)	ΔV (V)	$K_{e_a} \times 10^3$ $(\Omega\ cm)^{-1}$	pH_a	Phenol (mg/l)	Phenol (%)	T.O.C. (mg/l)	T.O.C. (%)	(Pb) (mg/l)
0	4.7	6.2	9.44	100	-	77		0.1
15	4.7		11.70	83	17	76	1	0.4
30	4.7	7.0	11.77	68	32	73	5	0.4
45	4.5		11.82	58	42	70	9	0.4
60	4.5	7.2	11.83	53	47	66	14	0.4
75	4.5		11.84	49	51	64	17	0.4
90	4.5	7.2	11.88	43	57	63	18	0.4
105	7.9		3.38	18	82	58	25	0.4
120	7.9	8.0	3.00	6	94	44	43	0.3
135	7.7		2.80	2	98	40	48	0.2
150	7.5	9.0	2.73	0	100	37	52	0.2

Note: Current was changed to 10 A at 90 min to observe pH response. During the high pH interval the solution had a brown-reddish colour and after the pH drop the colour changed to light yellow.

RUN 2-5

Membrane: IONAC MC-3470
I = 6 A c.d. = 315.8 A/m^2

Electrolyte	Concentration	$K_e \times 10^3$ $(\Omega\ cm)^{-1}$	pH
Anolyte	5 g/l Na_2SO_4 NaOH to adjust pH	6.2	9.42
Catholyte	25 g/l NaOH	15*	12.6*

t (min)	ΔV (V)	$K_{e_a} \times 10^3$ $(\Omega\ cm)^{-1}$	pH_a	Phenol (mg/l)	Phenol (%)	T.O.C. (mg/l)	T.O.C. (%)
0	5.8	6.2	9.42	85			
15			3.74	49	42	65	4
30	5.7	6.5	3.50	28	67	62	7
45			3.21	19	78	59	10
60	5.6	7.1	3.05	12	86	56	14
75			2.88	7	92	54	17
90	5.5	8.3	2.80	5	94	53	18
105			2.78	2	98	53	18
120	5.5	8.5	2.76	0	100	52	20

RUN 2-6

Membrane: IONAC MC-3470
I = 20 A c.d. = 1052.6 A/m^2

Electrolyte	Concentration	$K_e \times 10^3$ $(\Omega\ cm)^{-1}$	pH
Anolyte	5 g/l Na_2SO_4 0.44 g/l H_2SO_4	8.5	2.45
Catholyte	25 g/l NaOH	14*	12.7*

t (min)	ΔV (V)	$K_{e_a} \times 10^3$ $(\Omega\ cm)^{-1}$	pH_a	Phenol (mg/l)	Phenol (%)	T.O.C. (mg/l)	T.O.C. (%)
0	12.7	8.5	2.45	105		81	
15	12.4			24	77	81	0
30	9.7	12.5	1.80	5	95	80	1
45	8.9			2	98	78	4
60	8.7	15.5	1.67	1	99	72	11
75	8.4			0	100	66	18
90	8.2	17.0	1.58			59	27
105	7.9					52	36
120	7.8	17.5	1.50			42	48

RUN 2-7

Membrane: IONAC MC-3470
I = 10 A c.d. = 526.3 A/m^2

Electrolyte	Concentration	$K_e \times 10^3$ $(\Omega\ cm)^{-1}$	pH
Anolyte	5 g/l Na_2SO_4 0.44 g/l H_2SO_4	8.3	2.46
Catholyte	25 g/l NaOH	14*	12.7*

t (min)	ΔV (V)	$K_{e_a} \times 10^3$ $(\Omega\ cm)^{-1}$	pH_a	Phenol (mg/l)	Phenol (%)	T.O.C. (mg/l)	T.O.C. (%)
0	7.5	8.3	2.46	100	0	75	0
15				30	70		
30	6.7	10.5	1.96	8	92	74	1
45				4	96		
60	6.3	12.5	1.81	2	98	74	1
75				0	100		
90	6.0	14.0	1.72			72	4
105							
120	5.9	15.0	1.66			67	11

RUN 2-8

Membrane: NAFION 127
I = 10 A c.d. = 526.3 A/m^2

Electrolyte	Concentration	$K_e \times 10^3$ $(\Omega\ cm)^{-1}$	pH
Anolyte	5 g/l Na_2SO_4 0.44 g/l NaOH	8.0	12.03
Catholyte	25 g/l NaOH	14*	12.6*

t (min)	ΔV (V)	$K_{e_a} \times 10^3$ $(\Omega\ cm)^{-1}$	pH_a	Phenol (mg/l)	Phenol (%)	T.O.C. (mg/l)	T.O.C. (%)
0	5.3	8.0	12.03	95		76	
15			2.1	53	44	75	1
30	5.5	9.0	1.8	20	79	74	3
45				7	93		
60	5.2	11.0	1.54	3	97	73	4
75				1	99		
90	5.1	13.0	1.38	0	100	70	8
120	5.0	14.5	1.29			67	12
150	4.9	15.0	1.26			66	13

Note: Colour change observed from brown reddish to yellow when the pH dropped.

RUN 2-9

Membrane: NAFION 127
I = 20 A c.d. = 1052.6 A/m^2

Electrolyte	Concentration	$K_e \times 10^3$ $(\Omega\ cm)^{-1}$	pH
Anolyte	5 g/l Na_2SO_4 0.44 g/l H_2SO_4	8.2	2.48
Catholyte	25 g/l NaOH	15*	12.7*

t (min)	ΔV (V)	$K_{e_a} \times 10^3$ $(\Omega\ cm)^{-1}$	pH_a	Phenol (mg/l)	Phenol (%)	T.O.C. (mg/l)	T.O.C. (%)
0	8.5	8.2	2.48	102		85	
15	7.5			37	64	84	1
30	6.8	12.5	1.7	4	91	82	3
45	6.4			1	98	77	9
60	5.9	15.0	1.67	0	100	72	15
75	5.5			0	100	67	21
90	5.5	16.5	1.64			63	26
105	5.5					58	32
120	5.5	17.5	1.62			53	38

RUN 2-10

Membrane: NAFION 127
I = 20 A c.d. = 1052.6 A/m^2

Electrolyte	Concentration	$K_e \times 10^3$ $(\Omega\ cm)^{-1}$	pH
Anolyte	5 g/l Na_2SO_4 5 g/l NaOH	30	12.84
Catholyte	25 g/l NaOH	15*	12.7

t (min)	ΔV (V)	$K_{e_a} \times 10^3$ $(\Omega\ cm)^{-1}$	pH_a	Phenol (mg/l)	Phenol (%)	Total Carbon (mg/l)	Inorg. Carbon (mg/l)	T.O.C. (mg/l)	(%)
0	3.9	30.0	12.84	102	0	82	0	82	
15	3.9	23.5	12.66	92	10	82	2	80	2
30	4.9	17.0	12.54	69	32	82	4	78	5
45	5.0	11.0	12.24	36	65	82	8	74	10
60		7.0	2.15	15	85	72	5	67	18
75	5.0	9.5	1.56	3	97	62	2	60	26
90	5.0	11.0	1.40	0	100	55	3	52	37
105	5.0								
120	5.0	13.5	1.28			43	0	43	48
135	5.0								
150	5.0	14.0	1.26			39	0	39	52

Comments: The colour of the electrolyte changed from brown reddish to yellow when the pH drop was produced.

RUN 2-11

Membrane: IONAC MA-3475 (anionic)
I = 20 A c.d. = 1052.6 A/m^2

Electrolyte	Concentration	$K_e \times 10^3$ $(\Omega\ cm)^{-1}$	pH
Anolyte	5 g/l Na_2SO_4 0.44 g/l H_2SO_4	8	2.4
Catholyte	25 g/l NaOH	15*	12.7*

t (min)	ΔV (V)	$K_{e_a} \times 10^3$ $(\Omega\ cm)^{-1}$	pH_a	Phenol (mg/l)	Phenol (%)	Carbon (mg/l) Total	Carbon (mg/l) Inorg.	Carbon (mg/l) T.O.C.	Carbon (%)
0	7.7	8.0	2.40	94	0	78	0	78	0
15			2.80	26	72		2	76	3
30	7.6	8.1	3.15	9	90	78	3	75	4
45			8.33	4	96		7	71	9
60	7.4	8.2	11.20	2	98	78	18	60	23
75			11.75	0	100		33	45	42
90	7.1	8.3	12.08			78	45	33	58
120	7.0	9.5	12.38			78	52	26	67
150	6.6	10.0	12.53			78	60	18	77

Comment: The anionic membrane showed a change in colour (from yellow to brown) after the run.

RUN 3-1

Electrolyte	I(A)	c.d. (A/m^{-2})
5 g/l Na_2SO_4 NaOH to adjust pH	10	526.3

t (min)	ΔV (V)	$K_e \times 10^3$ $(\Omega\ cm)^{-1}$	pH	Phenol (mg/l)	Phenol (%)	T.O.C. (mg/l)	T.O.C. (%)
0	9.7	6.2	9.46	110		84	
15	10.5	6.5	3.78	60	45	80	5
30	9.7	6.7	3.62	40	64	78	7
45	9.1	6.8	3.52	19	83	77	8
60	8.9	6.9	3.46	9	92	75	11
75	8.7	6.9	3.42	3	97	71	15
90	8.5	7.0	3.39	1	99	67	20
120	8.5	7.0	3.36	0	100	60	29

RUN 3-2

Electrolyte	I(A)	c.d. (A/m^{-2})
5 g/l Na_2SO_4 0.44 g/l NaOH	10	526.3

t (min)	ΔV (V)	$K_e \times 10^3$ $(\Omega\ cm)^{-1}$	pH	Phenol (mg/l)	Phenol (%)	Carbon (mg/l) Total	Carbon (mg/l) Inorg.	Carbon (mg/l) T.O.C.	% T.O.C.
0	6.5	8.0	11.98	106		81	0	81	
15	6.4	7.5	11.88	71	33	81	5	76	7
30	6.3	7.2	11.81	52	51	81	7	74	9
45	6.3	7.0	11.72	34	68	81	8	73	10
60	6.3	6.9	11.67	18	83	81	10	70	13
75	6.4	6.8	11.58	12	89	81	13	68	16
90	6.5	6.8	11.57	9	92	81	18	63	22
120	6.6	6.7	11.54	5	95	81	26	55	32

RUN 3-3

Electrolyte	I(A)	c.d. (A/m^{-2})
5 g/l Na_2SO_4 0.44 g/l H_2SO_4	10	526.3

t (min)	ΔV (V)	$K_e \times 10^3$ $(\Omega\ cm)^{-1}$	pH	Phenol (mg/l)	Phenol (%)	T.O.C. (mg/l)	T.O.C. (%)
0	7.8	8.4	2.50	93		75	
15	7.3	8.6		28	70	75	0
30	7.2	8.8	2.45	12	86	74	1
45	6.9	8.9		4	95	71	5
60	6.7	8.9	2.43	2	98	69	7
75	6.5	8.9		1	99	68	9
90	6.4	8.9	2.41	0	100	65	13
120	6.4	8.9	2.39			61	19
150	6.4	8.9	2.38			56	25

RUN 3-4

Electrolyte	I(A)	c.d. (A/m^{-2})
5 g/l Na_2SO_4 0.44 g/l H_2SO_4	20	1052.6

t (min)	ΔV (V)	K × 10^3 (Ω cm)$^{-1}$	pH	T (°c)	Phenol (mg/l)	Phenol (%)	T.O.C. (mg/l)	T.O.C. (%)
0	9.6	8.5	2.47	23	95	-	73	-
15	9.7	9.1	2.28		23	75	71	3
30	9.2	9.2	2.28	25	10	89	68	7
45	8.4	9.2	2.27		3	97	64	12
60	8.2	9.2	2.25	26	2	98	59	19
75	8.2	9.3	2.24		1	99	54	26
90	8.2	9.4	2.22	27	0	100	47	36
120	9.3	9.5	2.20	28			34	53
150	10.7	9.6	2.19	28			23	68

$(Pb)^-$ = undetectable.

RUN 3-5

Electrolyte	I(A)	c.d. (A/m^{-2})
5 g/l Na_2SO_4 0.44 g/l NaOH	20	1052.3

t (min)	ΔV (V)	$K_e \times 10^3$ $(\Omega\ cm)^{-1}$	pH	T (°C)	Phenol (mg/l)	Phenol (%)	Carbon (mg/l) Total	Carbon (mg/l) Inorg.	Carbon (mg/l) T.O.C.	(%)	(Pb) (mg/l)
0	9.2	8.2	12.04	24	102		86	0	86	0	0.0
15	9.1	7.9	11.91		48	53	84	6	78	9	0.2
30	8.9	7.7	11.76	25	26	75	84	13	71	17	0.2
45	8.9	7.5	11.56		12	88	84	22	62	28	0.0
60	9.0	7.2	11.26	26	3	97	84	30	54	37	0.0
75	9.4	7.1	10.76		0	100	84	37	46	46	0.0
90	10.4	7.1	10.26	27			84	46	38	56	0.0
120	11.4	7.1	9.56	28			83	60	23	73	0.0
150	12.0	7.0	8.84	28			81	62	19	78	0.0

RUN 3-6

Electrolyte	I(A)	c.d. (A/m^{-2})
5 g/l Na_2SO_4 0.44 g/l H_2SO_4	30	1578.9

t (min)	ΔV (V)	$K_e \times 10^3$ $(\Omega\ cm)^{-1}$	pH	T (°C)	Phenol (mg/l)	Phenol (%)	T.O.C. (mg/l)	T.O.C. (%)
0	14.0	8.6	2.48	24	96	-	76	
15	11.9	8.9	2.40	26	20	79	71	7
30	11.6	9.1	2.36	28	4	96	68	11
45	11.4	9.3	2.32	29	1	99	61	20
60	13.0	9.5	2.30	31	0	100	47	38
75	14.0	9.6	2.28	33	0	100	37	51
90	15.0	9.7	2.26	34			28	63
120	15.5	9.8	2.25	36			24	69

(Pb): undetectable

RUN 3-7

Electrolyte	I(A)	c.d. (A/m^{-2})
5 g/l Na_2SO_4 0.44 g/l NaOH	30	1578.9

t (min)	ΔV (V)	$K_e \times 10^3$ $(\Omega\ cm)^{-1}$	pH	T (°C)	Phenol (mg/l)	Phenol (%)	Carbon (mg/l) Total	Carbon (mg/l) Inorg.	Carbon (mg/l) T.O.C.	(%)
0	11.9	8.1	12.08	23	110	0	86	0	86	0
15	10.7		11.97	25	36	67	74	10	74	14
30	10.4	7.6	11.80	26	12	89	61	22	61	29
45	10.5		11.47	28	1	99	48	35	48	44
60	12.9	7.2	10.80	29	0	100	32	51	32	63
75	13.4		10.43	31			25	58	23	73
90	13.5	7.3	10.18	32			16	64	16	81
120	13.6	7.0	9.5	35			7	73	7	92

[Pb]: undetectable

RUN 3-8

Electrolyte	I(A)	c.d. (A/m^{-2})
5 g/l Na_2SO_4 0.44 g/l H_2SO_4	10	526.3

t (min)	ΔV (V)	$K_e \times 10^3$ $(\Omega\ cm)^{-1}$	pH	Phenol (mg/1)	Phenol (%)	T.O.C. (mg/1)	T.O.C. (%)
0	4.5	30.5	2.5	108	0	83	0
15				33	70	80	4
30	4.2	31.0	2.44	13	88	79	5
45				5	95	77	7
60	4.1	31.5	2.42	1	99	72	13
75				0	100	68	18
90	4.1	31.5	2.40			67	19
120	4.1	31.5	2.38			61	27

RUN 3-9

Electrolyte	I(A)	c.d. (A/m^{-2})
5 g/l Na_2SO_4 0.44 g/l NaOH	10	526.3

t (min)	ΔV (V)	$K_e \times 10^3$ $(\Omega\ cm)^{-1}$	pH	Phenol (mg/l)	Phenol (%)	Carbon (mg/l) Total	Inorg.	T.O.C.	(%)
0	4.6	32	12.06	105		80	0	80	0
15	4.6	32	11.88	72	31	80	2	78	3
30	4.6	32	11.81	48	54	80	5	75	6
45	4.6	32	11.64	38	64	80	8	72	10
60	4.6	32	11.41	18	83	80	14	66	18
75	4.6	32	10.96	7	93	80	20	60	25
90	4.6	32	10.36	1	99	80	27	53	34
120	4.6	32	9.24	0	100	80	40	40	50
150	4.6	32	7.7			72	45	27	66

RUN 3-10

Electrolyte	I(A)	c.d. (A/m^{-2})
30 g/l Na_2SO_4 0.44 g/l	20	1052.6

t (min)	ΔV (V)	$K_e \times 10^3$ $(\Omega\ cm)^{-1}$	pH	T (°C)	Phenol (mg/l)	Phenol (%)	T.O.C. (mg/l)	T.O.C. (%)
0	6.6	32	2.46	25	98	0	80	0
15					20	80	77	4
30	6.1	32	2.42	25	7	93	75	6
45					3	97	70	13
60	6.0	32	2.40	26	1	99	65	19
75					0	100	58	28
90	6.2	32	2.38	28			54	33
120	6.4	32					40	50
150	6.7	32	2.36	28			28	65

RUN 3-11

Electrolyte	I(A)	c.d. (A/m^{-2})
30 g/l Na_2SO_4 0.44 g/l NaOH	20	1052.6

t (min)	ΔV (V)	$K_e \times 10^3$ $(\Omega\ cm)^{-1}$	pH	Phenol (mg/l)	Phenol (%)	Carbon (mg/l) Total	Carbon (mg/l) Inorg.	Carbon (mg/l) T.O.C.	(%)
0	4.4	32.0	12.03	113	0	87	0	87	
15				54	52	87	7	80	8
30	4.4	31.5	11.93	29	74	87	13	74	15
45				14	88	87	22	65	25
60	4.5	31.0	11.70	3	98	87	32	55	37
75				0	100	87	40	47	45
90	4.6	30.5	11.16			87	51	36	59
120	4.7	30.0	10.42			87	65	22	75
150						87	70	17	80

RUN 3-12

Electrolyte	I(A)	c.d. (A/m^{-2})
5 g/l Na_2SO_4 0.44 g/l H_2SO_4	10	526.3

t (min)	ΔV (V)	$K_e \times 10^3$ (Ω cm)$^{-1}$	pH	Phenol (mg/l)	Phenol (%)	T.O.C. (mg/l)	T.O.C. (%)
0	8.7	8.0	2.43	525	0	395	
15				320	39		
30	8.6	8.7	2.25	175	67	380	4
45				75	86		
60	8.5	9.3	2.18	25	95	375	5
75				15	97		
90	8.2	9.3	2.16	5	99	370	8
120	7.8	9.3	2.14	0	100	350	11

RUN 3-13

Electrolyte	I(A)	c.d. (A/m^{-2})
5 g/l Na_2SO_4 0.44 g/l H_2SO_4	10	526.3

t (min)	ΔV (V)	$K_e \times 10^3$ $(\Omega\ cm)^{-1}$	pH	Phenol (mg/l)	Phenol (%)
0	9.3	8.7	2.42	1100	0
15				792	28
30	8.3	8.9	2.32	506	54
45				341	69
60	8.0	8.9	2.28	187	83
75				88	92
90	7.9	9.1	2.27	22	98
120	7.8	9.2	2.26	5	100

Comment: The net change in T.O.C. was practically undetectable due to the high amount of carbon present in solution.

RUN 3-14

Electrolyte	I(A)	c.d. (A/m^{-2})
5 g/l Na_2SO_4 2.2 g/l H_2SO_4	10	526.3

t (min)	ΔV (V)	$K_e \times 10^3$ $(\Omega\ cm)^{-1}$	pH	Phenol (mg/l)	Phenol (%)	T.O.C. (mg/l)	T.O.C. (%)
0	5.4	13.5	1.8	90		77	
15	5.2	13.7		30	67	74	4
30	5.1	14.0	1.78	9	90	73	5
45	5.0	14.2		3	97	72	6
60	4.9	14.3	1.75	1	99	69	10
75	4.9	14.5		0	100	68	12
90	4.9	14.5	1.75			66	14
120	4.9	14.5	1.75			64	17

RUN 3-15

Electrolyte	I(A)	c.d. (A/m^{-2})	Q (ℓ/min)	P(Kpa)
5 g/l Na_2SO_4 0.44 g/l H_2SO_4	20	1052.6	0.55	145

t (min)	ΔV (V)	$K_e \times 10^3$ $(\Omega\ cm)^{-1}$	pH	Phenol (mg/1)	Phenol (%)	T.O.C. (mg/1)	T.O.C. (%)
0	12.1	8.3	2.5	105	0	79	0
15				28	73	74	6
30	10.5	8.5	2.43	9	91	71	10
45				2	98	69	13
60	10.9	8.7	2.40	1	99	62	22
75				0	100	55	30
90	11.1	8.8	2.38			48	39
120	12.0	8.9	2.37			36	54

RUN 4-1

Electrolyte	I(A)	c.d. (A/m^{-2})	$K_e \times 10^3$ $(\Omega\ cm)^{-1}$	pH	T_{in} (°C)	Phenol C_{in} (mg/1)
5 g/1 Na_2SO_4 0.44 g/1 H_2SO_4	10	526.3	7.9	2.5	24	100

Q (ℓ/min)	ΔV (V)	P (kPa)	T_{out} (°C)	Phenol C_{out} (mg/1)	(%)
0.11	8.7	108	32	9	91
0.25	8.6	120	28	42	58
0.40	8.3	129	26	55	45
0.55	7.9	143	25	67	33
0.85	7.4	184	24	75	25
1.10	7.1	232	24	79	21

RUN 4-2

Electrolyte	I(A)	c.d. (A/m^{-2})	$K_e \times 10^3$ $(\Omega\ cm)^{-1}$	pH	T_{in} (°C)	Phenol C_{in} (mg/l)
5 g/l Na_2SO_4 0.44 g/l H_2SO_4	10	526.3	8.1	2.5	24	105

Q (ℓ/min)	ΔV (V)	P (kPa)	T_{out} (°C)	Phenol C_{out} (mg/l)	(%)
0.25	8.6	119	27	43	60
0.40	8.5	129	26	60	44
0.55	8.3	143	25	71	34
0.85	7.8	184	25	80	26
1.10	7.3	232	24	85	21
1.30	7.0	280	24	90	17

RUN 4-3

Electrolyte	I(A)	c.d. (A/m^{-2})	$K_e \times 10^3$ (Ω cm)$^{-1}$)	pH	T_{in} (°C)	Phenol C_{in}(mg/1)
5 g/1 Na_2SO_4 0.44 g/1 H_2SO_4	10	526.3	8.0	2.5	23	95

Q (ℓ/min)	ΔV (V)	P (kPa)	T_{out} (°C)	Phenol C_{out}(mg/1)	(%)
0.250	8.7	108	27	39	59
0.400	8.6	120	25	53	44
0.550	8.3	129	24	63	34
0.850	7.9	143	24	72	24
1.100	7.4	184	23	76	20
1.300	7.1	232	23	81	17

RUN 4-4

Electrolyte	I(A)	c.d. (A/m^{-2})	$K_e \times 10^3$ $(\Omega\ cm)^{-1}$	pH	T_{in} (°C)	Phenol C_{in} (mg/l)
5 g/l Na_2SO_4 0.44 g/l H_2SO_4	10	526.3	8	2.45	23	580

Flow (ℓ/min)	ΔV (V)	P (kPa)	T_{out} (°C)	Phenol C_{out} (mg/l)	(%)
0.11	8.7	108	31	175	70
0.25	8.6	120	27	365	37
0.40	8.3	129	26	435	25
0.55	7.9	143	25	470	19
0.85	7.4	184	23	510	12
1.10	7.0	234	23	526	9

RUN 4-5

Electrolyte	I(A)	c.d. (A/m^{-2})	$K_e \times 10^3$ $(\Omega\ cm)^{-1}$	pH	T_{in} (°C)	Phenol C_{in} (mg/l)
5 g/l Na_2SO_4 0.44 g/l H_2SO_4	20	1052.6	7.9	2.43	24	110

Q (ℓ/min)	ΔV (V)	P (kPa)	T_{out} (°C)	Phenol C_{out} (mg/l)	(%)
.11	13.4	110	48	7	94
.25	13.4	122	38	40	63
.40	13.3	129	32	62	44
.55	12.6	145	27	73	34
.85	11.5	185	26	80	27
1.10	10.8	234	25	90	19

RUN 4-6

Electrolyte	I(A)	c.d. (A/m^{-2})	$K_e \times 10^3$ $(\Omega\ cm)^{-1}$	pH	T_{in} (°C)	Phenol C_{in} (mg/l)
5 g/l Na_2SO_4 0.44 g/l NaOH	20	1052.6	7.9	2.45	24	515

Q (ℓ/min)	ΔV (V)	P (kPa)	T_{out} (°C)	Phenol C_{out} (mg/l)	(%)
0.11	12.2	110	48	56	89
0.25	11.8	121	38	260	49
0.40	11.3	129	30	335	35
0.55	10.8	145	27	390	24
0.85	10.1	185	25	430	16
1.10	9.7	234	24	450	12

RUN 4-7

Electrolyte	I(A)	c.d. (A/m^{-2})	$K_e \times 10^3$ $(\Omega\ cm)^{-1}$	pH	T_{in} (°C)	Phenol C_{in} (mg/l)
5 g/l Na_2SO_4 0.44 g/l H_2SO_4	10	523.6	8.1	2.43	25	110

Q (ℓ/min)	ΔV (V)	P (kPa)	T_{out} (°C)	Phenol C_{out} (mg/l)	(%)
0.11	5.9	110	30	68	38
0.25	5.9	115	28	87	21
0.40	5.9	115	27	98	11
0.55	5.9	115	26	100	9
0.85	5.9	115	25	103	6
1.10	5.9	115	25	106	4

Note: The anode used was the feeder plate only (refer to general specifications). Therefore, the pressure was practically constant at 115 Kpa.

RUN 4-8

Electrolyte	I(A)	c.d. (A/m^{-2})	$K_e \times 10^3$ $(\Omega\ cm)^{-1}$	pH	T_{in} (°C)	Phenol C_{in} (mg/l)
5 g/l Na_2SO_4 0.44 g/l H_2SO_4	10	526.3	8.0	2.43	24	100

Q (ℓ/min)	ΔV (V)	P (kPa)	T_{out} (°C)	Phenol C_{out} (mg/l)	(%)
0.11	6.3	112	31	5	95
0.25	6.0	128	28	33	67
0.40	5.9	143	27	47	53
0.55	5.8	162	26	55	45
0.85	5.7	204	25	66	34
1.10	5.6	271	25	71	29

Note: This run corresponds to the smaller particle size ($0.7 < dp < 1.1$ mm). For bed data refer to general specifications.

APPENDIX 3

Mathematical Models

The electrochemical oxidation of phenol is a heterogeneous process that takes place on the surface of the anode. A simplified picture of the process is that the disappearance of phenol is the result of two steps which occur in series:

a) the transfer of phenol molecules or phenoxonium ions from the bulk of the solution to the surface of the electrode

b) an electrochemical reaction by which the phenol is converted into some oxidation products as discussed in Chapter 2.

Two limiting cases are considered in which either of the two steps are so slow that they control the overall rate of the process. Such models assume that adsorption phenomena and transfer of oxidation products from the electrode surface are not rate-limiting. A third case is also presented where both the resistance to mass transfer and to electrochemical reactions are comparable in magnitude.

1. Mass transfer controlled model

The model presented here deals with a packed bed electrochemical reactor operating continuously in plug flow.

Assumptions

- The resistance to the electrochemical reaction is negligible compared with the resistance to mass transfer. In other words, the concentration of phenol at the surface of the electrode is negligible

compared with the concentration of phenol in the bulk of the solution.

- Variations in phenol concentration in the directions perpendicular to the flow are neglected compared to the variations of concentration in the direction of flow.
- All the bed is active for phenol oxidation.

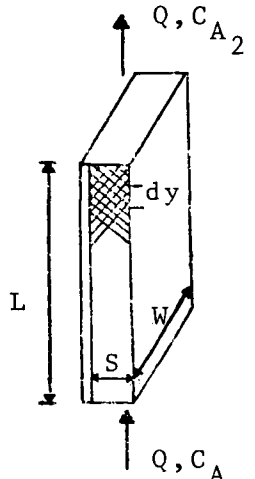

Fig.A-1 Plug-flow packed bed reactor

Mass balance for a differential height.

$$Q\, dC_{A_b} = - K_m\, a(S\, W\, dy)(C_{A_b} - C_{A_s}) \qquad [A.1]$$

The superficial velocity referred to the cross sectional area of the bed is given by:

$$u = Q/W\, S$$

Neglecting C_{A_s}, (Eq. A.1) can be expressed as:

$$dC_{A_b} = - \frac{K_m\, a\, dy}{u} C_{A_b}$$

integrating,

$$\int_{C_{A_1}}^{C_A(y)} \frac{dC_{A_b}}{C_{A_b}} = - \int_0^y \frac{K_m\, a\, dy}{u}$$

$$\ln \frac{C_A(y)}{C_{A_1}} = - \frac{K_m\, a\, y}{u} \qquad [A.2]$$

which can also be expressed in terms of the fractional conversion X, for $y = L, C_A(y) = C_{A_2}$

and

$$X = \frac{C_{A_1} - C_{A_2}}{C_{A_1}} = 1 - \frac{C_{A_2}}{C_{A_1}} \qquad [A.3]$$

then,

$$\ell n(1 - X) = - \frac{K_m \, a \, L}{u} \qquad [A.4]$$

The specific surface area of the bed is given by the sum of the specific surface area of the feeder plate plus the specific surface area of the particles, as

$$a = \frac{1}{S} + \frac{6(1 - \varepsilon)}{\xi \, dp} \qquad [A.5]$$

where ξ is a shape factor for the particles, and ε is the fraction of voids (49).

The average mass transfer coefficient can be estimated using the correlation by Pickett and Stanmore (45) as follows,

$$\frac{K_m \, dp}{D} = 0.83 \left(\frac{u \, dp}{\nu}\right)^{0.56} \left(\frac{\nu}{D}\right)^{1/3} \qquad [A.6]$$

for $23 < Re < 520$

This equation was developed using a single layer of spheres and correlated the experimental data within ± 10%.

It should be noted that the effect of gas evolution is not included in equation A.6. Studies of mass transfer on gas-evolving packed bed electrodes have been made recently (47), but for the case of a stationary solution where the motion of the electrolyte in the cell is only provided by gas bubbles. It was found that the rate of mass transfer was increased by gas evolution.

For the present case of forced convection, a correlation for mass transfer in gas evolving particulate electrodes could not be found in the literature. However, it is reasonable to expect that enhancement of the mass transfer coefficient due to gas bubbling is less significant than in free convection, since the electrolyte is mainly moved by mechanical circulation.

2. Electrochemical reaction controlled model

Assumptions

- The resistance to electrochemical reaction is so high that the concentration of phenol at the surface of the particles is equal to the concentration at the bulk of the solution.
- The oxidation reaction is assumed to be first order in phenol concentration.
- The electrode potential is assumed to be uniform all over the cell. This assumption represents a significant simplification because in reality an electrode potential distribution exists within and along the electrode (10).

In a differential length of the anode, the potential distribution would be as indicated in Fig. A-2.

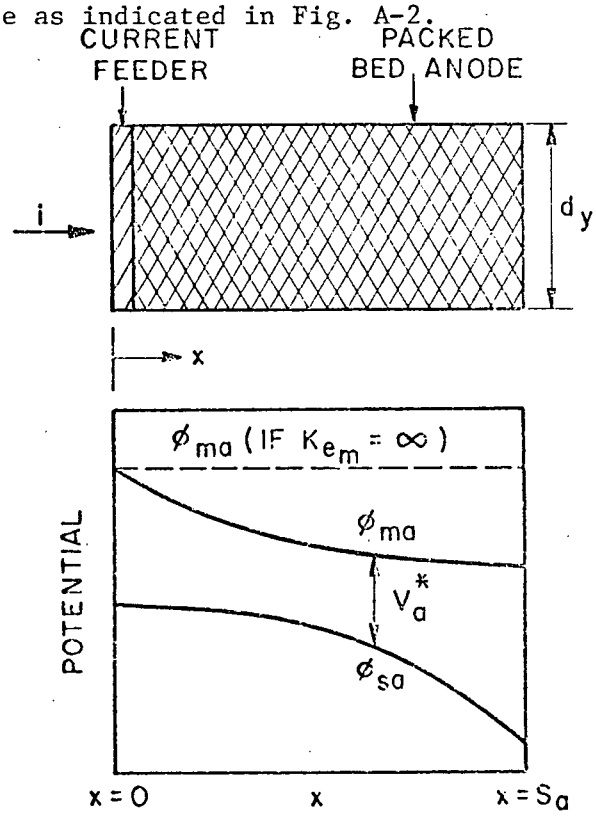

$$i_s = -K_{e_s} \frac{d\phi_s}{dx}$$

$$i_m = -K_{e_m} \frac{d\phi_m}{dx}$$

$$i = i_s + i_m.$$

The potential distribution in the x direction originates because the total charge at a central x is carried by both the metal and the solution.

Fig. A-2. Potential distribution in a particulate electrode.

The total charge at x = 0 is entirely carried by the metal of the feeder plate but at x = S_a the current is entirely carried by the solution. This implies that the metal potential presents its maximum gradient at x = 0 and the solution potential at x = S_a, so that the shape of the curves ϕ_m vs x and ϕ_s vs x are as indicated in the figure.

In the ideal case of a metal of infinite conductivity, the potential drop through the metal is zero and is represented by the horizontal dotted line. Generally, the conductivity of the metal is much greater than that of the electrolyte, therefore the solution potential drop would be greater than the metal potential drop. Thus, the electrode potential $V^* = \phi_m - \phi_s$ tends to increase towards x = S_a. This means that the side reactions are more likely to occur at the edge of the packed bed opposite to the feeder electrode.

A two dimensional model for potential, current, and concentration distributions has been developed (48) for a concentric cylindrical electrode, but the mathematical solution involved is extremely complicated.

The model to be presented here assumes that some average electrode potential exists within the cell. This permits a simple correlation of all the variables affecting the process.

For the case where the electrochemical reaction is the rate limiting step, the mass balance in a differential length of cell is:

$$Q\, dC_{A_b} = - K_{r_A}\, a\, S\, W\, dy\, C_{A_s} \qquad [A.7]$$

The electrochemical reaction coefficient K_r is related to the electrode potential by definition

$$K_{r_A} = K^{\circ}_{r_A} \exp \frac{\alpha_A z_A V^*_a F}{R\, T} \qquad [A.8]$$

Under the assumption of uniform electrode potential and $C_{A_s} = C_{A_b}$, eq. A.7 can be integrated (with u = Q/W S).

$$\int_{C_{A_1}}^{C_A(y)} \frac{dC_{A_b}}{C_{A_b}} = -\int_0^y \frac{K_{r_A}\, a\, dy}{u} = \ell n \frac{C_A(y)}{C_{A_1}} = -\frac{K_{r_A}\, a\, y}{u} \qquad [A.9]$$

for $y = L \quad C_A(y) = C_{A_2}$ and $X = 1 - \frac{C_{A_z}}{C_{A_1}}$

then, $$\ell n(1 - X) = -\frac{K_{r_A}\, a\, L}{u} \qquad [A.10]$$

a) Single reaction

If the only reaction occurring at the electrode is the electrochemical oxidation of phenol, a local reaction rate (referred to the true electrode area) would be given by:

$$\frac{i_A(y)}{z\, F} = K_r\, C_A(y) \qquad [A.11]$$

Solving for $C_A(y)$ from eq. A.9 and substituting in equation A.11

$$\frac{i_A(y)}{z\, F} = K_r\, C_{A_1} \exp\left(-\frac{K_{r_A}\, a\, y}{u}\right) \qquad [A.12]$$

the average true current density through the cell $\left(\bar{i}_A = \frac{I}{a}\right)$ is,

$$\bar{i}_A = \frac{\int_0^L i_A(y)}{\int_0^L dy} dy \qquad [A.13]$$

Substituting eq. A.12 into eq. A.13 and integrating, an average reaction rate can be obtained as:

$$\frac{\bar{i}_A}{z\,F} = \frac{C_{A_1} u}{a\,L}\left[1 - \exp\left[-\frac{K_{r_A}\, a\, L}{u}\right]\right] \qquad [A.14]$$

Equation A.14 implies that if the initial concentration of phenol is increased holding all the other parameters constant, the value of K_r will be lower to sustain the same current flowing. To illustrate this, eq. A.8 is combined with eq. A.14, to find the relation between the average reaction rate, and the electrode potential, as represented in Fig. A-3.

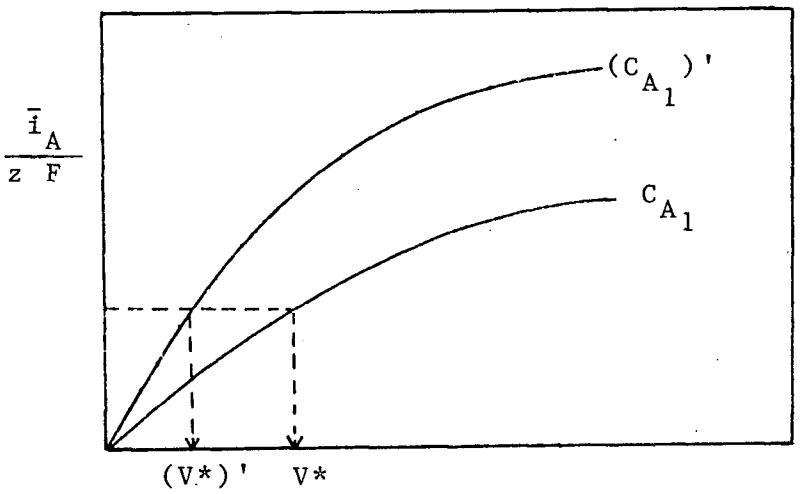

Fig A-3 Schematic representation of eq. A.14

If the initial concentration of phenol is increased from C_{A_1} to $(C_{A_1})'$ at a constant current input, the value of the electrode potential $(V^*)'$ will be lower, and therefore the value of K_r will drop too.

Analogous reasoning shows that K_r will also decrease if u is increased, or if a is increased at a constant applied current. Equation A.14 also implies that when the electrode potential tends to infinity, the

rate of reaction $\bar{i}_A/z\ F$ will tend to a maximum given by $\left(\frac{C_{A_1}\ u}{a\ L}\right)$.

b) More than one electrochemical reaction occurs at the electrode

If, for example, a side reaction of water electrolysis occurs in parallel to the phenol oxidation, the average current density will be given by the sum of the average current densities driving each reaction. If water electrolysis is represented with the subscript w, the current balance would be expressed by,

$$\bar{i} = \bar{i}_A + \bar{i}_w \quad \text{where} \quad \bar{i} = I/a$$

Using eq. A.14 for both partial average currents,

$$i = \frac{z_A\ F\ C_{A_1}\ u}{a\ L}\left(1 - \exp\left(-\frac{K_{r_A}\ a\ L}{u}\right)\right) + \frac{z_w\ F\ C_w\ u}{a\ L}\left(1 - \exp\left(-\frac{K_{r_w}\ a\ L}{u}\right)\right) \qquad [A.15]$$

where $K_{r_A} = K^\circ_{r_A} \exp\left(\frac{\alpha_A\ z_A\ V^*_a\ F}{R\ T}\right)$ [A.8]

and $K_{r_w} = K^\circ_{r_w} \exp\left(\frac{\alpha_w\ z_w\ V^*_a\ F}{R\ T}\right)$

Therefore, the average current density, referred to the true area of the bed, can be related to the electrode potential as represented in Fig. A-4, where it is assumed that both reactions take place at all potentials greater than zero. Figure A-4 shows that there is only one electrode potential at which $\bar{i}_A + \bar{i}_w = \bar{i}$ for each set of parameters a, L, u, C_{A_1}.

If the initial concentration of phenol is increased holding all other parameters constant, a lower value of V* will sustain the same total average current density $\bar{i}$.

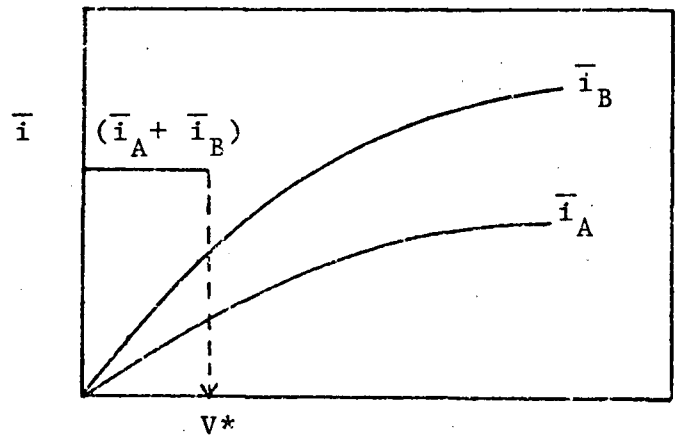

Fig.A-4 Schematic representation of eq. A.15

Analogously, if u or a is increased V* should also decrease, which means that the values of the reaction rate constants K_{r_A} and K_{r_w} would be lower.

3. Mass transfer and electrochemical reaction controlled model

The most general case to consider is when both resistances to mass transfer and to electrochemical reaction are comparable.

Under steady-state (when the concentration profiles have been developed), the rate of electrochemical reaction and the rate of mass transfer per unit area of the electrode, will be equal in a differential of cell length (dy),

$$- Q\, dC_{A_b} = K_m\, a\, S\, W\, dy\, (C_{A_b} - C_{A_s}) \qquad [A.1]$$

$$- Q\, dC_{A_b} = K_r\, a\, S\, W\, dy\, C_{A_s} \qquad [A.7]$$

Therefore, under steady-state,

$$K_m\, (C_{A_b} - C_{A_s}) = K_r\, C_{A_s}$$

which permits to express the concentration at the surface as a function of the concentration in the bulk of solution,

$$C_{A_s} = \frac{K_m C_{A_b}}{(K_m + K_r)} \qquad [A.16]$$

Substituting eq. A.16 into eq. A.1 with Q = u/W S, and integrating,

$$\int_{C_{A_1}}^{C_A(y)} \frac{dC_{A_b}}{C_{A_b}} = -\int_0^y \frac{K_m K_r \quad a}{(K_m + K_r) \quad u} dy$$

$$\ell n \frac{C_A(y)}{C_{A_1}} = -\frac{K_m K_r \quad a\ y}{(K_u + K_r) \quad u} \qquad [A.17]$$

for $y = L, C_A(y) = C_{A_2}$ and with $X = 1 - \frac{C_{A_2}}{C_{A_1}}$

$$\ell n(1 - X) = -\frac{K_m K_r \quad a\ L}{(K_m + K_r) \quad u} \qquad [A.18]$$

where

$$K = \frac{K_m K_r}{K_m + K_r} \qquad [A.19]$$

is the overall rate constant, which could also be found applying the concept of resistances in series as:

$$\frac{1}{K} = \frac{1}{K_m} + \frac{1}{K_r} \quad . \qquad [A.20]$$

Analogous to eq. A.15, in the general case when a side reaction of water electrolysis occurs in parallel to phenol oxidation, the total average current density would be given by,

$$\bar{i} = \frac{z_A F C_{A_1} u}{a L}\left(1 - \exp\left(-\frac{K a L}{u}\right)\right) + \frac{z_w F C_w u}{a L}\left(1 - \exp\left(-\frac{K_{r_w} a L}{u}\right)\right)$$

[A.21]

Note that K_{r_w} is used for the water electrolysis reaction, since it it is an activation controlled process and would not be affected by mass transfer. In this case, an increase in the phenol inlet concentration C_{A_1} or in the specific surface area of the bed, would result in lower values of K_r (or V*) for a same average current density, as discussed previously. However, an increase in the superficial velocity u would result in increased mass transfer coefficients (eq. A.6) but at the same time, lower reaction rate constants K_{r_A}, K_{r_w} should be expected.

4. Mass transfer model for a batch recirculation system

If the cell is operated in a batch recirculation system, as shown in Fig. A-5 both inlet and outlet concentrations will be a function of time.

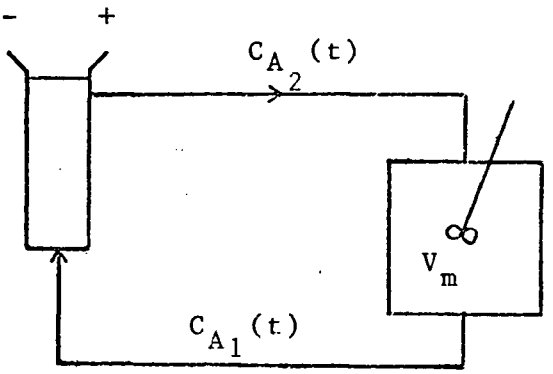

Fig. A-5 Schematic representation of a batch system

It is possible to find an expression to correlate the inlet and outlet concentrations with time, utilizing the approach of Pickett (32, p. 325).

From equations A.3 and A.4,

$$C_{A_2} = C_{A_1} \exp\left(-\frac{K_m a L}{u}\right) \qquad [A.22]$$

An instantaneous material balance over the recirculation tank would be written as,

$$C_{A_2} - C_{A_1} = t_m \frac{dC_{A_1}}{dt} \qquad [A.23]$$

with $$t_m = V_m/Q \qquad [A.24]$$

Combining equation A.22 with A.23 would give,

$$C_{A_1} \exp\left(-\frac{K_m\ a\ L}{u}\right) - C_{A_1} = t_m \frac{dC_{A_1}}{dt}$$

integrating,

$$\int_0^t \left(\exp\left(-\frac{K_m\ a\ L}{u}\right) - 1\right) \frac{dt}{t_m} = \int_{C_{A_0}}^{C_{A_1}} \frac{dC_{A_1}}{C_{A_1}}$$

yields,

$$\ln \frac{C_{A_1}}{C_{A_0}} = \left(\exp\left(-\frac{K_m\ a\ L}{u}\right) - 1\right) \frac{t}{t_m}$$

$$C_{A_1} = C_{A_0} \exp\left(\left(\exp\left(-\frac{K_m\ a\ L}{u}\right) - 1\right) \frac{t}{t_m}\right) \qquad [A.25]$$

Substituting C_{A_1} from eq. A.25 into eq. A.22,

$$C_{A_2} = C_{A_0} \exp\left(\left(\exp\left(-\frac{K_m\ a\ L}{u}\right) - 1\right) \frac{t}{t_m} - \frac{K_m\ a\ L}{u}\right) \qquad [A.26]$$

defining, $$t^* = \frac{t}{t_m} = \text{dimensionless time}$$

$$\theta = \frac{K_m\ a\ L}{u} = \text{dimensionless mass transfer group}$$

$$X = \frac{C_{A_0} - C_{A_2}}{C_{A_0}} = \text{fractional conversion}$$

Equation A.26 can be written as,

$$X = 1 - \exp[(\exp(-\theta) - 1)\ t^* - \theta] \qquad [A.27]$$

Note that if the reaction controls the process, an analogous mathematical solution for a constant applied current operation is not possible, because the value of K_r will change as the concentration C_{A_1} changes with time, as discussed from eq. A.14.

APPENDIX 4

Calculations

1. Batch experiments. Calculation of theoretical phenol fractional conversion if mass transfer controls.

This estimate will be suitable to compare all those experiments in groups No. 2 and No. 3, performed under the following experimental conditions,

Flow rate 1.12 ℓ/min

Particle size $1.7 < dp < 2.00$ mm

Particle weight 250 g

Particle volume $= \frac{250\ g}{9.375^{*}\ g/cm^3} = 23\ cm^3$ *density of PbO_2 from ref. (49)

Void fraction $(57-23)/57 = 0.60$

Specific surface area of the bed (eq. A.5)

$$a = \frac{1}{S} + \frac{6 \times (1 - \varepsilon)}{\xi \times dp}$$

taking $\xi = 0.75$ for A and, from ref. (49), and $dp = 0.185$ cm.

$$a = \frac{1}{0.3\ cm} + \frac{6 \times (1 - 0.57)}{0.75 \times 0.185} = 20.6\ cm^{-1}$$

Determination of the mass transfer coefficient from eq. A.6,

$$K_m = 0.83 \frac{D}{dp} (Re)^{0.56} (Sc)^{1/3}$$

Using an equation for diffusivity of liquids given by Wilke (50). (Original nomenclature.)

$$D = \frac{7.4 \times 10^{-8} \; (\phi_B \; m_B)^{\frac{1}{2}} \; T}{\mu \; \tilde{V}_A^{0.6}}$$

$$D = \frac{7.4 \times 10^{-8} \; (2.6 \times 18)^{\frac{1}{2}} \times 297}{1 \times (105)^{0.6}} = 9.2 \times 10^{-6} \text{ cm}^2/\text{s}$$

Superficial velocity of the liquid,

$$u = \frac{1.12 \text{ ℓ/min}}{5 \times 0.3 \text{ cm}^2} \times (10^3 \text{cm}^3/\text{ℓ}) \times (1 \text{ min}/60 \text{ s}) = 12.4 \text{ cm/s}$$

$$Re \simeq \frac{u \; dp}{\nu} = \frac{12.4 \text{ cm/s} \times 0.185 \text{ cm}}{0.01 \text{ cm}^2/\text{s}} = 229.4$$

$$Sc = \frac{\nu}{D} = \frac{0.01 \text{ cm}^2/\text{s}}{9.2 \times 10^{-6} \text{ cm}^2/\text{s}} = 1086$$

$$K_m = 0.83 \times \frac{9.2 \times 10^{-6}}{0.185} \; (229.4) \; (1086) = 8.7 \times 10^{-3} \text{ cm/s} \pm 10\%$$

Extreme values of K_m, taking into account the 10% error in correlation A.6,

$$K_m^- = 0.078 \text{ cm/s} \qquad K_m^+ = 0.0096 \text{ cm/s}$$

The dimensionless mass transfer group is given by

$$\theta = \frac{K_m \; a \; L}{u} = \frac{K_m \; 20.6 \text{ cm}^{-1} \; 38 \text{ cm}}{12.4 \text{ cm/s}}$$

Therefore, the extreme values of θ will be

$$\theta^- = 0.49 \qquad \theta^+ = 0.60$$

The phenol fractional conversion for mass transfer control is given by,

$$X = 1 - \exp[(\exp(-\theta) - 1) \; t^* - \theta] \qquad [A.27]$$

with $t^* = \frac{t}{t_m}$ and $t_m = \frac{5 \text{ ℓ}}{1.12 \text{ ℓ/min}} = 4.464$ min.

Using the extreme values of θ, equation A.27 is used to calculate the range of theoretical fractional conversion for mass transfer control at a given time, as shown in Table A-2.

TABLE A-2

THEORETICAL PHENOL FRACTIONAL CONVERSION VS TIME FOR A MASS TRANSFER--CONTROLLED BATCH SYSTEM

t (min)	t*	X^-	X^+
0	.00	0.39	0.45
15	3.36	0.83	0.88
30	6.72	0.95	0.97
45	10.08	0.99	0.99
60	13.44	1.00	1.00

A theoretical mass transfer controlled region is obtained in this manner which is represented in Fig. 28 for comparison with the experimental results.

2. Continuous experiments. Determination of experimental, mass transfer, and reaction rates constants.

Procedure

a) According to the plug flow equation,

$$\ell n(1 - X) = - \frac{K\ a\ L}{u} \qquad [A.18]$$

If $- \ell n/(1 - X)$ vs $\frac{1}{u}$ is plotted from the experimental data, a straight line should be obtained, with a slope equal to K a L. The experimental rate constant can be determined from the slope. The specific surface area of the electrode is calculated from eq. A.5.

b) Using the empirical equation for the mass transfer coefficient, K_m is estimated:

$$K_m = 0.83 \frac{D}{dp} (Re)^{0.56} (Sc)^{1/3} \qquad 22 < Re < 520$$

c) The reaction rate constant is then calculated from the equation of resistances in series:

$$\frac{1}{K} = \frac{1}{K_r} + \frac{1}{K_m} \qquad [A.20]$$

where

$$K_r = \frac{K_m K}{K_m - K}$$

TABLE A-3

CALCULATION OF EXPERIMENTAL, MASS TRANSFER AND REACTION RATE CONSTANTS FROM EXPERIMENTS 4-1, 4-2, 4-3* (USING AVERAGE PHENOL FRACTIONAL CONVERSION)

Q (ℓ/min)	u (cm/s)	u^{-1} $(cm/s)^{-1}$	X	$-\ln(1-X)$	Re	K_m (cm/s)	K_r (cm/s)
0.25	2.78	0.360	0.59	0.89	51.4	3.85×10^{-3}	15.65×10^{-3}
0.40	4.44	0.225	0.44	0.58	82.1	5.01×10^{-3}	8.06×10^{-3}
0.55	6.11	0.163	0.34	0.42	113.0	5.98×10^{-3}	6.39×10^{-3}
0.85	9.44	0.106	0.25	0.29	174.6	7.64×10^{-3}	5.19×10^{-3}
1.10	12.22	0.082	0.21	0.24	226.0	8.82×10^{-3}	4.76×10^{-3}
1.30	14.44	0.069	0.17	0.19	267.0	9.69×10^{-3}	4.54×10^{-3}

*For these experiments:

$C_{A_0} = 100 \pm 5$ mg/l $1.7 < dp < 2.00$ mm $a = 20.6\ cm^{-1}$ (from page 171)

From Fig. 32: Slope = 2.42 cm/sec $= K = \dfrac{2.42\ cm/s}{20.6\ cm^{-1} \times 38\ cm} = 3.09 \times 10^{-3}$ cm/s

$$Re = \frac{u\ dp}{\nu} = \frac{u \times 0.185\ cm}{0.01\ cm^2/s} = 18.5\ u$$

$$K_m = 0.83 \frac{D}{dp} (Re)^{0.56} (Sc)^{1/3} = 0.83 \times \frac{9.2 \times 10^{-6}}{0.185} \times Re^{0.56} (1086)^{1/3} = 4.24 \times 10^{-4}\ Re^{0.56}$$

TABLE A-4

CALCULATION OF EXPERIMENTAL, MASS TRANSFER AND REACTION RATE CONSTANTS FOR EXPERIMENT (4-4)*

Q (ℓ/min)	u (cm/s)	u^{-1} $(cm/s)^{-1}$	X	$-\ln(1-X)$	Re	K_m (cm/s)	K_r (cm/s)
0.25	2.78	0.36	0.37	0.46	51.4	3.85×10^{-3}	2.21×10^{-3}
0.40	4.44	0.225	0.25	0.29	82.1	5.01×10^{-3}	1.95×10^{-3}
0.55	6.11	0.163	0.19	0.21	113.0	5.98×10^{-3}	1.84×10^{-3}
0.85	9.44	0.106	0.12	0.13	174.6	7.64×10^{-3}	1.72×10^{-3}
1.10	12.22	0.082	0.09	0.09	226.0	8.82×10^{-3}	1.67×10^{-3}

*In experiment (4-4):

C_{A_0} = 580 mg/l 1.7 < dp < 2.00 mm a = 20.6 cm^{-1} (from page 171)

From Fig. 32: Slope = 1.1 cm/s = $K = \frac{1.1 \text{ cm/s}}{20.6 \text{ cm}^{-1} \times 38 \text{ cm}} = 1.405 \times 10^{-3}$ cm/s

with,

$$Re = 18.5\ u$$

and $K_m = 4.24 \times 10^{-4}\ Re^{0.56}$ (as in Table A-3)

TABLE A-5

CALCULATION OF EXPERIMENTAL, MASS TRANSFER AND REACTION RATE CONSTANT FOR EXPERIMENT (4-8)*

Q (ℓ/min)	u (cm/s)	u^{-1} $(cm/s)^{-1}$	X	$-\ln(1-X)$	Re	K_m (cm/s)	K_r (cm/s)
0.25	2.78	0.36	0.67	1.11	25	5.3×10^{-3}	2.68×10^{-3}
0.40	4.44	0.225	0.53	0.76	40	6.9×10^{-3}	2.40×10^{-3}
0.55	6.11	0.163	0.45	0.60	55	8.2×10^{-3}	2.27×10^{-3}
0.85	9.44	0.106	0.34	0.42	85	10.5×10^{-3}	2.14×10^{-3}
1.10	12.22	0.082	0.29	0.34	110	12.1×10^{-3}	2.09×10^{-3}

*In experiment (4-8) $C_{A_0} = 100$ mg/1 $0.7 < dp < 1.1$ $\varepsilon = 0.57$

Specific surface area of the bed (eq. A.5):

$$a = \frac{1}{0.3 \text{ cm}} + \frac{(1 - 0.57) \times 6}{(0.75)(0.09) \text{ cm}} = 41.5 \text{ cm}^{-1}$$

From Fig. 32: Slope = 2.81 cm/s $=$ $K = \dfrac{2.81 \text{ cm/s}}{(41.5 \text{cm}^{-1})(38 \text{cm})} = 1.78 \times 10^{-3}$ cm/s

$Re = u\, dp/\nu = u\, 0.09/0.01 = 9\, u$

$$K_m = 0.83 \times \frac{9.2 \times 10^{-6} \text{ cm}^2/\text{s}}{0.09 \text{ cm}} (Re^{0.56})(1086)^{1/3} = 8.72 \times 10^{-4} (Re)^{0.56}$$

3. Estimates of typical % current efficiency

a) Batch experiments

$$\% \text{ C.E.} = \frac{F\ z\ (\text{moles oxidized})}{I\ t} \times 100 \qquad \text{[Eq. 7]}$$

Assuming a 4-electron transfer from the phenol molecule as proposed by Covitz (Reaction R.11), the % C.E. can be calculated.

Sample calculation: Run 3-13, recirculation time = 15 min. For the calculation, it is supposed that after 15 min, recirculation is stopped and the volume remaining in the tank is treated continuously. The steady state final concentration at the outlet is assumed to be equal to the recorded at 15 min time.

total electrolysis time = 15 min + 5 ℓ/1.12 ℓ/min = 19.5 min

$$\text{moles phenol oxidized} = (1100-792)\text{mg/1} \times 5\ell \times 1\text{ g mol/94 g} \times 1\text{ g}/10^3\text{ mg} = 16.4\times10^{-3}\text{ g mol}$$

$$\% \text{ C.E.} = \frac{96500\text{ coul/eq} \times 4\text{ eq/mol} \times 16.4\times10^{-3}\text{ g mol}}{10\text{ A} \times 19.5\text{ min} \times 60\text{ sec/min}} \times 100 = 0.54$$

This is a sample calculation for Table 6, where % C.E. is given after 15 and 90 min recirculation times.

b) Continuous experiments

$$\% \text{ C.E.} = \frac{F\ z\ Q\ X\ C_{A_1}}{I} \times 100$$

Therefore, current efficiencies for phenol oxidation in a single pass, are a function of flow, conversion, initial phenol concentration, and current applied.

Sample calculation: Run 4-4, at Q = 0.25 ℓ/min,

$$\% \text{ C.E.} = \frac{96500\text{ coul/eq} \times 4\text{ eq/mol} \times 0.25\ \ell\text{/min} \times 0.37 \times 580\text{ mg/1}}{10\text{ A} \times 10^3\text{ mg/g} \times 94\text{ g/g mol} \times 60\text{ sec/1 min}} \times 100$$

% C.E. = 36.7.

4. Estimate of typical electrical energy requirements and costs

a) Batch experiments

$$\frac{\text{Energy requirements}}{\text{Moles of phenol oxidized}} = \frac{I\ \Delta V\ t}{V_m\ (C_{A_0} - C_{A_2})}$$

Sample calculation: Run 3-13, recirculation time = 15 min. As it was assumed in the previous section, after the batch operation the tank volume is treated continuously.

Total electrolysis time = 15 min + 5 ℓ/1.12 ℓ/min = 19.5 min

Average ΔV = 8.5 V

$$\frac{\text{Energy}}{\text{mol}} = \frac{10\ \text{A} \times 8.5\ \text{V} \times 1\ \text{kw}/10^3\ \text{w} \times 19.5\ \text{min} \times 1\ \text{h}/60\text{min}}{5\ell \times (1100\text{-}792)\ \text{mg}/1 \times 1\ \text{g}/10^3\text{mg} \times 1\ \text{g mol}/94\ \text{g}}$$

$$= 1.69\ \frac{\text{kw-h}}{\text{g mol}}$$

Power costs are taken as 2¢/kw-h for illustration,

Cost = 1.69 kw-h/g mol × 0.02 $/kw-h = 0.03 $/g mol

Energy requirements and costs are presented in Table 6 for the batch experiments Nos. 3-3, 3-12, 3-12 at 10 A, after 15 and 90 min recirculation time.

In Table 8 the energy requirements per volume of waste is estimated as follows: in Runs 3-12 and 3-13, 99% and 98% phenol removal is achieved at 90 min recirculation time.

Total electrolysis time = 90 mm + 5ℓ/1.12 ℓ/min = 94.5 min

$$\text{Energy} = \frac{10\ \text{A} \times 8.5\ \text{V} \times 94.5\ \text{min} \times 10^3\ \text{kw/w}}{5\ell \times 60\ \text{min}/1\ \text{h}} = 0.027\ \text{kw-h}/\ell$$

Energy = 0.027 kw-h/ℓ × 3.785 ℓ/1 gal = 0.1022 kw-h/gal

The electrical cost for treating 10^3 gal of waste would be:

$$102.2 \text{ kw-h/1000 gal} \times 0.02 \text{ \$/kw-h} \simeq 2 \text{ \$/1000 gal}$$

This would be the approximate cost for treating a 700 mg/l effluent with a 99% phenol removal, under the operating conditions of experiments 3-12 or 3-13.

b) Continuous experiments

$$\frac{\text{energy required}}{\text{mol phenol oxidized}} = \frac{I \ \Delta V}{Q \ (C_{A_1} - C_{A_2})}$$

Sample calculation: Run 4-4 at $Q \simeq 0.25$ ℓ/min,

$$\text{Energy} = \frac{10 \text{ A} \times 8.5 \text{ V} \times 10^3 \text{ kw/w} \times 10^3 \text{ mg/g} \times 94 \text{ g/g mol}}{0.25 \text{ ℓ/min} \times (580-365)\text{mg/l} \times 60 \text{ min/l h}} = 2.51 \text{ kw-h/g mol}$$

Cost of electrical energy per mol of phenol oxidized:

$$0.02 \text{ \$/kw-h} \times 2.51 \text{ kw-h/g mol} = 0.05 \text{ \$/g mol}$$

APPENDIX 5

Relevant Physical Data

TABLE A-6

pH OF SOLUTIONS OF NaOH AND H_2SO_4 AT 20°C (51)

N	Aq. NaOH solutions		Aq. H_2SO_4 solutions	
	g/l	pH	g/l	pH
.1	40.0	14	49.0	0.3
0.1	4.0	13	4.9	1.2
0.01	0.4	12	0.49	2.1

TABLE A-7

CONDUCTIVITIES OF AQUEOUS SOLUTIONS OF NaOH, H_2SO_4 AND Na_2SO_4 AT 20°C (51)

NaOH		H_2SO_4		Na_2SO_4	
conc. (g/l)	$K_e \times 10^3$ $(\Omega\ cm)^{-1}$	conc. (g/l)	$K_e \times 10^3$ $(\Omega\ cm)^{-1}$	conc. (g/l)	$K_e \times 10^3$ $(\Omega\ cm)^{-1}$
5	24.8	5.0	24.3	5.0	5.9
10.1	48.6	10.0	47.8	10.1	11.2
15.2	71.3	15.1	70.3	15.2	15.7
20.4	93.1	20.2	92.0	20.3	19.8
				25.5	23.9
				30.8	27.9

% phenol ionized vs pH at 20°C

dissociation constant $K_d = 1.28 \times 10^{-10}$ (51)

$K_d = [H^+]\ [C_6H_5O^-] \ / \ [C_6H_5OH]$

$\text{Ionized fraction} = [C_6H_5O^-] \ / \ [C_6H_5OH]$

$$\text{Ionized fraction} = \frac{K_d}{[H^+]} = \frac{K_d}{10^{-pH}} = \frac{1.28 \times 10^{-10}}{10^{-pH}}$$

% ionized = fraction/(fraction + 1) × 100

TABLE A-8

% PHENOL IONIZED VS pH

pH	2	4	6	8	10	12
ionized to unionized fraction	1.28×10^{-8}	1.28×10^{-6}	1.28×10^{-4}	1.28×10^{-2}	1.28	128
% ionized	1.28×10^{-6}	1.28×10^{-4}	1.28×10^{-2}	1.16×10^{-1}	56	99